

**Calcium and cAMP homeostasis determine network organisation of
respiratory pre-Bötzinger neurons in *Mecp2* null mice *in vitro***

Dissertation

for the award of the degree

“Doctor of Philosophy” Ph.D. Division of Mathematics and Natural Sciences

of the Georg-August-Universität Göttingen

within the biology doctoral program

of the Georg-August University School of Science (GAUSS)

submitted by

Ekaterina Skorova

from Moscow, Russia

Göttingen 2012

Thesis Committee

Prof. Dr. Andreas Stumpner, Abtl. Zelluläre Neurobiologie, Schwann-Schleiden-Forschungszentrum

Prof. Dr. Michael Hörner, Johann-Friedrich-Blumenbach-Institut für Zoologie und Anthropologie, Abt. Zelluläre Neurobiologie, c/o ENI

Members of the Examination Board

Reviewer: Prof. Dr. Andreas Stumpner, Abtl. Zelluläre Neurobiologie, Schwann-Schleiden-Forschungszentrum

Second Reviewer: Prof. Dr. Michael Hörner, Johann-Friedrich-Blumenbach-Institut für Zoologie und Anthropologie, Abt. Zelluläre Neurobiologie, c/o ENI

Further members of the Examination Board

Prof. Dr. Nils Brose, Max Planck Institute for Experimental Medicine, Dept. of Molecular Neurobiology

Prof. Dr. Uwe Groß, Göttingen University Medical School Institute for Medical Microbiology, Dept. of Medical Microbiology

Prof. Dr. Hansjörg Scherberger, German Primate Center, Research Group Neurobiology

Prof. Dr. Andreas Wodarz, Stammzellbiologie, Abt. Anatomie und Zellbiologie, GZMB

Date of oral examination: 27th of November 2012

Acknowledgements

Research presented in this thesis was carried out at the Department of Neurophysiology and Sensory Physiology, Georg-August University within the framework of the CMPB project. The author expresses her acknowledgements to those who helped along the way and influenced the evolution of her thinking. I would like to thank members of CMPB for support and personally Prof. Diethelm Richter for their warm encouragement.

I am deeply indebted to Prof. Michael Hoerner and Prof. Andreas Stumpner for their continuous support and thoughtful guidance during this work.

In particular, I wish to express my gratitude to Dr. Sergey L. Mironov for his extremely valuable experience, invaluable suggestions and the scientific hypothesis that formed my present understanding of the problem. In this I would also like to include my gratitude to Dr. Sebastian Kuegler who together with the members of his lab provided support to this research along the way. I am happy to acknowledge my debt to Nicole Hartelt, whose practical skills made this work possible.

Finally I would like to thank my family for the never-ending support.

Contents

1. Summary	6
2. Abbreviations	8
3. Introduction	13
3.1 Rett Syndrome (RS)	13
3.2 MeCP2.....	15
3.3 Mouse models of RS	17
3.4 RS and respiratory rhythmogenesis.....	18
3.5 Neurochemistry in the brainstem respiratory network in <i>Mecp2</i> null mice	22
3.5.1 Biogenic amines	23
3.5.2 GABAergic signalling.....	23
3.5.3 Second messenger signalling. ATP	23
3.5.4 Second messenger signalling. Ca ²⁺	25
3.5.5 Second messenger signalling. cAMP and PKA	26
3.5.6 BDNF	28
3.6 Transcription and neuronal activity.....	29
4. Methods	34
4.1 Ethical approval.....	34
4.2 Mouse strains.....	34
4.3 Cell culture	34
4.4 Organotypic culture.....	35
4.5 Immunofluorescence	36
4.5.1 Sensors	38
4.5.2 Chemical indicators.....	38
4.5.3 Genetically encoded calcium indicators.....	40
4.5.4 Genetically encoded cAMP indicators.....	41
4.5.5 Simultaneous calcium and cAMP imaging	42
4.6 Transduction of neurons.....	45
4.7 Patch clamp	46
5. Results	48
5.1. ATP-dependent potentiation of K-ATP channels	48

5.2. ATP-dependent modulation of action potentials.....	51
5.3 BDNF modifies activity of K-ATP channels	51
5.4. BDNF modulates excitability of granule cells and preBötC neurons	53
5.5. Interactions between ATP and BDNF signalling pathways.....	53
5.6. The electrophysiological study of <i>Mecp2</i> null mice	56
5.7 Distorted topology of the network in preBötC in model Rett mice	60
5.8 Impaired Ca ²⁺ homeostasis in MeCP2 deficient neurons and its correction by BDNF	63
5.9 Hypoxia and retraction of neurites	68
5.10. Neuron-specific expression of cAMP and calcium dependent changes	73
5.11 Deregulated cAMP homeostasis in <i>Mecp2</i> ^{-/-} neurons	81
6. Discussion.	86
6.1 Electrophysiology.....	86
6.2 Disturbances in network topology and neurite retraction in <i>Mecp2</i> KO mice.....	88
6.3 Impaired calcium homeostasis in the mouse model of Rett syndrome	94
6.4 Interplay between calcium and cAMP	94
7. References	98
8. Curriculum vitae.....	140

1. Summary

Rett Syndrome (RS) is a neurodevelopmental disorder caused primarily by mutations in a *Mecp2* gene on the X chromosome that encodes methyl-cytosine binding protein (MeCP2). MeCP2 acts as a transcriptional repressor and an activator for a number of genes such as *DLX5/Dlx5* and *Bdnf*. One of the effects of diminished *Mecp2* expression activity is the appearance of a Rett-like phenotype including tremors, severe breathing irregularities, and hypoactivity. Neurons of pre-Bötzinger complex (preBötC), the most important component of the complex respiratory network on which the generation of respiratory rhythm in mammals is relied were used to study possible origins of breathing disturbances. The research was focused on two major players of intracellular signal transduction, Ca^{2+} and cAMP, involved in various events of neuronal activity and plasticity, to establish disturbances in signal transduction, excitability, and higher vulnerability of the *Mecp2*^{-/-} (KO) preBötC neurons during early postnatal development. Using recently developed methods of transduction of living neural tissue with neuron-specific fluorescent sensors, D3cpv calcium sensor and exchange protein directly activated by cAMP (Epac1-camps) were introduced into the organotypic slices from wild-type (WT) and model knockout (KO) mice. Thereby differences in the spatial organisation of neurons in preBötC and disturbances in intracellular Ca^{2+} ($[\text{Ca}^{2+}]_i$) and cAMP ($[\text{cAMP}]_i$) homeostasis in mutant mice which appeared in RS mouse model during early postnatal development were observed.

Calcium buffering in KO neurons was indicated by increased amplitude and kinetics of depolarisation-induced calcium transients related to insufficient calcium uptake into the endoplasmic reticulum. Brief hypoxia and calcium release from internal stores induced global calcium increases, after which the processes of many KO neurons were retracted. The effects were restored after a treatment with BDNF while inhibition of BDNF signalling in WT neurons produced disturbances in calcium buffering similar to those observed in KO mice. The data obtained recently point to a direct connection between calcium homeostasis and long-term changes in neuronal connectivity. It can be therefore proposed that calcium-dependent retraction of neurites in preBötC neurons can retard the development of the neural network and set up conditions for appearance of breathing irregularities in RS.

Transduction of organotypic slices with a sensor based on a cAMP-dependent GTP-exchange factor (Epac1-camps) allowed us to measure the intracellular distribution of cAMP, its absolute levels and time-dependent changes in response to different physiological stimuli. After

modulation by adenylate cyclase (AC), inhibition of phosphodiesterase (PDE) and activation of G-protein-coupled metabotropic receptors, $[cAMP]_i$ changes in μM range were recorded. Membrane depolarisation and Ca^{2+} release from internal stores slowly increased $[cAMP]_i$ levels. These effects were suppressed after AC blockade with 2'5'-dideoxyadenosine, and potentiated after inhibiting PDE with isobutylmethylxanthine or rolipram. Inhibition of protein kinase A (PKA) with N-[2-(p-bromocinnamylamino)ethyl]-5-isoquinoline sulfonamide hydrochloride (H-89) in turn abolished these effects. This indicates the important role of phosphorylation of voltage-sensitive Ca^{2+} channels in the potentiation of $[cAMP]_i$ transients. A crosstalk between Ca^{2+} and cAMP signalling that revealed a synergism of actions of these two second messengers was investigated. Resting $[cAMP]_i$ levels in KO neurons were lower and transient $[cAMP]_i$ changes were smaller and faster, but both features were corrected by BDNF to those of the WT.

The results obtained indicate that KO neurons have significant disturbances in calcium and cAMP homeostasis that is possibly responsible for higher excitability and vulnerability of neurons. Calcium-induced retraction of neurites can retard formation of properly functioning respiratory network and produce instabilities in regular breathing. An important result that BDNF corrected both calcium and cAMP homeostasis corroborates the present view of the important role of MeCP2-regulated expression and secretion of BDNF in neuronal development. This supports the current opinion about the special role of BDNF in the development of RS that has been derived from biochemical and molecular biology studies.

2. Abbreviations

[Ca²⁺]_i – cytoplasmic free Ca²⁺;

[cAMP]_i – intracellular concentration of cAMP;

μOR – μ-opioid receptor;

AAV – adeno-associated virus;

AC – adenylate cyclase;

ACSF – artificial cerebro-spinal fluid;

AMPA – α-amino-3-hydroxy-5-methyl-4-isoxazolepropionate;

AP – action potential;

ATP – adenosine triphosphate;

BAPTA – 1,2-bis(o-aminophenoxy)ethane-N,N,N',N'-tetraacetic acid);

Bdnf – gene encoding BDNF protein;

BDNF – brain-derived neurotrophic factor;

bGH – bovine growth hormone derived polyadenylation site;

BrOMecAMP – 8-bromo-2'-OMe-cAMP;

BSA – bovine serum albumin;

CaM – calmodulin;

CaMK – calmodulin dependent protein kinases;

cAMP – cyclic adenosine monophosphate;

CCCP – carbonyl cyanide m-chlorophenyl hydrazone;

CCD – charge-coupled device;

CFP – cyan fluorescent protein;

CICR – Ca²⁺-induced Ca²⁺ release;

CNS – central nervous system;

CREB – CRE-binding protein;

CREs – Ca²⁺-response elements;

CREST – calcium-responsive transactivator;

CSF – cerebrospinal fluid;

DAG – diacylglycerol;

DDA – 2'5'-dideoxyadenosine;

DHPG – (S)-3,5-dihydroxyphenylglycine;

DIV – days *in vitro*;

D-MEM – Dulbecco/Vogt modified Eagle's minimal essential medium;

DMSO – dimethyl sulfoxide;

EDTA – ethylenediaminetetraacetic acid;

EGFP – enhanced green fluorescent protein;

EGTA – ethylene glycol tetraacetic acid;

Epac – cAMP-dependent exchange factor;

Epac1-camps – exchange protein directly activated by cAMP;

ER – endoplasmic reticulum;

FDA – The Food and Drug Administration government agency USA;

Fig. – figure;

FRET – fluorescence resonance energy transfer;

GABA – gamma-aminobutyric acid;

GFP – green fluorescent protein;

GPCR – G-protein-coupled receptor;

H-89 – *N*-[2-(*p*-bromocinnamylamino)ethyl]-5-isoquinoline sulfonamide hydrochloride;

HDAC – histone deacetylases;

HEK 293 – human embryonic kidney 293 cells;

hSyn1 – short human synapsin-1 gene promoter

IBMX – isobutylmethylxanthine;

ICAN – Ca²⁺-activated nonselective cationic current;

IGF-1 – insulin-like growth factor 1 (IGF-1), somatomedin C;

INaP – persistent sodium current;
Int – chimeric intron
IO – *inferior olive*;
IP(3)R – inositol triphosphate receptor;
IPSC – inhibitory postsynaptic current;
ITR – inverted terminal repeats of AAV-2;
K 252 – staurosporine aglycon;
K-ATP channels – ATP-sensitive potassium channels;
KO – *Mecp2*^{-/-} (null) mice;
L-NMMA – N-monomethyl-L-arginine;
LED – light-emitting diode;
LSM – laser scanning microscopy;
MAPK – mitogen-activated kinase
MBD – methyl-binding domain;
MBD – methyl-CpG binding domain;
mGluR1/5 – group I metabotropic glutamate receptor;
Mecp2 – MeCP2 coding gene;
MeCP2 – methyl-cytosine binding protein;
NA – *nucleus ambiguus*
NK1 – (TACR1, SPR) – neurokinin 1;
NMDA – N-methyl-D-aspartate;
NMRI – inbred line of mice for 51 generations, then transferred to the Naval Medical Research Institute;
NOS – nitric oxide synthase;
NTS – *nucleus tractus solitarius*;
ODQ – 1H-[1,2,4]-oxadiazolo-[4,3-a]-quinoxalin-1-one;
P2R – purinergic receptor ;

P2Y – G protein-coupled purinergic receptors;
P3-P49 – postnatal days 3-49;
PBS – phosphate buffered saline;
PDE – phosphodiesterase;
PFA – phosphate buffered formaldehyde;
pFRG – parafacial respiratory group;
PIP2 – phosphatidylinositol 4,5-bisphosphate
PLC – phospholipase C;
PKA – protein kinase A;
PKC – proteinkinase C;
preBötC – pre-Bötzinger complex;
PXX – postnatal day;
RS – Rett Syndrome;
RT – room temperature;
RyR – ryanodine receptor;
SERCA – Sarco/Endoplasmic Reticulum Ca²⁺-ATPase;
SNAP – S-nitroso-N-acetylpenicillamine;
SNpc – *substantia nigra pars compacta*;
SPR – substance P receptor;
SV40 – simian virus 40 derived polyadenylation site;
TACR1 – tachykinin receptor 1;
Tg – thapsigargin;
TRD – transcription repression domain;
TRH – thyrotropin-releasing hormone;
TrkB – tyrosine kinase B;
TRPM4 – calcium-activated nonselective cation channels;

UV – ultraviolet;

VGCC – voltage-dependent calcium channel;

VLM – ventrolateral medulla;

VRC – ventral respiratory column;

WPRE – woodchuck hepatitis virus posttranscriptional regulatory element;

WT – wild-type;

XII – *nucleus hypoglossus*;

YFP – yellow fluorescent protein.

3. Introduction

3.1 Rett Syndrome

Rett Syndrome (RS) is a neurodevelopmental disorder. It has been studied for more than 50 years since 1954 when a Viennese physician Rett first noticed its symptoms in two girls who were making the same characteristic repetitive hand-washing movements (Rett, 1966). In 1983 Hagberg and his colleagues finally raised the profile of RS and drew attention to this disorder (Hagberg et al., 1983). It was fairly soon discovered that the Rett Syndrome, named after its discoverer, affects primarily young females at the age of 6-18 months after an apparently normal period of growth and development, with an incidence of one per 10.000-15.000 by the age of 12 years (Francke, 2006; Chahrour and Zoghbi, 2007). In 1999 it was discovered that RS is caused primarily by a genetic mutation in the gene that encodes MeCP2 - methyl-cytosine binding protein (Amir et al., 1999) and can arise sporadically or from germline mutations. This mutation was found in more than 95% of those meeting criteria for typical RS and more than 50% for atypical RS. The discovery of a monogenic origin of RS promoted it from a set of symptoms to the system disorder with a genetically defined origin and yet unknown development.

MeCP2 is a member of the family of proteins capable of binding to methylated DNA and recruiting chromatin-modifying activities that causes the deacetylation and condensation of chromatin. As a result, MeCP2-binding regions in DNA become no more accessible to the transcription machinery and the corresponding genes cannot be expressed. *Mecp2* mutation does not directly induce neurodegeneration but rather leads to the MeCP2-regulated changes in transcription patterns. These signalling moieties are required during the development that eventually leads to an RS-like phenotype including tremors, breathing irregularities and hypoactivity. The areas of the brain disrupted in RS are the frontal, motor, and temporal cortex, brainstem, basal forebrain, basal ganglia (which control many basic functions, such as movement), and they are critical for the normal development of the cortex or higher brain centre in late infancy.

It is generally assumed that RS patients and *Mecp2* null mice do not exhibit gross morphological abnormalities in brain organisation or detectable cell loss (Ogier and Katz, 2008). Reasonable reduction of brain size in RS is associated with marked reduction in dendritic

branching of pyramidal neurons in the frontal, temporal and motor cortices, and neurons in the subiculum (Armstrong, 2005), as well as shortening of dendritic spines in the frontal cortex (Belichenko et al., 1994). Neuronal size is reduced in the cortex, thalamus, basal ganglia, amygdala, and hippocampus (Kitt and Wilcox, 1995). *Mecp2*^{-/y} mice also show a decreased cortical dendritic arborization (Kishi and Macklis, 2004), delayed neuronal maturation and synaptogenesis in the cerebral cortex (Fukuda et al., 2005), and reduction in synapse number in the hippocampus (Chao et al., 2007). Mutation in *Mecp2* produces primarily changes in cellular organisation of the neural centres that control both movement and emotion (Budden et al., 2005), whereas their morphological appearance is not substantially changed (Ogier and Katz, 2008).

Severity of RS can vary: since females have two X chromosomes, the normal version of the gene can compensate for much of the dysfunction. For males there is no compensation: males die young, within the first year of life (Schanen et al., 1998). In general, the disease is considered as embryonically lethal in males. There are still some ways to overcome this rule: genetic mosaicism is believed to be the reason for the survival of some individuals (Clayton-Smith et al., 2000; Renieri et al., 2003), and a boy with 47,XXY karyotype has been described as well (Schwartzman et al., 1998). At present it is now known that MeCP2 can underlie various disorders which are not related to RS (Gonzales and LaSalle, 2010). *Mecp2* mutations have been identified in children with schizophrenia (Shibayama et al., 2004) and some forms of autism (Beyer et al., 2002; Carney et al., 2003), as well as in those with severe mental retardation associated with movement disorders (Van Esch et al., 2005). Some women with very mild learning disabilities have also been found to carry *Mecp2* mutations although in most cases mutations in *Mecp2* led to the characteristic set of clinical signs (Wan et al., 1999).

Clinically, the affected girls have a normal *in utero* development followed by a normal postnatal period extending up to 18 months. The symptoms appear at a stage when development slows down and gives way to stagnation and regression of previously acquired social skills and abilities to walk and to talk. Such patients have a severe mental retardation and demonstrate a language and motor milestone regress, a sudden arrest of brain development, and loss of purposeful hand use, followed by repetitive hand movements (clapping, tapping, wringing). Rett Syndrome Diagnostic Criteria Working Group (1988) reported that there were additional problems such as cognitive impairment and seizures, scoliosis, spasticity, breathing anomalies (for example Hagberg and colleagues (1883) identified hyperventilation, apnea, or sighing, and

epilepsy), abnormal blood circulation, and partial loss of verbal skills. Recent RS studies show that there are physiological dysfunctions that possibly underlie the clinical symptoms, such as EEG abnormalities, atypical brain glycolipids, elevated CSF levels of glutamate and beta-endorphins, and reduction of substance P. The persons with Rett Syndrome symptoms that were recognized during their first 3 – 4 years may remain stabilized for interaction and cognitive function such as making choices for many decades. A final stage is characterized by reduced mobility so that even previously mobile patients lose their ability to walk. The life expectancy for patients with RS is around 50 years (Akbarian, 2002).

3.2 MeCP2

Almost 10 years after the discovery of the first mutations in Mecp2 causing RS and 16 years after the discovery of the gene itself in the mouse genome, the exact function of the MeCP2 protein is still unknown and remains the subject of many debates and many research projects!

Medical Genetics & Functional Genomics Group,

http://www.germaco.net/intro_rett_gb.html

The *Mecp2* gene controls production of MeCP2 protein which was first identified in mice in 1992 by the group of Adrian Bird (Lewis et al., 1992). The human gene was cloned in 1996 (D'Esposito et al., 1996). Now there are three different transcripts found in human (Pelka et al., 2005) with still unclear differences in their function and distribution. MeCP2 is a member of the family of proteins able to bind to methylated DNA that represents an essential mechanism to repress transcription both in the heterochromatin and in regions which are transiently repressed. Methylation itself is not sufficient to repress the expression of a gene, but if additional proteins are recruited at these methylated sites the repression becomes possible (for a review, see Ulrey et al., 2004). MeCP2 has been initially shown to promote transcriptional repression through its binding of methyl-binding domain (MBD) to CpG dinucleotides and its subsequent recruitment by the transcription repression domain (TRD) of histone deacetylases (HDAC) that may modify the chromatin structure and make it inactive. However, MeCP2 protein is able to modify chromatin structure by histone deacetylase-independent mechanism of repression (Yu et al., 2000) or without a need in methylated DNA (Georgel et al., 2003). Another way of transcription repression mediated by MeCP2 is a blockade of binding sites for transcription factors (di Fiore et al., 1999).

Although multiple mechanisms of regulation were revealed recently in searching of MeCP2 target proteins (for further details see Table 1), it is not possible to detect massive deregulation of gene transcription when the *Mecp2* gene product is absent. MeCP2 proteins are able to regulate the promoter III of the brain-derived neurotrophic factor (*Bdnf*) gene, which is responsible for the production of a protein playing essential role both for the growth and survival of neurons (Martinowich et al., 2003; Chen et al., 2003). *Bdnf* repression by MeCP2 is a dynamic process: membrane depolarization leads to a dissociation of MeCP2 from a *Bdnf* promoter and hence to an increased *Bdnf* expression. This is accompanied by chromatin changes at this site (Nelson et al., 2006; Martinowich et al., 2003).

Mecp2 gene is ubiquitously expressed. Although early developmental stages show the low levels of expression, *Mecp2* is widely active in various types of embryonic and adult tissues and represented in different cell types. In the brain, it is found in high concentrations in the neurons and is associated with maturation of the central nervous system (CNS) being primarily involved in formation of synaptic contacts (LaSalle, 2007). A last year report (Ballas et al., 2009) showed that MeCP2 protein is also expressed in glial cells, where it was previously supposed to be absent. This raises an important issue whether glial cells in the mice lacking MeCP2 protein are responsible for neuronal defects. A large-scale mapping of MeCP2 binding sites in neurons demonstrated that only 6% of the binding sites are in CpG islands, 63% of MeCP2-bound promoters are actively expressed and only 6% are highly methylated (Lewis et al., 1992). This indicates that MeCP2 protein represents not only a global transcriptional regulator its main function is different from that of silencing methylated promoters. Modern studies demonstrate that MeCP2 acts not only as a transcriptional repressor but also as an activator for a number of genes through a recruitment of the transcription factor CREB1 (see Table 1). In fact, the majority of genes that are regulated by MeCP2 are rather activated than repressed (Chahrour et al., 2008).

Recent studies (Guy et al., 2007) showed that neurological deficits resulting from a loss of MeCP2 can be reversed upon a restoration of gene function, indicating therefore a possibility of disease reversal. The neurons suffered from the loss of MeCP2 function can potentially regain functionality once MeCP2 is provided gradually and delivered at correct places. These findings provide a hope for restoring neuronal function in patients with RS (Ogier and Katz, 2008).

Table 1. MeCP2 Target Genes (from Chahrour and Zoghbi, 2007)

MeCP2 Target Gene	Function	References
<i>Bdnf</i>	neuronal development and survival	Chen et al., 2001; Martinowich et al., 2003
<i>xHairy2a</i>	neuronal repressor	Stancheva et al., 2003
<i>DLX5/Dlx5</i>	neuronal transcription factor	Horike et al., 2005
<i>Sgk1</i>	hormone signaling	Nuber et al., 2005
<i>Fkbp5</i>	hormone signaling	Nuber et al., 2005
<i>Uqcrc1</i>	mitochondrial respiratory chain	Kriaucionis et al., 2006
<i>ID1-3/Id1-3</i>	neuronal transcription factors	Peddada et al., 2006
<i>FXYD1/Fxyd1</i>	ion channel regulator	Deng et al., 2007
<i>IGFBP3/Igfbp3</i>	hormone signaling	Itoh et al., 2007
<i>Crh</i>	neuropeptide	McGill et al., 2006
<i>UBE3A</i>	ubiquitin ligase	Samaco et al., 2008
<i>GABRB3</i>	GABA-A receptor	Samaco et al., 2008

3.3 Mouse models of RS

Mouse models (Guy et al., 2001) have set out a major breakthrough in the understanding of RS and MeCP2 function (Viemari et al., 2005; Nelson et al., 2006; Wang et al., 2006; Zhou et al., 2006; Chao et al., 2007; Stettner et al., 2007; Fischer et al., 2009). Observed similarities between RS in mice and in humans support a frequently encountered point of view (Gaultier and Gallego, 2008) that mutant newborn mice with targeted deletions of genes are a valuable research object for the development of new treatments for RS disorders in humans. Both in mice (Larimore et al., 2009) and humans (Wenk, 1997), post-mortem RS brains show a reduced overall size, a decrease in the size of individual neurons and a reduction of dendritic arborisation. At the same time there are some differences between the species discussed by Sun and Wu, 2006. In humans three different transcripts of *Mecp2* (1.8; 7.5 and 10 kb) are present and their functional significance is yet unknown. In mice at least four different transcripts of *Mecp2* have been shown to possess potential tissue-specific function in the regulation of MeCP2 protein synthesis at different ages (Pelka et al., 2005). This result makes the extrapolation of data obtained from different experimental models less obvious.

Similar to human RS patients, homozygous female *Mecp2* murine mutants are not viable whereas heterozygous females are phenotypically heterogeneous due to variable patterns of X-

chromosome inactivation. Therefore, the mayor part of research projects is focused on the effects of MeCP2 loss of function in hemizygous males (*Mecp2*^{-/y}), which are completely devoid of MeCP2. As a result males tend to be more phenotypically homogenous than female heterozygotes (see Bissonnette and Knopp, 2006; Bissonnette and Knopp, 2008; Bissonnette et al., 2007). At least five RS mouse models have been created so far (Ogier and Katz, 2008) including 1) *Mecp2*^{-/y} mice that has extended exonic deletion of the *Mecp2* gene (Chen et al., 2001; Guy et al., 2001; Pelka et al., 2006), 2) *Mecp2*³⁰⁸/*y* mice with truncation of MeCP2 protein at amino acid 308, a human RS mutation (Shahbazian et al., 2002), 3) *Mecp2*^{2Fllox/y} mice expressing a hypomorphic *Mecp2* allele (Samaco et al., 2008), and 4) *Mecp2*^{2Tg1} mice that overexpress MeCP2 protein (Luikenhuis et al., 2004). The data obtained from these models are presented on Table 2. In the third mouse model an N-terminal truncated form of MeCP2 is produced instead of the normal protein. These mice have a less severe phenotype with stereotypic forelimb movements, thus resembling a human phenotype more closely (Shahbazian et al., 2002). Human *Mecp2* is mildly overexpressed in the forth model described by Luikenhuis et al. (2004). All these models mimic different degrees of severity of the human phenotype with large deletions of the protein leading to more serious forms of the disease. Yet not all the signs of RS clearly appear in each of them. Luikenhuis and colleagues (2004) showed that a *Tau-Mecp2* transgene expressed exclusively in neurons could rescue the phenotype of *Mecp2* mutant animals which means that the phenotypes of these models are indeed due to loss of function of MeCP2, particularly in neurons. Therefore the mouse models seem to be well suited to study the molecular mechanisms underlying the disease.

3.4 RS and respiratory rhythmogenesis

Breathing dysfunction in RS has complex pattern and is highly variable among affected individuals. It depends on the personal pattern of x-chromosome inactivation and on the level of behavioral arousal. In general, the RS breathing phenotype is characterized by forced and apneustic breathing, increased occurrence of apneas, and highly unstable breathing patterns including periods of breath-holds and hyperventilation and heterogeneous breath duration (Weese-Mayer et al., 2006). *Mecp2*^{-/y} male mice develop breathing abnormalities similar to human RS; however, significant differences in respiratory phenotype exist among known strains (Ogier and Katz, 2008). The two main strains studied thus far, *Mecp2*^{tm1.1Bird} (Guy et al., 2001) and *Mecp2*^{tm1.1Jae} (Chen et al., 2001) both exhibit increased variability in breath duration and

Table 2. Phenotypic features of the five mouse models established for RS (after Roloff 2005).

Publication	Genetic modification/Strains	Phenotypic features
Chen et al., 2001	CNS-specific deletion of exon 4 by cre/loxP system with a nestin promoter B6;129- <i>Mecp2</i> ^{tm1Jae} /Mmcd B6.Cg- <i>Mecp2</i> ^{tm1.1Jae} /Mmcd STOCK <i>Mecp2</i> ^{tm1.1Jae} /Mmcd	<i>Mecp2</i> null mice (normal until ~5 weeks): nervousness body trembling pilo erection variability in breath duration and episodes of hyperventilation: hard breathing disordered breathing: alternating periods of high respiratory frequency apneas Unlike <i>Mecp2</i> ^{tm1.1Bird} mice, mean breathing frequency (and minute ventilation) is significantly increased in 5-week-old <i>Mecp2</i> ^{tm1.1Jae} null mice compared to wildtype controls by approximately 20%, similar to human RS patients (Weese-Mayer et al., 2006). At later stages: - overweight - physical deterioration - hypoactive - death at ~10 weeks - reduced brain size and weight <i>Mecp2</i> ^{+/-} females (normal for ~4 months): - weight gain - reduced activity - ataxic gait
Guy et al., 2001	Excision of exons 3 and 4 by cre/loxP system B6;129P2- <i>Mecp2</i> ^{tm1Bird} /J B6.129P2(C)- <i>Mecp2</i> ^{tm1.1Bird} /J B6.129P2- <i>Mecp2</i> ^{tm2Bird} /J	<i>Mecp2</i> null mice (normal until ~3-8 weeks): - stiff, uncoordinated gate - hind limb clasping - irregular breathing variability in breath duration and episodes of hyperventilation Male <i>Mecp2</i> ^{tm1.1Bird} null mice develop erratic breathing increased variability in the duration of the respiratory cycle alternating periods of fast and slow breathing frequencies apneas (Viemari et al., 2005). Initial breathing disturbances worsen between the first and second months and the mice eventually die from fatal respiratory arrest (Viemari et al., 2005; Roux et al., 2007; Stettner et al., 2007; Zanella et al., 2008)

		<p>apart from breathing they have:</p> <ul style="list-style-type: none"> - uneven wearing of teeth - misalignment of jaws - rapid weight loss and death at ~54 days - reduced brain size and weight - males had internal testis - <i>Mecp2</i>^{+/-} females: - inertia and hindlimb clasping after 3 months
Shahbazian et al., 2002	<p>Remature stop codon at aa 308 leaves MBD and TRD intact</p> <p>B6.129S-<i>Mecp2</i>^{tm1Hco/J} (<i>MeCP2</i>³⁰⁸)</p>	<p><i>Mecp2</i>^{308/y} mice (normal until ~6 weeks):</p> <ul style="list-style-type: none"> - first symptom is a subtle tremor when suspended by tail - tremor worsens with age - stereotypic forelimb motions and clasping when hung by tail - progressive motor dysfunction - decreased activity - kyphosis in 40% - fur oily and disheveled - spontaneous myoclonic jerks and seizures - normal brain size and weight <p><i>Mecp2</i>^{+/-} females:</p> <ul style="list-style-type: none"> - milder and variable phenotype
Collins et al., 2004	<p>Slight over-expression of human <i>Mecp2</i> from a PAC clone</p> <p><i>MeCP2</i>^{Tg1}</p>	<ul style="list-style-type: none"> - normal until ~10-12 weeks - forepaw clasping when hung by tail - aggressiveness - hypoactivity - seizures - spasticity - kyphosis - premature death
Samaco et al., 2008	<p><i>Mecp2</i>^{Flxy} mice expressing a hypomorphic <i>Mecp2</i> allele with weaker phenotypic features compare to native <i>Mecp</i></p> <p><i>Mecp2</i>^{flxy}; <i>Dlx5/6-Cre</i></p>	<ul style="list-style-type: none"> - increased weight gain, - progressive motor impairments - altered social interaction. - increased respiratory variability and apneas - no change in the mean breathing frequency

episodes of hyperventilation (Viemari et al., 2005; Ogier et al., 2007; Zanella et al., 2008). Differences in the breathing phenotypes of *Mecp2^{tm1.1Jae}* and *Mecp2^{tm1.1Bird}* mice could result either from subtle differences in the exonic deletion between the two strains or due to the fact that these two mouse strains have different genetic background. For example, the fact that C57BL/6 mice are particularly prone to spontaneous apneas from central origin (Stettner et al., 2008a; Stettner et al., 2008b) might explain why the apneic phenotype is more pronounced in *Mecp2^{tm1.1Bird}* mice, engineered on a pure C57BL/6 background, compared to *Mecp2^{tm1.1Jae}* null mice, engineered on a mixed C57BL/6, 129/sv, Balb/c background.

Breathing abnormalities usually occur in mutant newborn mice deficient in genes involved in the development and modulation of rhythmogenesis of the respiratory network. Its most important element is pre-Bötzinger complex (preBötC) identified as a kernel of brainstem interneurons that are necessary and sufficient for generating inspiratory activity translated into a stable respiratory rhythm in mammals (Smith et al., 1991). The specific mechanisms that control rhythm generation are still subject to research; nevertheless it was established that preBötC includes glutamatergic network of rhythmic neurons (Bianchi et al., 1995; Ramirez et al., 1997) that is non-NMDA receptor-mediated (Thoby-Brisson and Greer, 2008). It was proposed that the neurons endow hyperpolarization-activated cationic channels (Rekling et al., 1996; Mironov et al., 2000; Thoby-Brisson et al., 2000) and the substance P receptor neurokinin 1 (NK1) (Gray et al., 1999; Wang et al., 2001; Stornetta et al., 2003; Pagliardini et al., 2003). In addition, it was proposed that preBötC neurons coexpress NK1R and μ -opioid receptor (μ OR) (Gray et al., 1999) and show prominent tyrosine kinase B (TrkB) immunoreactivity which overlaps with the distribution of NK1R (Thoby-Brisson et al., 2003). Although most neurons in the preBötC may be not pacemakers (Del Negro et al., 2005), they can be recruited for rhythmic activity during inspiration, post-inspiration and expiration. NaP (Pena et al., 2004), CAN (Del Negro et al., 2002), and TRPM4 (Mironov, 2008) channels were proposed for the initiators of ‘synaptic drive’ promoting bursting activity. Synaptic inhibition also plays an important role in network function as it is active not only while a given neuron is ‘silent’ (e. g., during expiration for an inspiratory neuron), but also during its active phases (Ramirez et al., 2005). Thus, the activity in a pacemaker cell in preBötC is determined by its intrinsic bursting properties and the concurrently occurring inhibitory and excitatory synaptic inputs, which both can be modulated through various neurotransmitters activating various intracellular signalling pathways.

Electrophysiological investigations of the RS-induced abnormalities in neuronal activity demonstrated that RS patients exhibit numerous manifestations of cortical hyperexcitability, including a higher incidence of seizures and appearance of rhythmic slow theta activity (Ramirez et al., 2005; Ogier and Katz, 2008). In MeCP2 deficient mouse models the imbalance between excitatory and inhibitory neurotransmission was reported (Dani et al., 2005; Moretti et al., 2006). The effects were different depending on the brain region and mouse strain used for experiments. Spontaneous neuronal activity was reduced in adult cortical slices (Dani et al., 2005), as well as in a number of hippocampal excitatory glutamatergic synapses *in vivo* (Chao et al., 2007). Nelson and colleagues (2006) obtained similar results for spontaneous excitatory synaptic transmission in cell culture. Changes in synaptic plasticity and long-term potentiation in *Mecp2* null hippocampal slices were shown by different research groups (Collins et al., 2004; Asaka et al., 2006; Moretti et al., 2006). Note to say that *Mecp2* null mice reported to have an excitatory/inhibitory imbalance in the mouse brainstem, including cell groups involved in regulation of breathing (Stettner et al., 2007). This suggests that the origin of the respiratory phenotype in *Mecp2* null mice (and possibly RS patients) consists of generating breathing arrhythmias and increasing incidences of apneas. Moreover, laboratory results listed above allow one to associate upper airway-related problems in RS, including apneas with laryngeal closure and loss of speech (Budden et al., 1990), weak coordination of breathing and swallowing (Morton et al., 1997; Isaacs et al., 2003).

3.5 Neurochemistry of the brainstem respiratory network in *Mecp2* null mice

The above considerations about the state of art of the problem of the generation and modulation of respiratory activity points to importance of the analysis of protein expression and functional differences of neurotransmitter systems in the *Mecp2* null mice as a model organisms for RS research. The primary objects of interest were BDNF, biogenic amines (norepinephrine and serotonin), and the inhibitory transmitter gamma-amino butyric acid (GABA), which are all involved in respiratory rhythmogenesis and can play specific roles in neurodevelopment.

3.5.1 Biogenic amines

Norepinephrine, dopamine, and serotonin levels in the *Mecp2* null brain as a whole exhibit significant gradual decline after birth compared to wild type (WT) animals (Ide et al., 2005). In the brainstem a postnatal deficit in norepinephrine is associated with a decrease in the number of neurons among cell groups expressing the catecholamine-synthesizing enzyme tyrosine hydroxylase (Viemari et al., 2005; Roux et al., 2007). These results give an impetus to pre-clinical and clinical studies of the efficacy of increasing noradrenergic signalling for improving respiratory function in RS which are currently in progress (Ogier and Katz, 2009).

3.5.2 GABAergic signalling

Spontaneous synaptic current carried by GABA(A) receptors are suppressed in rostral ventrolateral medullary neurons in *Mecp2* null mice, but glycinergic signalling is not affected (Medrihan et al., 2008). Diminished GABAergic transmission correlates with decreased expression of both pre- and post-synaptic markers of GABA signalling indicating both decreased presynaptic levels of GABA and vesicular inhibitory amino acid transporter.

3.5.3 Second messenger signalling. ATP.

Respiration rhythm in mammals is persistently maintained to adjust continuously the concentration of vital gases in the blood. It is finely tuned to other movements such as swallowing, phonation and locomotion. On the neuronal level, the breathing is regulated through numerous neuromodulatory inputs to the respiratory network, e. g., preBötC, where the rhythmic motor output is produced. Various G-protein-coupled receptors (GPCR) are important in the slow modulation mechanisms which coordinate the rhythm generation. Muscarinic acetylcholine, tachykinin (substance P), serotonin, thyrotropin-releasing hormone (TRH), μ -opioid, α -adrenergic, and GABAB receptors differentially modulate respiratory frequency and amplitude (Murakoshi et al., 1985), possibly mediating it via cell-to-cell communication in the respiratory network. Many preBötC neurons endow different types of GPCR as demonstrated by studies of single preBötC neurons in the respiratory network (Johnson et al., 1996; Reikling et al., 1996; Gray et al., 1999; Shao and Feldman, 2000). Downstream effectors of GPCRs often converge on cAMP-PKA pathway in neurons (Wojcik and Neff, 1984; Felder, 1995; Khawaja and Rogers, 1996; Lukyanetz and Kostyuk, 1996; Oka et al., 1996; Nestler, 1997; Badie-Mahdavi et al., 2001;

Browning and Travagli, 2001; Cai et al., 2002).

Although ATP is a ubiquitous cellular energy source, it participates in some signal transduction pathways by acting as an intercellular messenger molecule itself. It is claimed (Abbracchio et al., 2009) that purinergic receptors are the most abundant receptors in living organisms and their signalling role is important in both central and peripheral nervous system. Purinergic receptors are important in functioning of the autonomic nervous system at different levels. For example, ATP is involved in the autonomic reflex pathways ranging from the transduction of sensory information to neuroeffector transmission (Gourine et al., 2009). Purinergic receptors recognise ATP, ADP or adenosine produced due to activity-dependent release of ATP from nerve terminals, axons, and glia (Fields and Burnstock, 2006).

Several studies performed in the last decade revealed multiple roles played by purinergic receptor (P2R) signalling in respiratory control. They are gated by extracellular ATP and subdivided into ionotropic (P2X₁₋₇) and metabotropic (P2Y_{1,2,4,6,11-14}) receptors (Mironov, 1995). At the periphery, P2X₂Rs on the afferent terminals of the carotid sinus nerve in the carotid body are required for the hypoxic ventilatory response (Rong et al., 2003). P2Rs are expressed in spinal and brainstem respiratory motoneurons, where their activation by ATP potentiates output of respiratory motoneurons *in vitro* (Funk et al., 1997; Miles et al., 2002). P2XRs (Kanjhan et al., 1999; Yao et al., 2000) and P2YRs (Fong et al., 2002) are also expressed throughout the ventrolateral medulla (VLM), including respiratory-related regions of the brainstem (Thomas et al., 1999; Spyer and Thomas, 2000; Thomas and Spyer, 2000; Thomas et al., 2001; Fong et al., 2002; Lorier et al., 2007). Some inspiratory and expiratory neurons increase discharge frequencies in response to ATP (Gourine et al., 2003) and therefore were declared as uniquely sensitive to ATP, but further studies showed similar sensitivity to ATP for all classes of respiratory neurons. Lorier and colleagues (2008) concluded that P2Y₁R-mediated frequency increase in activity seemingly reflects activation of a mixed cationic conductance in multiple types of preBötC neurone rather than excitation of one, highly sensitive group.

Recent use of ATP biosensor technology demonstrated a physiological role of endogenous ATP and P2R signalling in central respiratory control. Gourine et al., (2005 a,b) showed that ATP is released in response to hypercapnia or hypoxia and that the resultant activation of P2Rs on cells near the ventral medullary surface or within the *ventral respiratory column* (VRC) contributes to the hypercapnic and hypoxic ventilatory responses (Lorier et al., 2008).

3.5.4 Second messenger signalling. Ca^{2+}

Ca^{2+} is one of the most important intracellular messengers in many eukaryotic signal-transduction pathways. Calcium complexes must be kept in low concentration to prevent cell damage. This is maintained by transport systems which mediate calcium extrusion from the cytoplasm or uptake into intracellular organelles. Nevertheless, in living cells Ca^{2+} interferes with many regulatory circuits which are especially important (Berg et al., 2002). For instance, in neurons changes in $[\text{Ca}^{2+}]_i$ regulate different events from triggering of neurotransmitter release at presynaptic terminals to bursting activity. Ca^{2+} participates in rapid processes as well as in lasting for many days (Augustine et al., 2003). The characteristics of Ca^{2+} transients are shaped by Ca^{2+} influx through voltage- and ligand-gated channels, intracellular release and endoplasmic reticulum (ER) buffering. Intrinsic Ca^{2+} buffering in preBötC neurons may be limited (Alheid et al., 2002), suggesting that Ca^{2+} transients could play a particular role in generation of respiratory rhythm and origin. The contribution of Ca^{2+} and Ca^{2+} -dependent conductances to membrane potential variations in respiratory neurons has been studied both *in vivo* (Pierrefiche et al., 1995; Pierrefiche et al., 1999; Haji and Ohi, 2006) and *in vitro* (Onimaru et al., 1996; Elsen and Ramirez, 1998; Mironov and Richter, 1998). Optical imaging studies using cell permeant forms of Ca^{2+} -sensitive dyes (e.g., fura-2 and fluo-3) reveal Ca^{2+} transients during inspiration both in active preBötC neurons (Fremann et al., 1999; Koshiya and Smith, 1999; Barnes et al., 2007; Funke et al., 2007; Mironov, 2008) and in respiratory-modulated motoneurons (Ladewig and Keller, 2000).

In active preBötC neurons somatic Ca^{2+} transients occur during the inspiratory burst only as the consequence of action potentials (APs), while in the absence of APs the inspiratory drive potential was unaffected but somatic Ca^{2+} transients could not be detected (Morgado-Valle et al., 2008), suggesting that such transients do not contribute to the inspiratory drive recorded in soma, the principal determinant for generation of APs.

Imaging of somatic Ca^{2+} transients in phase with preBötC neuron inspiratory activity was used by many researches to study respiratory network connectivity, distribution, and development (Koshiya and Smith, 1999; Thoby-Brisson et al., 2005; Barnes et al., 2007; Funke et al., 2007). Ca^{2+} plays an essential role in termination of bursts of APs through activation of SK and BK K^+ channels (Richter et al., 1993). This output is supported by an observation that inhibition of BK channels reduces inspiratory burst frequency (Zhao et al., 2006) and can

increase AP duration in preBötC neurons (Onimaru et al., 2003). Single neuron Ca^{2+} imaging established that high voltage-dependent calcium channels (VGCCs) are the dominant source of somatic Ca^{2+} in rhythmic respiratory neurons (Fermann et al., 1999). Somatic Ca^{2+} signals seen in active preBötC neurons are due to somatic APs induced by the inspiratory drive potential, and not by the inspiratory drive potential per se. Somatic $[\text{Ca}^{2+}]_i$ was proved to arise due to a voltage-dependent process rather than due to a process following activation of second messenger signalling cascades that release Ca^{2+} from intracellular stores much more slowly (Morgado-Valle et al., 2008). Activation of somatic TRPM4-like channels by Ca^{2+} was proposed as the mechanism generating the inspiratory drive (Mironov, 2008). In active preBötC inspiratory neurons, somatic Ca^{2+} transients do not significantly contribute to the inspiratory drive. It was proposed that dendritic Ca^{2+} transients in preBötC neurons play critical role in determining their excitability and ultimately their contribution to rhythm generation (Mironov, 2008; Morgado-Valle et al., 2008).

Intracellular PKA, PKC, cAMP, and Ca^{2+} signalling pathways have functional significance in modulating the behavior of medullary respiratory neurons. Persistent activation of these pathways produces significant increases of excitability in medullary respiratory neurons. Neuromodulators including 5-HT, catecholamines, acetylcholine, adenosine, and opioids also act on the PKA, PKC and Ca^{2+} signal pathways to alter synaptic processes and current flow through voltage- and ligand-gated membrane channels (Champagnat et al., 1979; Pierrefiche et al., 1993; Bonham, 1995). Such receptor-mediated regulation of intracellular signal pathways may stabilize the respiratory rhythm and produce functional flexibility that is advantageous for fine tuning of depth, frequency, and pattern of breathing (Richter et al., 1997).

3.5.5 Second messenger signalling. cAMP and PKA

ATP is used as metabolite in many signal transduction processes by various kinases in phosphate transfer reactions and by adenylate cyclase (AC) to produce the second messenger molecule cyclic AMP (Alberts et al., 2002). cAMP-dependent pathway is often initiated by activation of GPCRs. Increases in cAMP lead to activation of cyclic-nucleotide-gated ion channels, exchange proteins (Epacs) or cAMP-dependent protein kinase A (PKA). PKA participates in different cellular processes through phosphorylation of cellular proteins such as ion channels and receptors that modulates neuronal excitability and excitatory synaptic

transmission through the phosphorylation of glutamate receptors (Greengard et al., 1991; Wang et al., 1991; Wang et al., 1993; Blackstone et al., 1994; Colwell and Levine, 1995; Roche et al., 1996; Traynelis and Wahl, 1997; Banke et al., 2000). For example, PKA potentiates the current induced by activation of AMPA glutamate receptors in hippocampal neurons (Greengard et al., 1991; Wang et al., 1991) via increasing the opening frequency and the mean open time of AMPA glutamate receptors (Greengard et al., 1991). This possibly occurs through PKA-mediated phosphorylation of one subunit of the pentameric AMPA receptor (Roche et al., 1996) that increases peak open probability of AMPA receptors (Banke et al., 2000). The PKA modulation of postsynaptic AMPA receptors plays a role in synaptic plasticity by modulating synaptic strength and has significant implications for network behavior in many brain structures including hippocampus, the neostriatum, and the cerebral cortex (Blackstone et al., 1994; Colwell and Levine, 1995; Kameyama et al., 1998; Lee et al., 2000; Soderling and Derkach, 2000).

PKA suppresses voltage- and calcium-gated K^+ channels that regulate duration of action potentials and afterhyperpolarizations, as well as GABAB receptor-gated potassium channels (Laurenza et al., 1989; North and Uchimura, 1989; Greengard et al., 1991; Schwartz et al., 1991; Swope et al., 1992). In the expiratory neurons these effects control persistent and synaptically-controlled K^+ outward currents and depolarizing inward cation currents (Haji et al., 1996; Lalley et al., 1997).

Enhancement of PKA activity in the preBötC increases the frequency of respiratory-related rhythmic motor output, while inhibition of PKA activity decreases the frequency. PKA activation induces a tonic inward current, increases the endogenous inspiratory drive currents, as well as the exogenous AMPA-induced currents (Shao et al., 2003). On the other hand, modulation of AMPA receptors or associated synaptic proteins through inhibition of phosphatase, which counteracts with the effects of PKA, increases respiratory frequency, as well as the excitability of individual respiratory-related neurons (Ge and Feldman, 1998). AMPA receptors are critically involved in rhythm generation (Funk et al., 1993) and it has been observed that enhancement of PKA activity potentiates the AMPA-induced current in preBötC inspiratory neurons. One can conclude that the modulatory effects of PKA on respiratory rhythm are primarily due to phosphorylation of AMPA receptors or related synaptic proteins mediating excitatory synaptic transmission (Shao et al., 2003). Another protein kinase C (PKC) depends on both intracellular calcium and diacylglycerol formed after activation of metabotropic

neurotransmitter receptors via phospholipase C (PLC), additionally enhances GABA-mediated inhibitory postsynaptic currents within respiratory neurons (Richter, 1996).

3.5.6 BDNF

BDNF is a member of the neurotrophin family of growth factors known to be involved both in long-term processes of neuronal survival (Levi-Montalcini, 1987; Davies, 1994; Lewin and Barde, 1996) and long-time potentiation (Korte et al., 1995; Patterson et al., 1996). It also participates in rapid events of ion channel activity, neurotransmitter release, and axon pathfinding (Song and Poo, 1999; Schinder and Poo, 2000; Kovalchuk et al., 2004). BDNF influences the expression of voltage-dependent conductances in both cell lines and neurons (Gonzalez and Collins 1997; Lesser et al., 1997; Oyelese et al., 1997; Sherwood et al., 1997) and modifies the intrinsic excitability of cortical neurons (Desai et al., 1999). In addition to its action as a neuronal survival factor, BDNF modulates synaptic function in newborn and adult animals in *nucleus tractus solitarius* (NTS) (Balkowiec et al., 2000), preBötC complex (Thoby-Brisson et al., 2003), Kölliker-Fuse nucleus (Kron et al., 2007a; Kron et al., 2007b) and spinal phrenic motoneurons (Baker-Herman et al., 2004), regulates synaptic plasticity (Bramham and Messaoudi, 2005; Turrigiano, 2007) and neuronal membrane conductances (Blum et al., 2002).

It has been long known that the respiratory rhythm development is severely disrupted in mice carrying a targeted deletion in the gene encoding BDNF (Erickson et al., 1996; Balkowiec and Katz, 1998). Recent experimental studies implicate an involvement of *Bdnf*, one of the identified transcriptional targets of MeCP2 (Chen et al., 2003; Martinowich et al., 2003), in the development of RS both in mice (Chen et al., 2003; Zhou et al., 2006; Ogier et al., 2007; Larimore et al., 2009) and in humans (Francke, 2006; Nectoux et al., 2008). Many of its actions are mediated by tyrosine kinase B receptors (Martinowich et al., 2003) which are proved to be expressed in preBötC (Thoby-Brisson et al., 2003). BDNF regulates respiratory rhythmogenesis by modulating activity of rhythmically active neurons in the preBötC (Thoby-Brisson et al., 2003), expressing TrkB receptors important in the generation of the respiratory rhythm (Bouvier et al., 2008). Neurons in *Mecp2* null mice showing clear signs of breathing irregularities express significantly lower levels of BDNF (Ogier et al., 2007) that may contribute to suppressed synaptogenesis (Zoghbi, 2003).

3.6 Transcription and neuronal activity

Brain development is modified by the environment through a release of neurotransmitters at specific synapses and their binding to appropriate receptors on the postsynaptic neuron. This binding induces a variety of biochemical signalling events among which is a rapid and local increase in calcium levels within the postsynaptic specialization. Depending on the cellular context, it results in a number of synapse-specific alterations: a modification of glutamate receptor subunits, an alteration of the synaptic protein function via posttranslational modifications, and a stimulation of the translation or degradation of proteins at the synapse. Together, these events lead to changes in the synaptic function (reviewed in Catterall and Few, 2008; Higley and Sabatini, 2008; and Wayman et al., 2008). Calcium influx into the postsynaptic neuron initiates local changes as well as a cascade of signalling events leading to the activation of a program of gene expression in nucleus that promotes dendritic growth, synapse development, and neuronal plasticity (Greer and Greenberg, 2008).

Numerous researchers showed that there are several hundred genes regulated by neuronal activity when synapses are forming and maturing (Nedivi et al., 1993; Altar et al., 2004; Hong et al., 2004; Li et al., 2004; and Park et al., 2006). Many of these activity-regulated genes encode transcription factors that mediate the cellular response to synaptic stimulation. They are believed to activate target genes important for cell survival, shaping, synaptic development, and synaptic plasticity. Many of them are regulated directly by neuronal activity encode proteins that act specifically on synapses to control various aspects of the synaptic development and function. These include *Bdnf* that participates in neuronal surviving; *Arc* that controls glutamate receptor endocytosis; *Cpg15* that regulates survival and dendritic growth; and *Homer1a*, which controls the formation of synaptic protein complexes (Kang and Schuman, 1995; Korte et al., 1995; McAllister et al., 1995; McAllister et al., 1997; Nedivi et al., 1998; Cantallops et al., 2000; Sala et al., 2003; Chowdhury et al., 2006; Rial Verde et al., 2006).

Neurons, being excitable cells, maintain low basal levels of intracellular calcium by pumping calcium into either ER or extracellular space. Therefore a neuron is able to respond rapidly and effectively to an increase in intracellular calcium concentration in multiple ways. Cytoplasmic calcium levels can rapidly increase in the postsynaptic neuron either by a calcium release from ER, or by an entrance of extracellular Ca^{2+} into the cytoplasm through voltage-gated calcium channels or ligand-gated ion channels. As it was shown by Jonas and Burnashev (1995)

and Berridge (1998), two types of the ligand-gated ion channels participate in this process: the NMDA or AMPA glutamate receptors. Depending on the mode of entry, quite different responses in terms of gene induction can be observed (Bading et al., 1993) although all of them lead to the significant increases in the calcium concentration. For instance, BDNF is highly induced in excitatory neurons after calcium entry through L-type voltage-sensitive calcium channels, but the response to the calcium influx through NMDA receptors or N-type calcium channels is less effective (Westenbroek et al., 1992; Ghosh et al., 1994). This variability initially led to speculation that the specific channel through which calcium enters the neuron determines the pattern of gene induction. Recent studies demonstrated that triggering a gene expression response by the calcium influx depends on a variety of features of calcium channels. The channel conductance, open time, localization of the channel, ability to trigger an increase in the calcium concentration within the nucleus, and association with key signalling molecules – all these channel properties are essential for the trigger definition. Calcium influx through NMDA or AMPA receptors or L-type VSCCs triggers the expression of new gene products via a number of signalling molecules and pathways. The later in turn modify the activity of transcription factors and, hence, the transcription of several hundred genes. The pathways that respond to calcium influx via signalling cascades induced by calcium influx include the Ras/ mitogen-activated kinase (MAPK) pathway, calcium/calmodulin-dependent protein kinases, phosphatase calcineurin, and Rac GTPases. The mechanism of biological processes affected by calcium-responsive genes on example of *Bdnf* regulation is described in Fig.1. Over 300 genes were shown to be regulated in response to neuronal activity, and each of them has a unique time course and magnitude of induction (Lin et al., 2008). *Bdnf* is one of the two genes precisely examined for such behaviour. Its transcription was preferentially activated in response to neuronal activity and hence was induced primarily in neurons (West et al., 2001). The proper balance of excitatory and inhibitory synaptic input is important for processing sensory information as well as for higher cognitive functions. An increasing number of human neurological disorders are characterized by imbalances in excitatory and inhibitory synaptic strength. Although, as was postulated by Cline (2005), the mechanism by which neuronal activity regulates inhibitory synapse development and maturation is still unknown (Cline, 2005), some researchers postulated that development and/or maintenance of inhibitory synapses was controlled by the activity-dependent gene network.

Transcriptional regulator for multiple genes, MeCP2 was shown to specifically control the

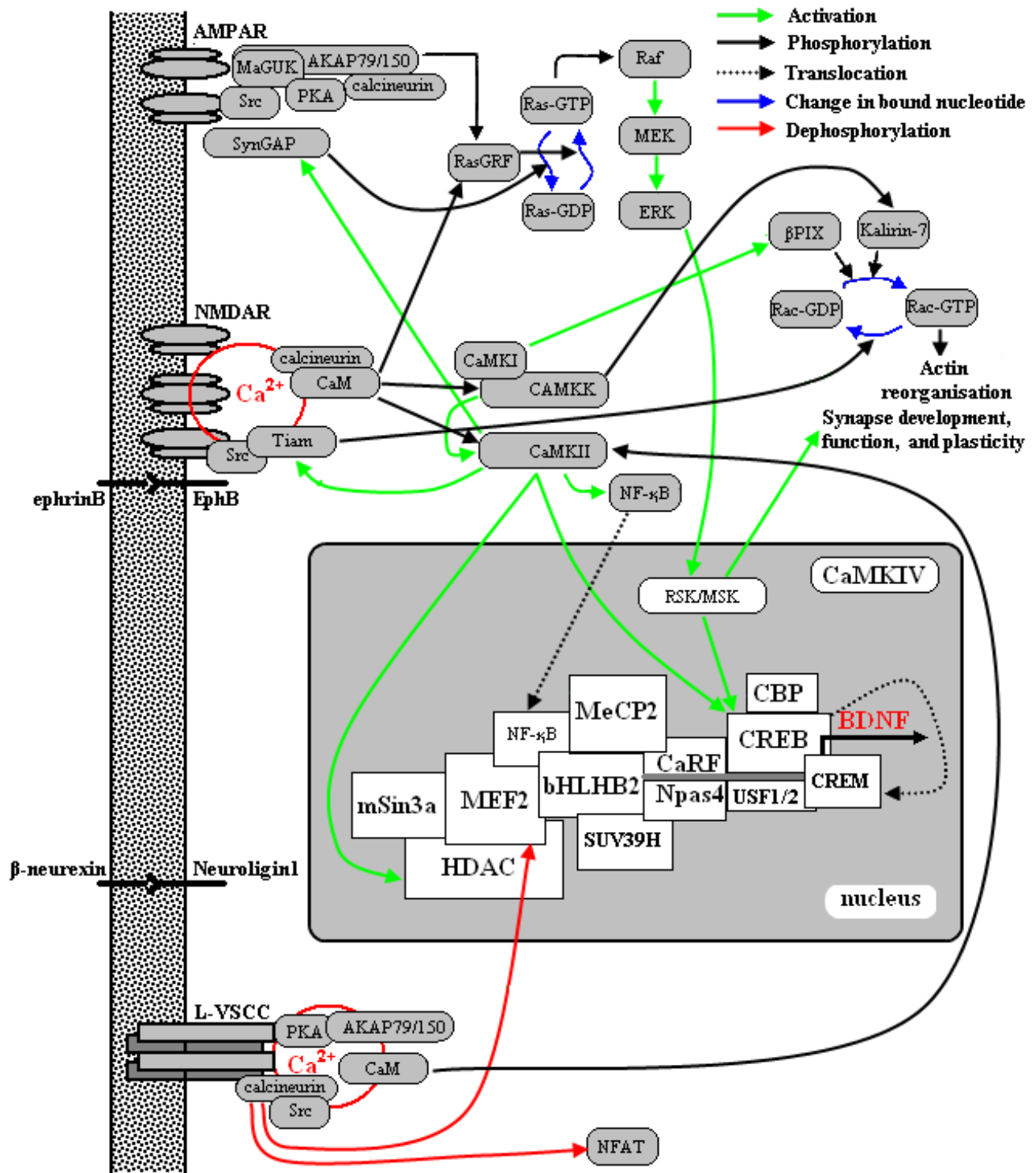


Figure 1. Signaling Pathways that Lead to Calcium-Mediated Transcription of BDNF (modified from Zieg et al., 2008)

strength of excitatory synaptic connections (Dani et al., 2005). Cortical pyramidal neurons from *Mecp2* knockout (KO) mice had reduced spontaneous synaptic activity. The data obtained from these mice allow one to assume that the alteration in excitability in *Mecp2* KO mice is due to a change in the balance of excitatory and inhibitory synaptic strength. The effects of NPAS4, MEF2, and MeCP2 on the balance between excitation and inhibition are partially explained by their ability to regulate *Bdnf* promoter IV transcription. A study performed by Hong and colleagues (2008) supports the idea that activity-dependent transcription of *Bdnf* controls excitatory/inhibitory balance. Mice with modification in *Bdnf* promoter IV transcription have similar levels of BDNF in the absence of stimulation and reduced levels of *Bdnf* promoter IV-dependent mRNA transcripts following synaptic stimulation. Notably, in these KO mice significantly fewer inhibitory synapses form on excitatory neurons, so one can suggest that activity-dependent *Bdnf* transcription plays a key role in regulating the number of inhibitory synapses (Linn et al., 2008).

During early postnatal development activity-dependent genes are highly induced and experience-dependent synaptic remodelling is peaking. This is the time when many disorders of human cognition appear. The possibility that defects in the Ca²⁺-dependent gene program are responsible for some disorders of human cognition is therefore postulated. This assumption is supported also by the evidence that mutations in a large number of the components of the activity-dependent gene program give rise to disorders of human cognition (Fig. 2).

Mutation in a number of molecules that regulate *Bdnf* transcription results in a variety of human cognitive disorders. Mutation in Ca_v1.2 transcription mechanism causes Timothy Syndrome, in RSK2 - Coffin-Lowry syndrome, in CBP - Rubenstein-Taybi Syndrome, in *Bdnf* itself - memory disturbances and psychiatric disorders, and finally mutation of *Mecp2*, an activity-regulated repressor of *Bdnf* promoter IV transcription, results in Rett Syndrome. All these mutations lead to disorders, including autism, and are first detected within first days and months of life following apparently normal early development. These symptoms arise during the period of development that is characterised by activity-dependent transcription during synaptic development (Zoghbi, 2003). Such coincidence of events raises the possibility that Rett Syndrome is a result of disturbances in activity-dependent gene transcription that depends on intracellular cascades (Greer and Greenberg, 2008).

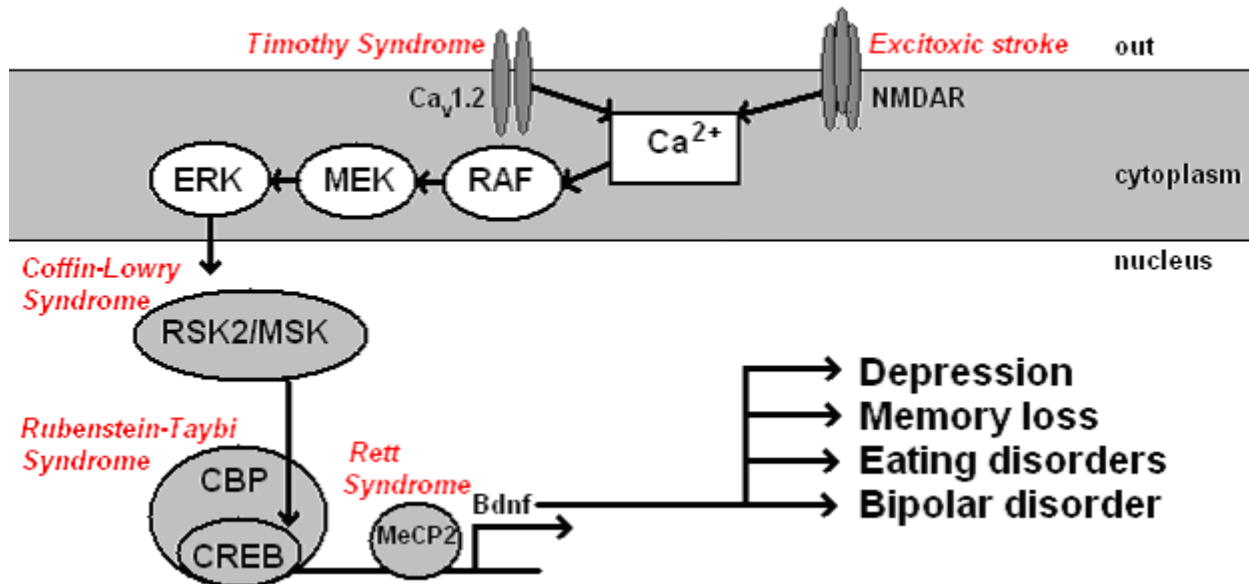


Figure 2. Mutation of components of the activity-dependent Bdnf expression program lead to human cognitive disorders (adopted from Greer and Greenberg, 2008)

As it is seen from the extended review presented above different approaches were intended lately to solve complex problem of Rett syndrome development. Mecp2 structure and functions were investigated on different levels of complexity. By now some of these aspects are pretty well revealed. Nevertheless there is not much known about processes lying in the gap between molecular composition of MeCP2 protein and changes in brain morphology as a complex network, caused by mutation in *Mecp2* gene.

This situation stimulates us to focus on physiological processes that underlie Rett syndrome development in respiratory neurons of pre-Bötzing. In this work we are interested in getting more insight in the possible mechanism that lead to higher vulnerability of the *Mecp2*^{-/-} (KO) preBötC neurons during early postnatal development. Based on the recently obtained results presented in the papers observed above we have chosen for further research two major players of intracellular signal transduction, Ca^{2+} and cAMP, both involved in various events of neuronal activity, signal transduction, excitability and plasticity.

Hereafter we use new methods to study differences in intracellular Ca^{2+} ($[Ca^{2+}]_i$) and cAMP ($[cAMP]_i$) homeostasis that lead to reorganisation of neurons in preBötC and might cause breathing irregularities.

4. Methods

4.1 Ethical approval

All animals were housed, cared for and euthanized in accordance with the recommendations of the European Commission (No. L358, ISSN 0378-6978), and protocols approved by the Committee for Animal Research, Göttingen University.

4.2 Mouse strains

Experiments were performed using the *Mecp2* null mice as a model for RS. Two lines were maintained on a C57BL/6J background. The *Mecp2* null mouse strain B6.129P2(C)-*Mecp2*^{tm1-1Bird} (Guy et al., 2001) was obtained from the Jackson Laboratory (Bar Harbor, ME, USA). B6.129P2(C)-*Mecp2*^{tm1-1Bird} mice with deleted *Mecp2* exons 3 and 4 are known to have normal development until 3-8 weeks. After approximately one month first signs of RS symptoms appear. Initial breathing disturbances became worse between the first and second months and the mice eventually die from fatal respiratory arrest (Viemari et al., 2005). All mice were genotyped in accordance with the Jackson Laboratory genotyping protocols described by Stettner and colleagues (2007). Studies were carried on hemizygous males because individual differences in X-inactivation pattern among heterozygous mice can result in variability in phenotype. Hemizygous mutant *Mecp2*^{-/y} males (denoted hereafter as KO mice) were generated whereas MNRI males were crossed with heterozygous *Mecp2* +/- females. The mice were examined blind and the data were then assorted into the two pools - the knock-outs and wild type (WT) – determined by their genotype.

4.3 Cell culture

Experiments were performed on neuronal cultures of brain stem containing functional respiratory network of mice. Preparations were made at postnatal day P3-P5. Animals were decapitated at the C3-C4 spinal level, the brain was isolated and placed in ice-cold artificial cerebrospinal fluid (ACSF) saturated with 95% O₂, 5% CO₂. ACSF contained 128 mM NaCl, 25 mM NaHCO₃, 1 mM NaH₂PO₄, 3 mM KCl, 1 mM MgSO₄, 10 mM glucose, and 1.5 mM CaCl₂. The brainstem was fixed by acrylic glue and sliced serially with a vibrotome from rostral to caudal direction until the beginning of preBötC was reached. The rostral boundary of the pre-

Böttinger complex is indicated by anatomical marks such as the *inferior olive* (IO), nucleus *tractus solitarii* (NTS), *hypoglossal nucleus* (XII), and *nucleus ambiguus* (NA) and by disappearance of the *facial nucleus* (Ruangkittisakul et al., 2006) as presented in Fig. 3. For isolation of preBötC neurons, a single thick transverse slice (650-750 μm) was cut and preBötC region was isolated by sucking into a large (ca. 1 mm inner diameter) bore fire-polished glass pipette. The piece of tissue was dispersed and trypsinised (1% trypsin, 0.25% EDTA, 5-10 min). The cell suspension was placed on poly-D-lysine-coated 18 mm glass coverslips in the D-MEM solution contained 85% of D-MEM (GIBCO, INVITROGEN), horse serum, 1% of Penicillin/Streptomycin, 15 mM of KCl, 1 mM of Na-pyruvate and 2 mM of L-glutamine. After the cells settled down in 4-well plates containing coverslips, the preparation was placed in the CO₂-incubator. Next day the medium was changed to Neurobasal-A medium (GIBCO, INVITROGEN), with B-27 supplement, L-glutamine, and Penicillin/Streptomycin and every second day afterwards.

Experiments were usually performed from 5 to 10 days *in vitro* (DIV). Coverslips with cultured neurons were mounted in the experimental chamber on a microscope table and the neurons were continuously perfused with warm ACSF.

Data were collected only from viable cells, i.e., from cells showing intracellular calcium increases in Fluo-3 or Fura-2-stained after short challenges to membrane depolarisations elicited by application of 50 mM K⁺ (high-K⁺). The time of solution exchange was less than 1 second. High-K⁺ solution was prepared by exchanging equivalent amount of Na⁺ in ACSF.

4.4 Organotypic culture

For the preparation of organotypic culture we used 250 μm -thick brainstem slices which contained preBötC (see above). Mice were prepared at P2–P4 and P18–P20 (denoted hereafter as P3 and P19, respectively). The preparation itself and all further manipulations were conducted on ice in ACSF solution saturated with 95% O₂ and 5% CO₂. After preparation the slices were placed on support membranes. Neurobasal-A medium (1 ml) was added so that the surface of the slice was continuously exposed to the incubator gas mixture, and balance between respiration and nutrition was achieved. We found that the organotypic slice cultures survived best in the culture medium containing 50% MEM with Earle's salts, 25 mM HEPES, 6.5 mg/ml glucose, 25% horse serum, 25% Hanks solution buffered with 5 mM Tris and 4 mM NaHCO₃, pH 7.3. This medium

was changed every other day. Maintenance of the slice on the boundary between medium and humidified carbonate atmosphere in a thermostat under conditions mentioned above allowed us to increase the life-time in the culture to up to 2 months without significant changes in viability or morphology.

The morphology of neurons from WT and KO mice was examined in groups at an interval of 1 week starting from P14. Approximately equal numbers of neurons from the respective groups were measured in parallel. All data were acquired and analysed blinded to genotype. Each test in this study was repeated with at least four different preparations and the mean data were obtained by analysing responses of 6–12 neurons in the image field. After performing the experiments, the slices were fixed and the immunocytochemical analysis was made to reveal NK1 putative receptors as described below. For the immunocytochemical experiments the surrounding membrane was removed, slices were fixed on the 18 mm glass coverslip with acrylic glue (Loctite 401) and mounted in the experimental chamber on a microscope table and immobilized with silicon Basilone-paste 35 (GE Bayer) in order to avoid accidental movements during imaging.

4.5 Immunofluorescence

Transverse brainstem sections containing the respiratory kernel (Ruangkittisakul et al., 2006) were examined in the presence of specific receptors using the antibodies to the tachykinin receptor 1 (TACR1) also known as neurokinin 1 receptor (NK1R) or substance P receptor (SPR). This G protein coupled receptor is abundant in neurons of the ventral respiratory group (Gray et al., 1999; Wang et al., 2001). NK1 receptor was proposed to endow specifically preBötC neurons for the following reasons: 1) immunohistochemical labelling for NK1R co-stains the population of glutamatergic respiratory neurons within the preBötC; 2) injection of Substance P, a putative NK1R ligand, into the preBötC markedly increases the respiratory frequency, and 3) a targeted destruction of NK1R-positive preBötC neurons with a toxic complex Substance P – aporin disrupts the rhythmic motor output *in vivo* (Gray et al., 1999; Gray et al., 2001; Manzke et al., 2003; Stornetta et al., 2003; McKay et al., 2005;). Based on these observations, it is proposed that the subset of preBötC neurons expressing NK1R can play a crucial role in the rhythm generation.

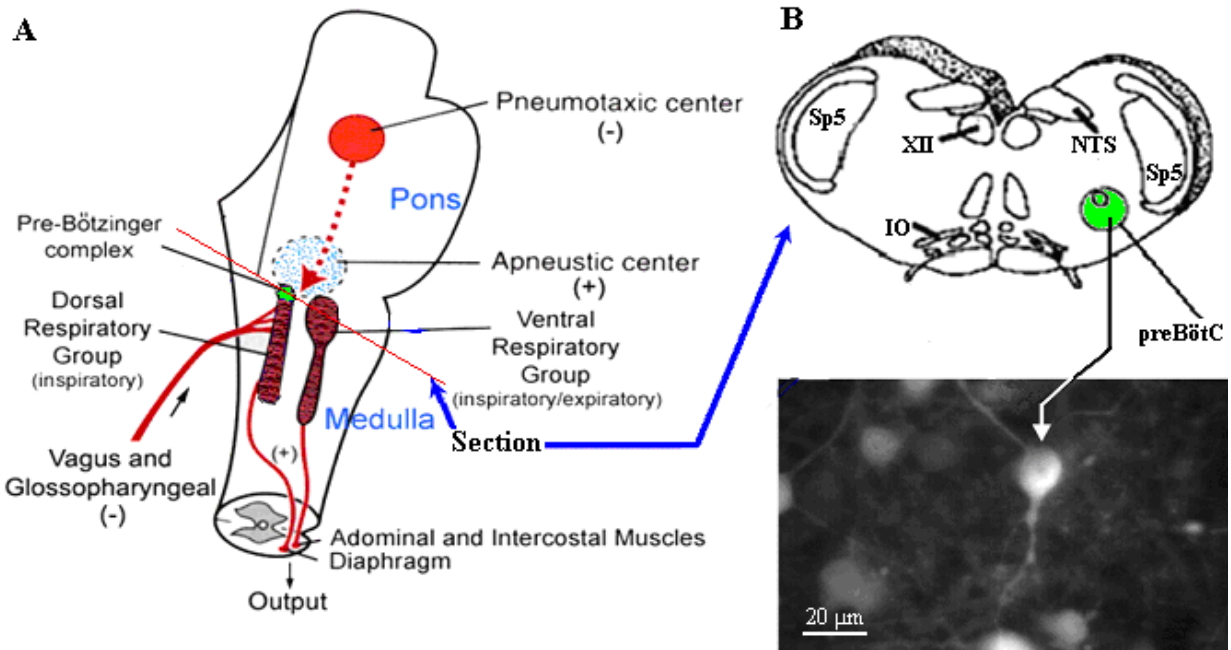


Figure 3. Anatomical localisation of preBötC in mouse brain stem.

(A) Schematic drawing of a rostrocaudal section of the brain stem area, corresponding to the border between medulla and pons. PreBötC marked with green (modified from Lynch). (B) Schematic drawing of transverse section of the brain stem corresponding to preBötC. XII – *Hypoglossal nucleus*; IO – *Inferior olive*; Sp5 – *Spinal trigeminal tract*; NTS – *Nucleus tractus solitarius*. PreBötC marked with green. (C) Representative image of a spontaneously active neuron from preBötC region stained with fluo-3.

For immunocytochemistry slices of the organotypic brainstem culture were fixed with 4% phosphate buffered formaldehyde (PFA). After a removal of the supporting membrane, the slice was permeabilized with 0.2% Triton X-100 for 30 min at room temperature (RT) and washed two times with phosphate buffer saline (PBS; pH 7.4). Non-specific binding was blocked with PBS containing 5% bovine serum albumin (BSA) for 1 h at RT. After washing three times with PBS (10 min each), the slices were incubated for 6 h at RT or, alternatively, 24–72 h at 4 °C with the primary rabbit anti-NK1R antibody solution (Chemicon; 1:200 in 2% BSA/PBS) followed by three cycles of washing for 15 min each. Slices were incubated for 4 h at RT in darkness with secondary Alexa 555-conjugated donkey antirabbit IgG antibodies (Molecular Probes; 1:500 in 2% BSA/PBS) followed by extensive washing (three cycles, 30 min each). For the examination the slices were placed on microscope slides and covered with fluorescent mounting medium (DAKO). Neuronal immunofluorescence analysis was performed with a confocal laser-scanning microscope (Meta-LSM 510, Zeiss, Germany) using the wavelengths 488 nm (Ar/Kr laser) and 543 nm (He/Ne laser). The overlay of two channels from confocal images (2048×2048 pixels) was merged using Zeiss software and imported into Adobe Photoshop CS2.

4.5.1 Sensors

Calcium imaging was performed with commercially available chemical sensors (fura-2 and fluo-3 from Molecular Probes) and genetically encoded indicators (D3cpv, designed in the lab of Roger Tsien, see chapter 4.5.3 for further details). After loading the neurons with a sensor protein or expressing the protein indicator, the fluorescence was excited at appropriate wavelength and collected using Zeiss Axioscop microscope, captured by a CCD Andor iXon camera (ANDOR, Offenbach).

4.5.2 Chemical indicators

For imaging of intracellular calcium, 10 μM fluo-3/AM or 3 μM fura-2/AM were added to ACSF as the aliquot of DMSO-based stock solution. The staining mixture was sonicated and slices were incubated with the dye for 20 min at 37 °C, followed by a 30 minutes-long wash-out to allow deesterification of ester precursor. Spectra of excitation and emission for these Ca²⁺ sensors and reporter proteins are presented in Fig. 4. Fura-2 was excited at 350 and 380 nm, fluo-3 was excited at 470 nm and the emission of either dye was collected at 535 nm. Exposure times

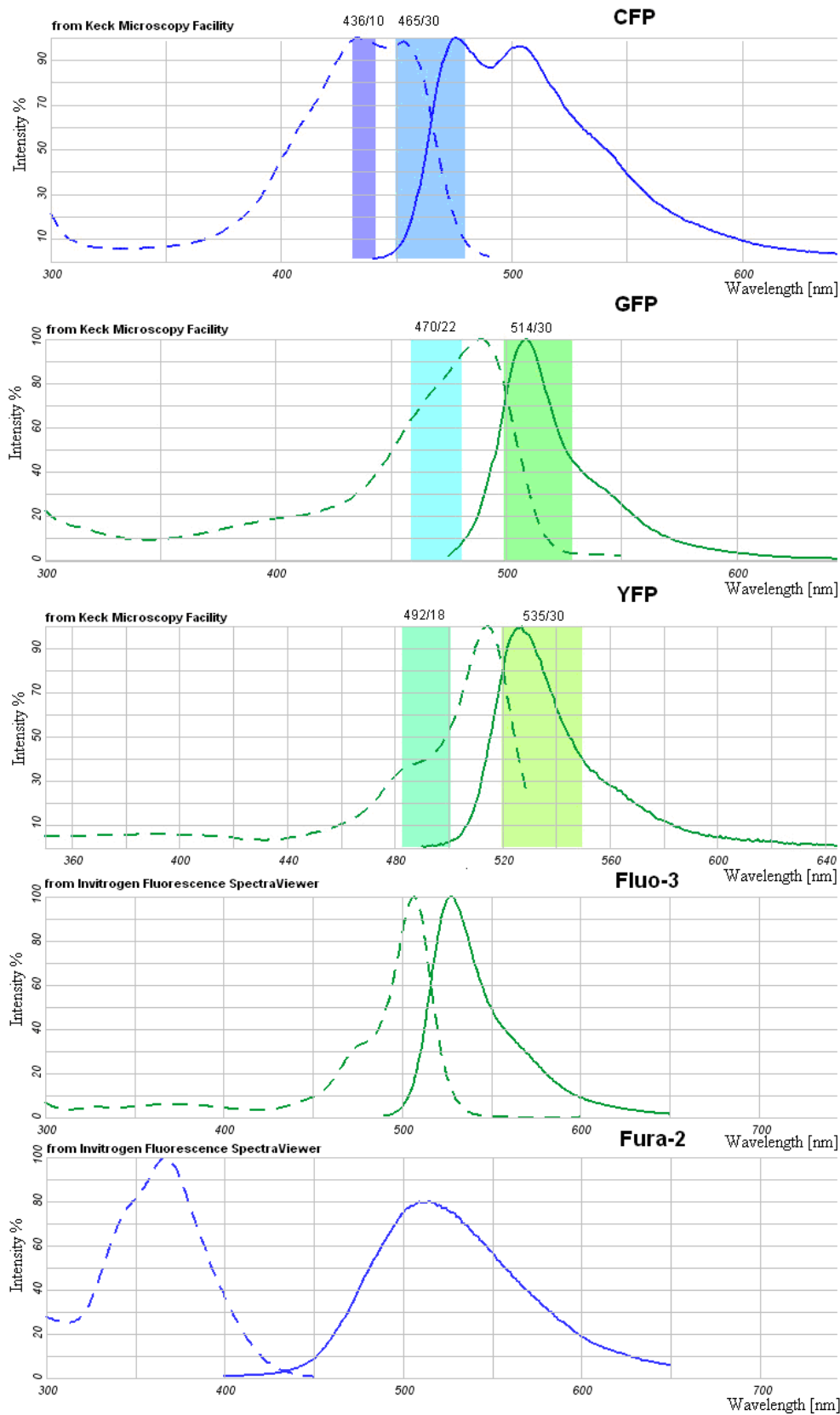


Figure 4. Spectra of excitation and emission for the Ca^{2+} sensors and reporter proteins.

ranged from 300 to 500 ms and the frames were collected every 1 s and analyzed off-line using MetaMorph software (Universal Imaging Corporation, West Chester, PA, USA). $[Ca^{2+}]_i$ increases were estimated from fluo-3 changes and from fura-2 ratios as described previously (Mironov and Hermann, 1996; Mironov and Langohr, 2005). Calcium changes were induced by applying membrane depolarisation with high- K^+ (5 to 10 s), calcium release with 1 mM ATP (10 s), chemical hypoxia with application of KCN (200 μ M 2 to 3 min), or evoking calcium release from internal stores (ER, 1 μ M thapsigargin (Tg), and mitochondria 1 μ M CCCP). All testing solutions were produced by adding aliquots of corresponding stock solutions directly to perfusing ACSF.

4.5.3 Genetically encoded calcium indicators

Calcium sensors are fluorescent proteins derived from green fluorescent protein or its variants (GFP, YFP, CFP), fused with calmodulin (CaM) and the M13 domain of the myosin light chain kinase, which binds CaM. Genetically encoded indicators are produced within cells after their transfection. We used calcium sensor D3cpv designed in the lab of Roger Tsien (Palmer et al., 2006; Palmer and Tsien, 2006; Wallace et al., 2008). In order to obtain a neuron-specific transduction (Kügler et al., 2003; Shevtsova et al., 2005), the sensor was embedded into a recombinant adeno-associated virus (AAV) vector. For transduction, we applied 1 μ l of AAV solution ($\approx 1 \times 10^9$ viral genomes) directly at the surface of the slice. The expression of D3cpv was detectable two days after transduction, reached a steady state after four to six days, and then remained constant over six weeks. D3cpv was excited at 430 nm by the LED (20 mW, Roithner Lasertechnik) generated light. Corresponding signals were separated with Optosplit (BFI Optilas, Puchheim) using dichroic mirror (495 nm) and 470 ± 12 and 535 ± 15 nm filters. Free calcium levels were obtained by rationing the emission of cyan fluorescent protein (CFP) at 470 nm to FRET signal between CFP and yellow fluorescent protein (YFP; emitted at 535 nm). Images were captured by a cooled CCD iXon camera (ANDOR, Offenbach) and collected with ANDOR software (500 x 500 pixels at 12 bit resolution). Fluorescence signals were analysed offline with the MetaMorph software (Universal Imaging Corporation, West Chester, PA, USA). Cytoplasmic calcium levels were evaluated from ratios of FRET and CFP signals (R) using the formula first derived for fura-2 (Grynkiewicz et al., 1985).

$$[\text{Ca}^{2+}]_i = K_d \frac{R - R_{min}}{R_{max} - R}. \quad (1)$$

The dissociation constant $K_d = 0.6 \mu\text{M}$ was taken from Palmer et al., 2004 and the values of $R_{min} = 1$ and $R_{max} = 80$ were determined from calibration experiments with ionomycin (Palmer and Tsien, 2006). D3cpv has better technical characteristics than fura-2 not only because it is selectively expressed in neurons, but also due to a broader range on Ca^{2+} dynamic detection (0.6–6 mM) and greater resistance to photobleaching. This allows one to perform continuous imaging of the cells for about 1 h without significant deterioration of fluorescence signal.

4.5.4 Genetically encoded cAMP indicators

For cAMP imaging we used the sensor derived in the lab of Martin Lohse (Nikolaev et al., 2004), namely Epac1-camps. It was excited at 430 nm with light generated by an LED (20 mW, Roithner Lasertechnik). Structure and emission spectrum of Epac1 fusion protein are presented in Fig. 5. Values of $[\text{cAMP}]_i$ were obtained from the ratio of Epac1-camps fluorescence (R) excited at 430 nm and emitted at 535 nm (FRET) and 470 nm (CFP). Calibration of cAMP levels *in vivo* using membrane-permeable 8-Bromo-2'-O-methyl-cAMP (BrOMecAMP), a specific activator of Epac (Kang et al., 2003) presented in Fig. 6B. Measured changes in ratio R were well fitted with the Michaelis–Menten–like equation

$$R = \frac{R_{max}C}{K_d + C}, \quad (2)$$

where C is the concentration of nucleotide and K_d is the dissociation constant for Epac1-camps (Fig. 6B). In estimating R_{max} we accounted for the basal $[\text{cAMP}]$ level by making a calibration after suppressing AC activity with DDA (see Results, page 87). Absolute cAMP levels were obtained as

$$C = \frac{K_d R}{R_{max} - R}. \quad (3)$$

The basal $[cAMP]_i$ was $0.49 \pm 0.03 \mu M$ ($n = 16$) whereas all $[cAMP]_i$ observed changes were well below $5 \mu M$ (Tables 3 and 4) indicating that the probe has an optimal dynamic range for cAMP imaging in neurons. One can see from Eqs. (2) and (3) that $[cAMP]$ is approximately proportional to the measured ratio for $[cAMP]$ levels which are less than K_d of the sensor ($1.5 \mu M$, see below). Since this condition is not satisfied automatically, presentation of $[cAMP]$ changes in the ratio form may show erroneous kinetics.

Using previously described procedures (Nikolaev et al., 2004) we calibrated Epac1-camps protein *in vitro*. Briefly, HEK293 cells were transfected with Epac1-camps. Cells were washed three times and resuspended in 5 mM Tris, 2 mM EDTA, pH 7.4 buffer 24 h after transfection. At the next step disruption with an Ultraturrax device for 40 s on ice and 20 min centrifugation at 80000 rpm was performed. Fluorescence emission spectra of the supernatant (excitation at 436 nm, emission range 460 - 550 nm) were measured with a fluorescence spectrometer LS50B (Perkin Elmer Life Sciences) before and after adding various concentrations of cAMP and a specific activator of Epac BrOMecAMP (Biolog Life Science Institute, Bremen, Germany). The concentration of fluorescent Epac1-camps protein was 50 nM. Ratios of FRET/CFP were calculated by dividing the peak emission intensities at 524 nm (FRET) and 477 nm (CFP) and analyzed using Origin 6.1 (Origin Lab Corporation, Northampton, MA, USA). The use of emission wavelengths with wider slits (such as set up in Optosplit) gave similar ratios. The curves for BrOMecAMP *in vivo* and *in vitro* were identical. They were close to the dose-response curve obtained for sensor in slices. K_d values *in vivo* and *in vitro* were 1.6 and 1.5 μM for BrOMecAMP, respectively, and 1.2 μM for cAMP.

4.5.5 Simultaneous calcium and cAMP imaging

During simultaneous calcium and cAMP imaging, we were concerned with possible contamination of the recorded fura-2 signal by CFP fluorescence from Epac1-camps which can be potentially excited by UV (Harbeck et al., 2006). Two pairs of Epac1-camps (470 and 535 nm emission at 430 nm excitation as presented in Fig. 5), and fura-2 signals (535 nm emission at 350 and 380 nm excitation) recorded during the stimulation with high- K^+ are demonstrated in Fig. 6C. Imaging of cells which were not loaded with fura-2 demonstrated that excitation of CFP at 380 nm produces the fluorescence at 535 nm that is only $10 \pm 2 \%$ ($n = 24$) of that recorded at 430 nm excitation. This estimation is in good agreement with the excitation spectrum of Epac1-camps *in*

vitro (Nikolaev et al., 2004). The two lowermost traces presented in Fig. 6C show the effect of such bleeding of Epac1-camps fluorescence into the fura-2 channel. Offline subtraction of 15 % Epac1-camps signal (Ex 430 nm, Em 535 nm) from the signal recorded in fura-2 channel (Ex 380 nm, Em 535 nm) does not change the traces significantly.

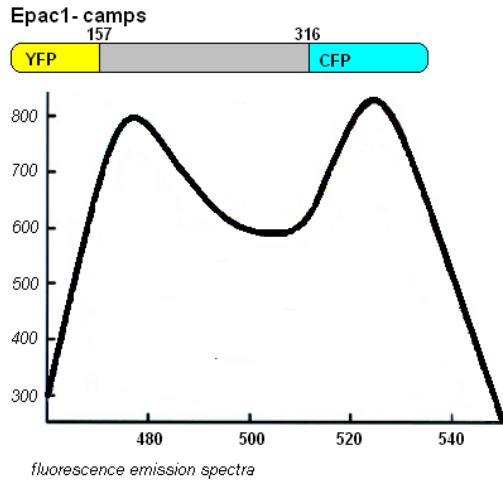


Figure 5. Structure and emission spectrum of Epac1 fusion protein (adopted from Nikolaev et al., 2004).

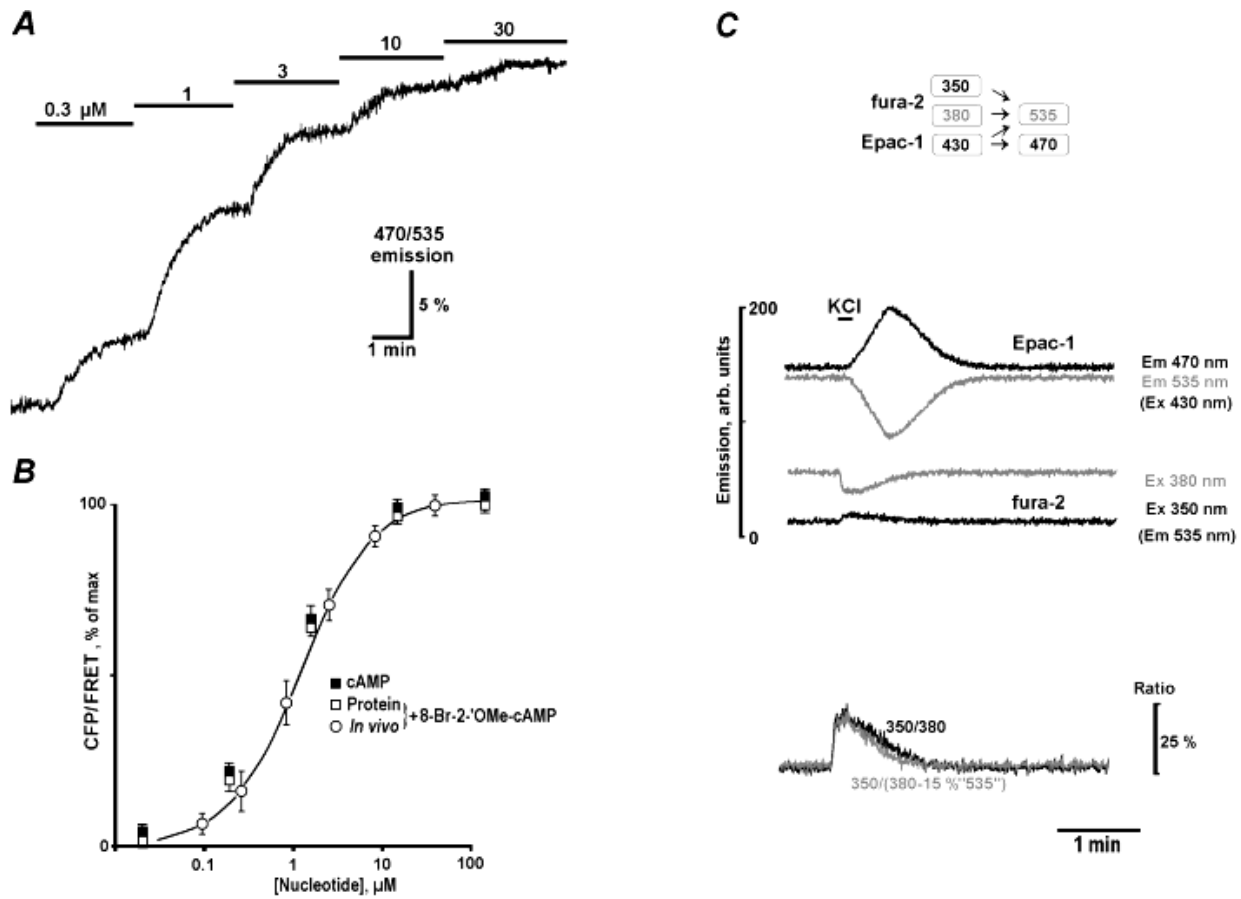


Figure 6. Calibration of cAMP levels in neurons (from Mironov et al., 2009b).

(A) Increases in 470/535 nm emission ratio during sequential addition of specific membrane-permeable Epac agonist 8-Bromo-2'-OMe-cAMP. (B) Calibration of Epac-1-camps. Mean ratios \pm S. E. M were obtained for 8-Bromo-2'-OMe-cAMP *in vivo* and *in vitro*, and for cAMP *in vitro*. The data are plotted against nucleotide concentration and the smooth curve is drawn according to the Michaelis – Menten-like equation with $K_d = 1.5 \mu\text{M}$. (C) Typical Ca^{2+} -dependent changes in [cAMP] after membrane depolarisation. The raw traces of Epac-1-camps emission at 470 nm (CFP) and 535 nm (FRET) excited at 430 nm and of fura-2 emission at 535 nm excited at 350 and 380 nm as indicated. The lower two traces demonstrate changes in the fura-2 ratio at excitation wavelengths 350 and 380 nm and changes obtained after subtraction of 15 % of Epac1-camps signal (Ex 430 nm, Em 535 nm) from fura-2 signal (Ex 380, Em 535 nm).

4.6 Transduction of neurons

Adeno-associated virus of the mosaic serotype 1/2 was constructed as described (Shevtsova et al., 2005; Kügler et al., 2007). The vector genome consisted of AAV-2 inverted terminal repeats flanking the neuron-specific human synapsin1 gene promoter (Kügler et al., 2001); EGFP, the woodchuck hepatitis virus posttranscriptional regulatory element (WPRE) for enhanced transgenic expression and a bovine growth hormone polyadenylation site (Fig. 7). This virus demonstrates greatly enhanced transduction of neurons in primary culture and was thus chosen for gene transfer into living slice cultures (Shevtsova et al., 2005).

The slices were transduced at 3 to 6 DIV, when they acquired a flattened form and became more transparent, and when cells damaged during dissection, de- or regenerated. For transduction, we applied 1 μ l of AAV solution (1×10^9 viral genomes) directly to cover only the slice surface. When AAV diffused into the slice, expression of EGFP became detectable after 24 h. It reached maximum 5 to 7 days after transduction and remained stable thereafter. The slices were taken into experiments at the times corresponding to about P12–P18 *in vivo*. We noticed no significant differences in the functional properties of the slices within this life span.

All chemicals used for transduction were from Sigma (Deisenhofen) and the fluorescent probes were from Molecular Probes (Leiden, Netherlands). Each test in this study was repeated with at least four different preparations.

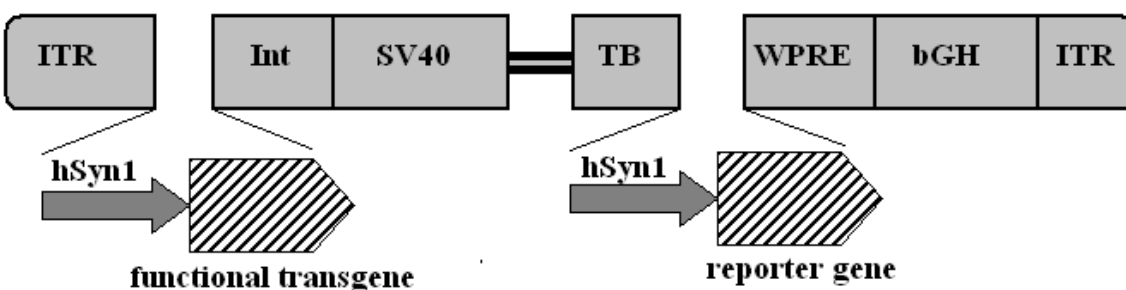


Figure 7. Structure of AAV vector (after Shevtsova et al., 2005).

ITR – Inverted terminal repeats of AAV-2; Int – 146 bp chimeric intron; SV40 – Simian virus 40 derived polyadenylation site; WPRE – Woodchuck hepatitis virus post-transcriptional 3'-control element; bGH – 3'-control element - bovine growth hormone derived polyadenylation site; hSyn1 – Short human synapsin-1 gene promoter; Reporter gene – Independent expression cassette for green fluorescent protein (EGFP).

4.7 Patch clamp

Ion channels are known to mediate a controlled passage of ions through the membrane that underlies many forms of cell communication. Specialised structure within channel pores allow them to switch between open and closed state, determined by intrinsic properties of the channel protein which can in turn be changed by various intracellular signaling pathways. The channel behavior is controlled either chemically (ligand-gated channels) or electrically (voltage-gated channels in excitable cells). However, the basic pattern is the same for any type of channel: when the gate opens, the current flows across the membrane; it stops when the gate is closed.

Despite these properties of ion channels were foreseen, the confirmation was acquired only after introduction of patch-clamp method representing a unique tool to examine properties of single ion channels. Openings and closings of the channel produce two different current levels that correspond to two membrane conductances. The probability of opening of the channel (which is a function of the number of openings and their duration) depends on the control mechanism which is determined by intrinsic properties of the channel protein and cell potential itself. These factors can be changed while representing a cellular reaction to various physiologically relevant processes.

In our studies we examined ATP sensitive potassium (K-ATP) channels that are abundant in neurons and other cells (Richter et al., 1993). Their opening probability directly depends on the intracellular ATP/ADP levels. It means that they are directly coupled to the metabolic state of a neuron to its electrical activity. K-ATP channels were described and characterised in the respiratory neurons (Mironov et al., 1998; Haller et al, 2001) and their physiological role in glucose sensing (Yamada and Inagaki, 2002), brain hypoxia (Mironov et al., 1998), and chronic neurodegenerative diseases (Liss and Roeper, 2001; Soundarapandian et al., 2001) are well established.

Patch-clamp recordings were performed on 5-10-days-old cultured neurons and 4-14 days old organotypic slices under visual control. Coverslips were placed in a perfusion chamber of a microscope with a continuous flow of ACSF. Perfusion was maintained by a cassette pump coupled with water heating system that maintained a constant temperature 34 °C in the experimental chamber. Pipettes were manufactured from a borosilicate glass capillars (Clark Instruments, Pangbourne, UK) using horizontal micropipette glass puller. Their tip openings had diameter of 1.5–2 µm and resistances of 1.5–2.5MΩ. The electrodes were filled with intrapipette

solution contained 140 mM D-gluconic acid, 0.5 mM CaCl₂, 1 mM MgCl₂, 10 mM HEPES, 1 mM NaCl, 1 mM EGTA and 1 mM Na₂ATP, with pH adjusted to 7.4 with KOH.

When approaching the cell, a gentle pressure was applied to prevent the tip from incidental contact with the cell or cell debris. For the gigaseal formation, the electrode was centred above the chosen cell and a gentle sucking was applied to stimulate the formation of a gigaseal (generally with resistance higher than 2 GΩ) in cell-attached recordings. The whole-cell mode was obtained by rupturing the plasma membrane.

K-ATP channels were measured in the cell-attached mode at a range of holding potential from 0 to -50 mV together with the action potentials indicating the activity of the cell. Intracellular signals were amplified through an EPC-7 patch-clamp amplifier (ESF, Friedland, Germany) as described previously (Mironov et al., 1998). They were filtered at 3 kHz (-3 dB) by L/M-PCA amplifier (E.S.F, Friedland, Germany), digitized and transmitted with Pulse program (Acquisition interface LIH 1600 by HEKA Elektronik) and stored for further off-line analysis. Single-channel data measured in a cell-attached mode were presented with the inverted currents, i.e., their values were assumed to be the difference between the value inside and outside the cell, according to conventional definitions of voltage and current directions in the neuron.

All patch-clamp data were primarily analyzed in QuB program (Version 1.4.0.2. The State University of New York, Buffalo, NY, USA) using principles of Markov model. Long-lasting single channel recordings were splitted to sequence of 2s intervals that were analyzed separately. Obtained parametras of each interval such as number of channel openings, probability of open state and mean duration of open state were transferred into Excel (Office XP Professional, Microsoft Deutschland GmbH, Unterschleißheim, Germany) for further statistical analysis. Data with action potentials were analyzed separately, while in that case we were interested only in number of events. Based on these calculations three time intervals of the same length vere chosen for further analysis and mean data from these intervals were obtained. Graphs and diagrams were plotted in Matlab and Excel based upon these values.

5. Results

In our electrophysiological study we used primary cultures of both cerebellum granule cells and preBötC neurons. These areas of brain are thought to be involved in the RS development and appear to be preferentially affected from the standpoint of both neuropathology and clinical signs (Oldfors et al., 1990; Murakami et al., 1992). The most characteristic aspects of RS-based changes in these areas should be connected with specific neuronal dysfunctions of cerebellum and preBötC involved the control of motor reflexes and rhythmogenesis. To unravel possible differences in neuronal network activity in the mouse RS model, we examined patterns of channel and neural activities. In what follows, we describe the effects of modulation of K-ATP channels in cerebellum granule cells and preBötC neurons via G-protein coupled receptors (ATP), neurotrophins (BDNF), as well as regulation of action potentials in the spontaneously active neurons in cerebellum and in preBötC and in particular their changes during development. The results obtained in isolated cells in the primary neuronal culture of cerebellum and preBötC were then complemented by studies of the organotypic slices, which more close correspond to the native nervous tissue.

5.1 ATP-dependent potentiation of K-ATP channels

Most single-channel recordings were made at the -20 mV holding potential that would roughly correspond to channel activity at rest. All recordings were made in the cell-attached mode, as described above in section 4.7 “Methods”. Application of ATP induced in both cerebellum and preBötC neurons gave rise to two effects: 1) fast activation followed by 2) slow inhibition of channel activity. The former was indicated by an increase in the probability of channel opening (Fig. 9A traces 2, 3) and attained its maximum in the interval of 10 to 30 s after ATP was introduced into the bath medium (Fig 9B, phase 2, Fig. 9 C). This short activation was then replaced with the inhibition of the channel activity which developed slowly and was long-lasting (Fig. 9 B, phase 3). The ATP-induced decrease in K-ATP channel activity (Fig. 9A trace 6) emerged 40 s after the application and the initial levels of channel activity were achieved only after washing out ATP for 10 to 15 s (Fig. 9A trace 4). Repetitive applications of ATP to the same cell induced smaller effects (Fig. 9A trace 5), but the time to recover from inhibition increased from about ~20 s to no recovery at all. This effect likely reflected certain underlying

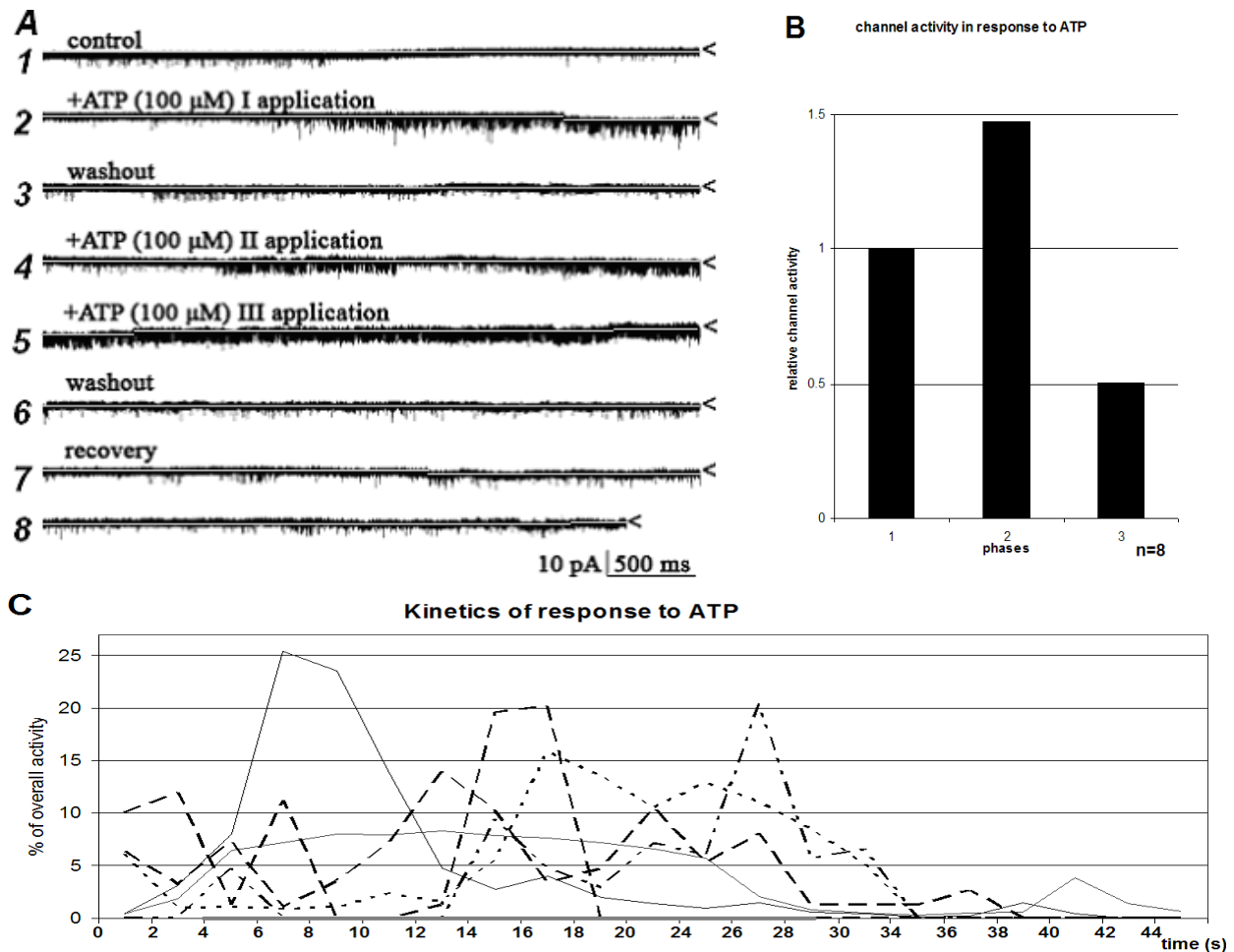


Figure 9. ATP-dependent modulations of the activity of K-ATP channels.

(A) Cell-attached patch clamp of cerebellum granule cell demonstrated ATP-induced changes in K-ATP channel activity. Initially active cell (1) treated with ATP (2) showed increase in channel activity (2, 3). Enhanced response of the same cell to the second exposure to ATP (4, 5) was fully reversible. Recovery developed after approx. 10 minutes of washout (6). Traces (7, 8) represents slowly-developing effect of ATP-based inhibition. Closed state of the K-ATP channel referred to a “<” sign. (B) Mean number of events (e.g. K-ATP channel openings) on each stage of developing effect demonstrated ATP-induced changes in K-ATP channel activity. Mean number of events in intact cells was referred to 1. Phase 1 illustrated mean initial activity of cells, phase 2 referred to mean activity at a stage of fast activation, phase 3 – to mean activity at a stage of slow inhibition of the channels. (C) Distribution of channel activity during the time demonstrated that most peaks of activity arised during interval of 25s (marked on x axis with grey). This fact allowed us to define time intervals for further analysis (phase 1, 2, 3). Number of all events during whole period of observation was defined here as 100%. . Experiments have been performed under -20mV of holding potential.

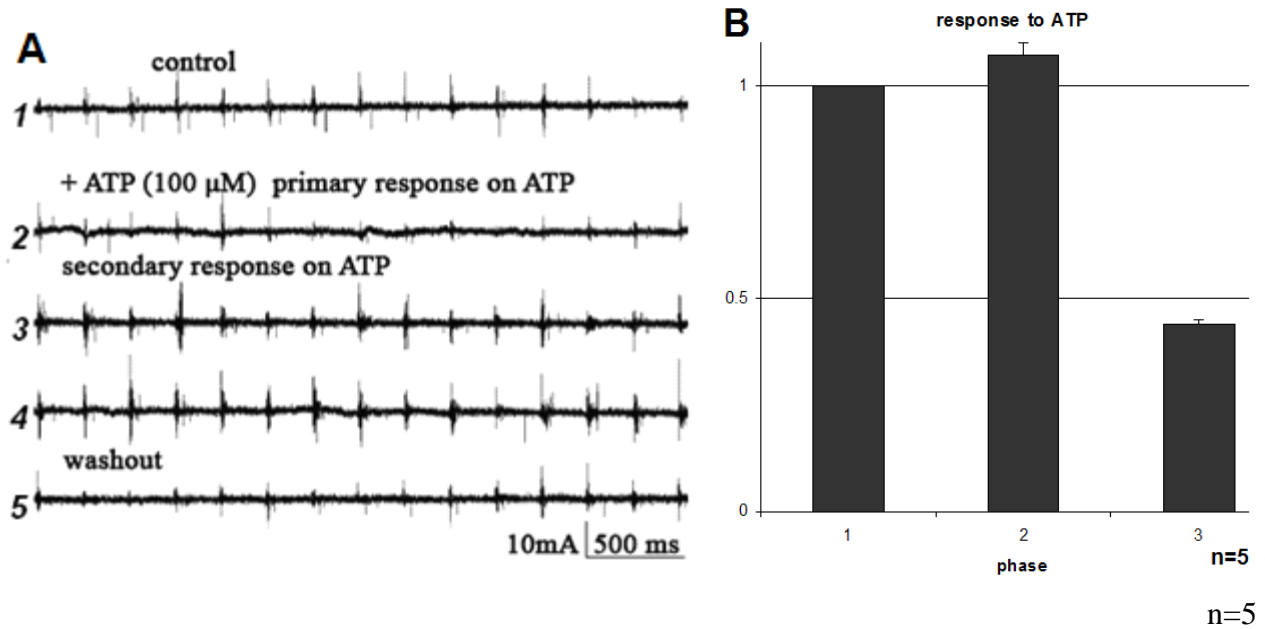


Figure 10. ATP-dependent modulations of APs activity.

(A) Actipon potential frequency is modulated by ATP in spontaneously active respiratory neuron from preBötC. Intact cell that spontaneously generates APs (1) exhibited primary effect of ATP application with the decrease in the number of spikes during the interval (2). Secondary, longer-developed activating effect of ATP application (3, 4) was followed by suppressed activity of spontaneously active cell (5). Constant frequency is typical for respiratory pacemaker cell. Experiments have been performed under -20mV of holding potential. (B) Mean number of APs on each phase of developing effect demonstrated ATP-induced changes in bursting activity of spontaneously active cells. Mean number of APs per second before ATP was added to the medium was referred to 1. Phase 1 illustrated mean initial activity of cells, phase 2 referred to mean activity at a stage of ATP-dependent activation, phase 3 – to mean activity at a stage of slow inhibition.

biochemical processes which developed slowly and were fully activated after several applications of ATP (Fig. 9A trace 7). However, the two subsequent applications of ATP were found to be reversible.

5.2 ATP-dependent modulation of action potentials

Patch-clamp recordings in cell-attached mode allow one to record the action potentials showing the patterns of intrinsic neuronal activity. Application of ATP to spontaneously active preBötC neurons and bursting cerebellum granule cells induced specific changes in their activity. The burst frequency was not changed by ATP, but the number of spikes per burst decreased (Fig. 10 A) and 30 s after adding ATP into the medium a clear depression of neuronal activity was observed indicating a slowly-developing inhibition effect (Fig. 10 A, B).

5.3 BDNF modifies activity of K-ATP channels

Next we examined the effects of BDNF, a neurotrophin that plays an important role in the development of Rett Syndrome. Its application to the neurons also produced two different effects on K-ATP channel activity: 1) fast-developing activation that took place during the first 2 minutes after BDNF had been added into the medium and 2) slowly developing inhibition that lasted up to 30 minutes. Fast BDNF dependent activation both in cerebellum and preBötC neurons was a result of an increase in the open probability of the channel (Fig.11A, B). Such potentiation developed about 1 min after BDNF addition and lasted for about 20 to 30 s (Fig. 11A, trace 2, Fig 11B, phase 2); after that a repression of channel activity was observed (Fig. 11A, trace 3, Fig 11B, phase 3). A decrease in the channel activity was manifested by an appearance of long-term closures (Fig. 11A trace 4) that reached the maximum after about 2 min and lasted for 5 minutes. Washing out BDNF for 10 to 30 minutes relieved the inhibition. The main effect was a steady disappearance of the long closures of the channel accompanied by an increase in the channel open time. Notably, a decrease in the lengths of closures resulted in the irregular pattern of channel openings (Fig. 11A, trace 6). A partial recovery took about 20 minutes; however, after 50 minutes of washout the long-lasting periods of inactivation were still present. Such events were not typical for “naïve” cells which had not been subject to BDNF before.

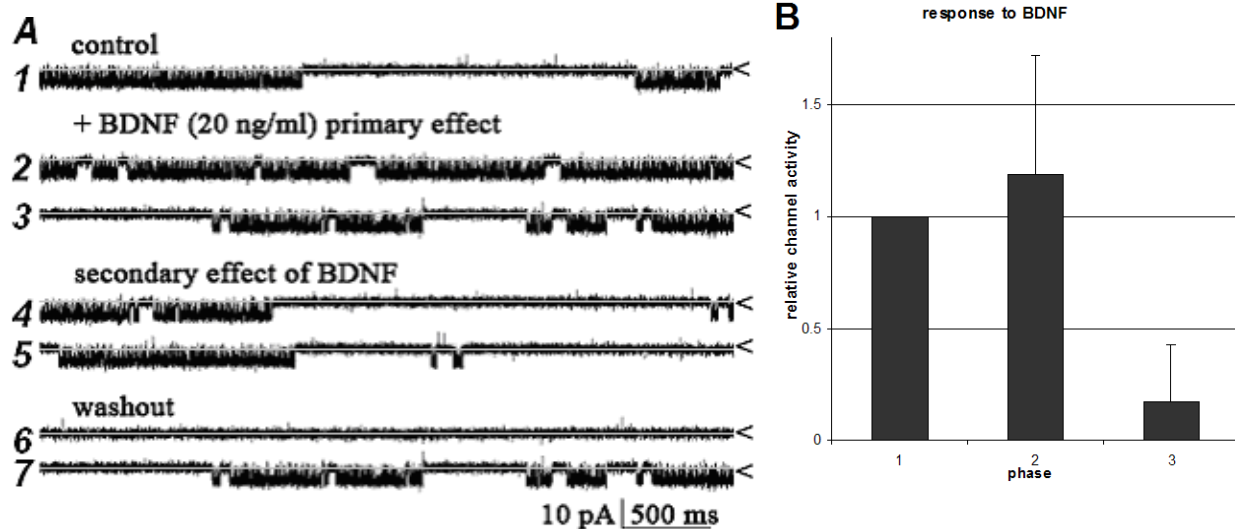


Figure 11. Modification of the K-ATP channel activity by BDNF.

(A) Recording of cell-attached patch clamp represents BDNF dependent modulation of the activity of K-ATP channel of granule cell from cerebellum. Initial K-ATP channel activity (1) is changed to the fast-developing BDNF-based activation of the channel (2) with decrease in inactive periods and increased number of opening per second. Activation of K-ATP channel (2) substituted by long-developing effect of inhibition (3), long silencing periods arise. Development of BDNF-based inhibition (4) results in the long-term inhibition (5) with continuous silencing periods (6). Full recovery (7) takes place after 20 minutes of washout. Closed state of the K-ATP channel refers to a “<” sign. Experiments were conducted under -20mV of holding potential. (B) Mean number of K-ATP channel openings on each stage of developing effect demonstrated BDNF-induced changes in K-ATP channel activity. Mean number of channel openings in intact cells was referred to 1. Phase 1 illustrated mean initial activity of cells, phase 2 referred to mean activity at a stage of activation, phase 3 – to mean activity at a stage of inhibition of the channels. Time intervals that were analysed as phase 1, phase 2 and phase 3 were defined by the same algorithm as for ATP-induced effect. . Experiments have been performed under -20mV of holding potential.

5.4 BDNF modulates excitability of granule cells and preBötC neurons

Spiking neurons of the primary neural culture were incubated with BDNF for at least 5 minutes to reveal BDNF-dependent modification of the APs development. Whole-cell recordings showed fast temporary increase in the frequency of action potentials (Fig. 12A trace 2, recorded at -50 mV of holding potential, Fig. 12C phase 2). This effect developed for 20-40 s (Fig. 12D) and then led to the transformation of burst activity into tonic activity within next 3-5 minutes (Fig. 12A trace 3, Fig. 12C). At the same time depression of action potentials was clearly seen (Fig. 12A traces 4, 5). This reduction of signalling activity was irreversible in 90% of cases. In less than 10% cases the initial level of activity was retained, although the origin of spikes was different. APs were not coupled as it was seen for the intact cells of the primary culture (Fig. 12A traces 5, 6). This allows us to speculate upon the possibility of a BDNF-dependent desynchronization of the spontaneous activity. BDNF-based effect on spontaneously active cells developed from the same origin in both cell cultures (Fig. 12B). In case of initial organisation of APs in bursts in preBötC neurons, effect of desynchronization was seen much more obvious (Fig. 12B traces 4, 5). In this case continuous washout was not efficient, because partial desynchronization remained even in 60 minutes after BDNF removal (Fig. 12B trace 6). This suggested that neurons producing bursts of APs (mainly respiratory neurons of preBötC) were more sensitive to BDNF. The latter suggestion had been proved by the previously obtained data from rhythmic slices (Thoby-Brisson et al., 2003; Bouvier et al., 2007) showing higher sensitivity of preBötC neurons to incubation with BDNF.

5.5 Interactions between ATP and BDNF signalling pathways

Since ATP and BDNF produce similar biphasic effects on channel activity, next we examined the crosstalk between the underlying pathways. The agents were sequentially applied in the same and reverse order and the resulting patterns of channel activity were examined. Addition of ATP to granule cells of cerebellum in the presence of BDNF did not change the pattern and time-course of the effect on channel activity. At the same time the open probability of K-ATP channels slightly increased that might result from complimentary actions of ATP and BDNF. The long closures characteristic for the effect of BDNF application were present, but the increase in

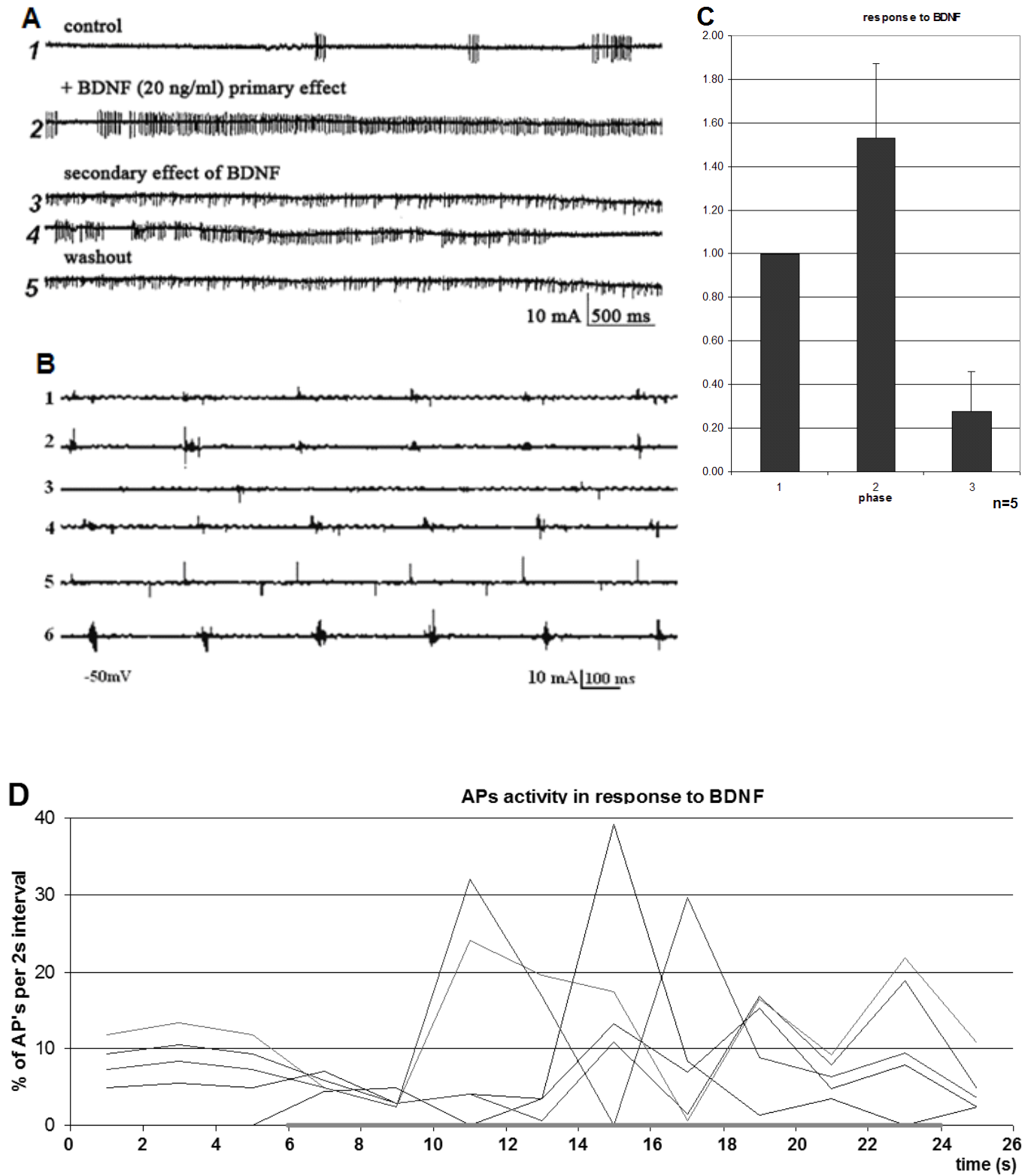


Figure 12. Modification of the Aps activity by BDNF.

(A) BDNF dependent modulation of excitability of granule cells (1) with fast-developing activation of spontaneous activity (2) substituted with tonic activity (3). 4, 5 – Slowly-developing augmentation of action potentials (3, 4) and desynchronization of currents develops in the end of incubation period (4, 5) was not fully reversible. After 60 minutes of washout action potentials are still inhibited (6), no bursts of spikes can be seen, desynchronization still persists. Experiments were conducted under -50mV of holding potential. **(B)** BDNF-based modulation of APs of the spontaneous active (1) neuron from preBötC. Spikes are grouped in bursts and the activity of the cell is enhanced during 20 s after addition of BDNF which is referred to the fast activation (2). Fast-developed activation is substituted by slowly-arising inhibitory effect (3, 4). Note uncoupled currents appearing after 40 s (4, 5). The lowermost trace (6) demonstrates partial desynchronization still remaining after 60 minutes of continuous washout. Experiments were conducted under -50mV of holding potential. **(C)** Mean number of APs on each phase of developing effect demonstrated BDNF-induced changes in activity of spontaneously active cells. Mean number of APs before BDNF was added to the medium was referred to 1. Phase 1 illustrated mean initial activity of cells, phase 2 referred to mean activity at a stage of BDNF-dependent activation, phase 3 – to mean activity of the cells at a stage of slow inhibition. **(D)** Distribution of AP activity during the time demonstrated that most peaks of activity developed during interval of 18-20s after BDNF was added (marked on x axis with grey). This fact allowed us to define time intervals for further analysis (phase 1, 2, 3). Number of all events during whole period of observation was defined here as 100%.

the open probability was evident due to an increase in the number of opening events during the periods of high activity (Fig. 13A traces 4 and 3 respectively, Fig. 13C traces 4 and 2). Although the short-time activity of the K-ATP channels seemed to enhance dramatically, an overall increase in channel activity was not appreciably augmented due to the existence of long closures in the presence of BDNF (Fig 13E). This indicates that the long-term BDNF modulation of the K-ATP channel persists even when the channel activity is seemingly recovered. On the other hand, in the presence of ATP the time-course of the BDNF effect was clearly different from the one observed in the naive cells (Fig 13F). However, although the pattern of the response was the same, the response to BDNF was developed about 60% faster (Fig. 13F).

The changes in neuronal responses to BDNF and ATP were modified after pre-incubation with cholera toxin (CT, 50 ng/ml 3.5-5.5 h), blocking GTPase-activity of inhibitory G-protein. They are coupled to adenylate cyclase and through this blockade adenylate cyclase becomes permanently activated that leading to elevation of cAMP. The experiments performed together with Sebastian Gliem (ENI rotation) demonstrated that after a pretreatment with the toxin, the number of channel openings and the open state probability decreased almost twice (from 4.1 – 21.5% to 1.4 – 1.8% per second). It is plausible that the changes in ATP-mediated effects arise from the selective inhibition of signal transduction between P2Y receptors and G-proteins. Since CT also modified the response to BDNF, the BDNF-dependent modulation of K-ATP channels can be also attributed to modification of G-protein / P2Y-receptor interplay. This complements the previous conclusion that in preBötC cAMP increase suppresses activity of K-ATP channels that in turn reinforces the respiratory motor output (Mironov et al., 1999).

5.6 The electrophysiological study of *Mecp2* null mice

Modulation of K-ATP channel and neuronal activities by ATP and BDNF in cerebellum granule and preBötC cells were qualitatively similar. In *Mecp2* null mice the activity of K-ATP channels was much reduced (Fig. 14B). This effect is manifested by distinctly lower probability of opening. The activation of K-ATP channels leads to membrane hyperpolarization and enhances stability of the resting state (“a decreased vulnerability”, Yamada et al., 2001; Allen and

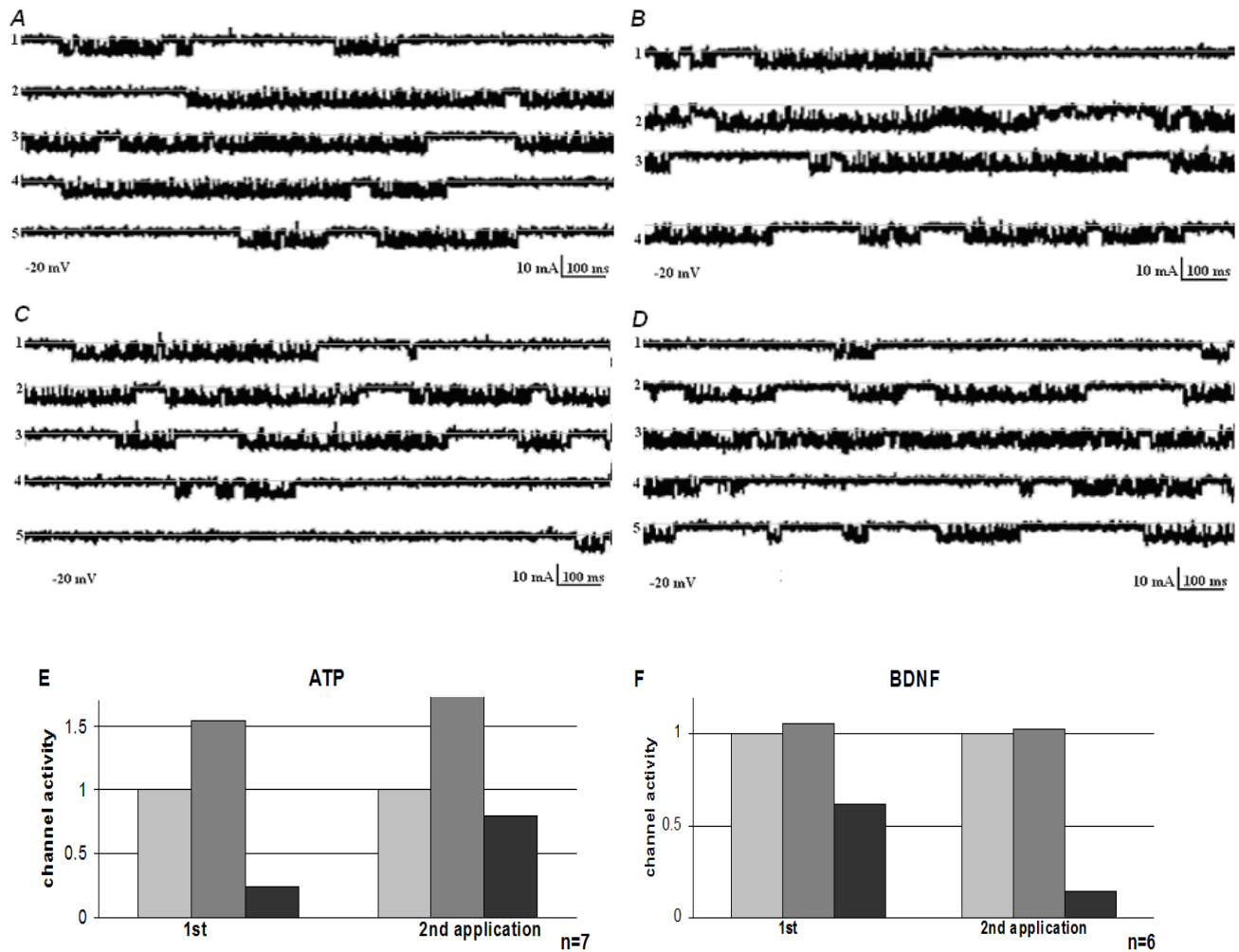


Figure 13. Differences in channel responses during multiple applications of ATP and BDNF.

Four applications of either ATP or BDNF on the same cell under the same holding potential of -20 mV are demonstrated. Grey line refers to the closed state of the channel. **(A)** Primary application on cerebellum granule cell (1). Incubation with BDNF represented typical combination of fast activation (2, 3) and slow augmentation (4, 5) due to developed periods of silence. **(B)** Secondary application of ATP resulted in the overlapping effects: periods of silence still remained (1, 3) but the activity of the channel increased (2, 3). **(C)** BDNF application on the same cell demonstrated slightly enhanced effect of both activation (1, 2) and inhibition (4, 5) of channel activity. Periods of silence were much longer (3, 4) and developed faster than during the first application. **(D)** ATP-dependent activation of the same cell resulted in the change in the kinetics of response. Period of ATP-dependent activation was longer (2, 3, 4, 5) even though it was overlapped with inhibitory effect of BDNF (long pauses at traces 4 and 5) period of ATP-dependent activation lasted longer than those for the single incubation with ATP. Panels **(E)** and **(F)** presented comparison of effect of primary and secondary application on number of channel openings. Mean number of events before reagent was added to the medium was referred to 1. Phase 1 marked with light grey illustrated mean initial activity of cells, phase 2 (dark grey) referred to mean activity at a stage of BDNF-dependent activation, phase 3 (black) – to mean activity of the cells at a stage of slow inhibition. Intervals corresponding to phases were defined based on the origin of first application.

Brown, 2004). This means that *Mecp2* $-/-$ neurons should possess an enhanced excitability as compared to the wild-type neurons. Such differences may underlie intrinsic disturbances in calcium and cAMP homeostasis in *Mecp2* $-/-$ neurons as described below. Notably, after pretreatment with exogenous BDNF K-ATP channels in the *Mecp2* $-/-$ neurons showed activity which was close to that observed in the wild-type (Fig. 14C).

Patch-clamp recordings performed in organotypic brainstem slices showed that both ATP and BDNF elicited the effects similar to those observed in the primary culture of preBötC neurons. This substantiates the results of detailed investigations of K-ATP channels in culture suggesting common operating mechanisms. The only difference between the effects in slices and in culture was the time-course of the responses that can be attributed to a slower delivery of the drugs to the bulk of the slice. The increased vulnerability of *Mecp2* null neurons due to weaker activity of ‘protective’ K-ATP channels may influence the development of synapses. The positive effects of BDNF indicate that the improper development and disorders, caused by low concentration of BDNF in both cerebellum and brain stem (preBötC), responsible for locomotion and respiratory rhythm generation, respectively, can be compensated. Thus the subcellular effectors of BDNF, e.g., K-ATP channels, intracellular calcium, and cAMP highlight the new targets for Rett Syndrome therapie.

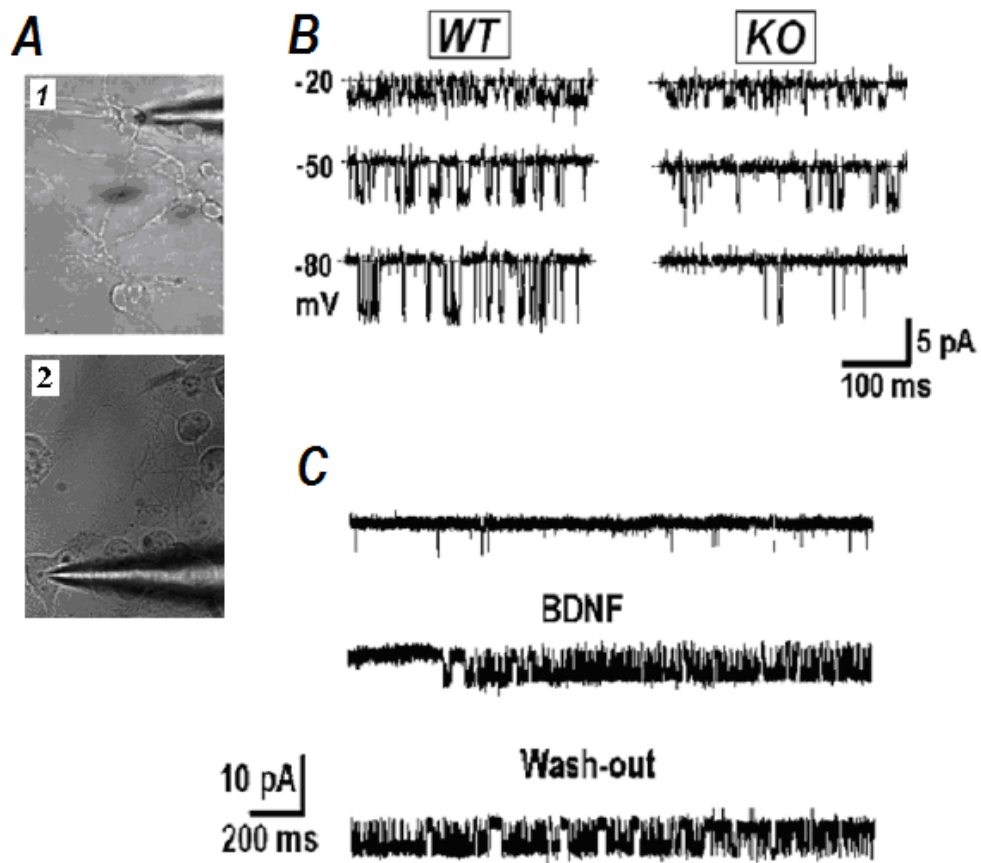


Figure 14. Appearance, channel activity, and BDNF-dependent potentiation of the *Mecp2* null neurons.

(A) *Mecp2* $-/-$ neurons from preBötC (1) and from cerebellum (2) in culture. (B) Decreased activity of K-ATP channels in preBötC neurons from *Mecp2* $y/-$ mutant. (C) Long-term potentiation of channels after application of BDNF (20 ng/ml for 5 min). Note that potentiation persisted 10 min after BDNF was washed out. The data indicate decreased expression of K-ATP channels in the KO cells that can underlie enhanced excitability in ‘Rett’ mice and its apparent correction by BDNF.

5.7 Distorted topology of the network in preBötC in model Rett mice

Neuronal organisation and function of cerebellum and brain stem are severely distorted in Rett syndrome. The changes develop in humans within first 6 to 18 postnatal months that corresponds to about 2 postnatal months in mice. Many factors participate in neurodevelopment and their actions frequently involve specific changes in the concentration of two second messengers, namely calcium and cyclic AMP, which regulate underlying processes either up- or downstream. We therefore examined the mechanisms of calcium and cAMP homeostasis and how they were related to neurodevelopment in Rett Syndrome using a model *Mecp2* null mice. We tested whether BDNF was able to correct the disturbances in calcium and cAMP regulation.

A low-resolution (x10) image of a transverse brainstem slice transduced with neuron-specific fluorescent Ca^{2+} -sensor D3cpv is shown in Fig. 15A. It demonstrates the organisation of neurons in the transverse slice and location of preBötC and other anatomical markers. At higher resolution (x40) fine details of neuronal processes are revealed (Fig. 15B, C). Images that were obtained using selective expression of calcium sensor in neurons sharply contrast with those obtained by bulk loading of slices with conventional calcium probes such as fura-2 (Hartelt et al., 2008), which are blurred leaving only neuronal somata visible. In contrast, the D3cpv sensor completely filled the interior of neurons after expression with only slight regional variations that allowed us to perform analysis of network wiring. The images were thresholded to produce contiguous masks of neurons (see the insets in Fig. 15B). The wiring diagrams within network were generated by applying the algorithms described previously (Hartelt et al., 2008). In the preparations of organotypic slices of preBötC from the WT mice, the morphology of neurons and their organisation was not changed significantly within the first two postnatal months. On the contrary the network in KO mice was apparently reorganized during this period of time, namely, the number of neurons and connections decreased as compared to those in WT. Such changes in the organisation of the network during the first month are presented in Fig. 15C. Already at P14 (that corresponds to 11 DIV in a preparation made at P3) these values were significantly smaller and the differences between WT and KO became even greater at later examination times. KO neurons had smaller dimensions (mean diameter was 14.1 ± 1.2 vs. 19.2 ± 1.4 μm at P28, $n = 64$, $P < 0.05$), that, among other

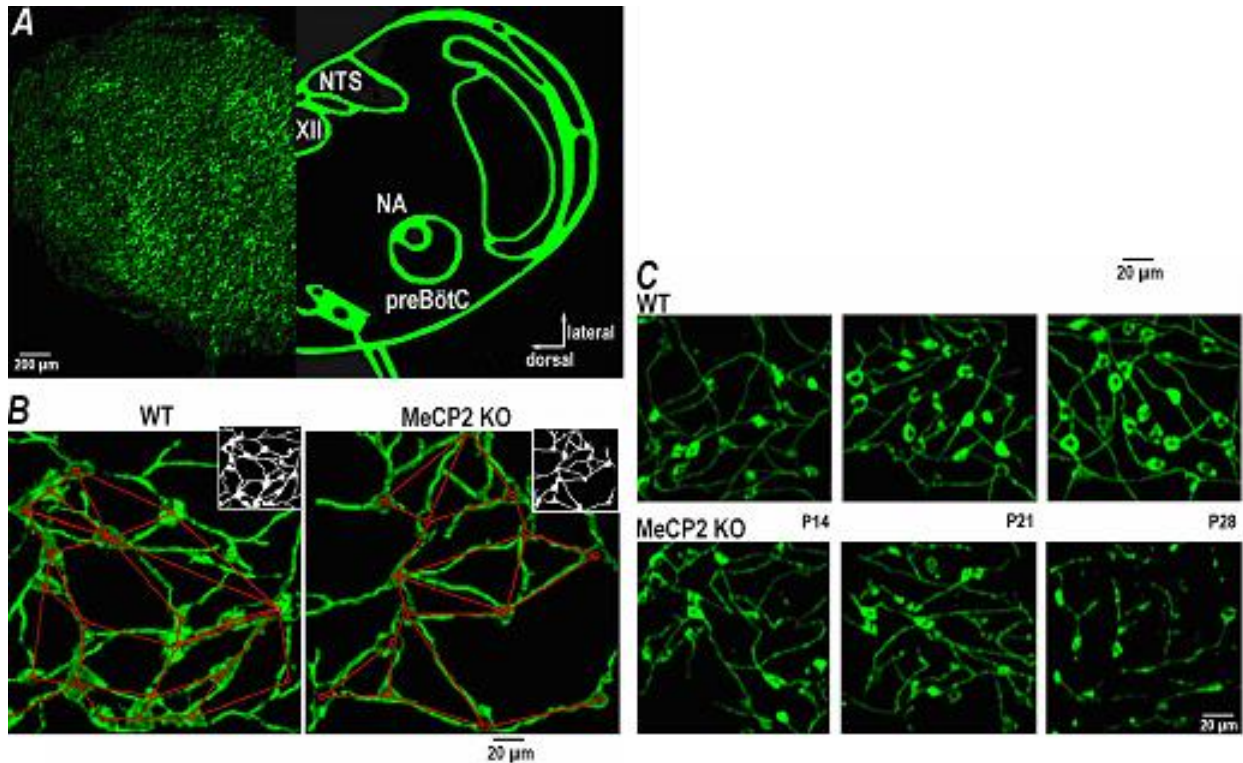


Figure 15. Topology of the WT mice respiratory network and its modification in *Mecp2* null mice (Mironov et al., 2009a).

(A) Image of the transverse WT slice transduced with AAV-D3cpv at P28 (left) and schematic presentation of main anatomical nuclei (right) in this brain stem section (NA – *Nucleus ambiguus*, XII – *Nucleus hypoglossus*, NTS – *Nucleus tractus solitarii*, preBötC – pre-Bötzinger complex). (B) Part of preBötC region in WT and *Mecp2*^{-/-} (KO) mice at P21. The binary images shown in right upper insets were used to obtain the wiring diagrams within a preBötC network. Nodes (the cell bodies) are indicated by red circles. The lines approximate interconnecting neural processes and represent the edges of the network. In these two images of WT (KO) network 20 (14) nodes and 25 (18) edges were counted. (C) Typical appearances of preBötC network at different postnatal days in culture.

morphological features, represents a morphological hallmark of RS both in mice (Larimore et al., 2009) and humans (Wenk, 1997). All slices were transduced during the first postnatal week. The neurons in slices maintained production of the sensor in the culture. Hence one can conclude that these changes in morphology cannot be related to the differential expression of D3cpv in WT and KO preparations. Culturing conditions might have influenced the difference in maturation between WT and KO neurons. To exclude this possibility, the slices from both types of mice were prepared at P19 and the measurements were repeated. Appearances of slices in the two preparations as well as morphological data were similar at the same postnatal day. Similarity of the overlapped data obtained in P3 and P19 slices justifies the absence of particular changes in the developmental program in culture as factors that might explain the differences between WT and KO mice. When the slices derived from P3 KO mice were cultured in the presence of BDNF (10 ng/ml), the number of neurons and connections showed no significant differences from those in WT mice. This fact indicates a positive influence of BDNF during the maturation of KO slices. These data are in agreement with the fact that RS is connected with the deficiency in BDNF production and secretion (see subsection 3.5.6 Introduction for further details). Morphological changes in the brainstem cytoarchitecture of the Rett mice are probably caused by intracellular calcium that is known to participate in the processes of neuronal maturation, shaping, and synaptogenesis. Ca^{2+} resting values were higher in all KO preparations (compared to WT); and this might result in reduction of the number of connections and in smaller dimensions of KO neurons. Both effects were corrected to the normal values by incubation with BDNF (Fig. 16C) which acts as a factor for neuronal surviving. This effect of BDNF also supports electrophysiological observations described above and shows a long-term activation of 'stabilizing' K-ATP channels. After pretreatment with exogenous BDNF, the KO neurons acquired wild-type patterns such as their channel activity. Elevated resting $[\text{Ca}^{2+}]_i$ levels point to particular disturbances in calcium homeostasis in KO neurons that may be responsible for the long-term changes observed in the morphology of neurons and their connectivity.

5.8 Impaired Ca²⁺ homeostasis in MeCP2 deficient neurons and its correction by BDNF

Resting [Ca²⁺]_i is normally controlled by the processes of slow Ca²⁺ buffering which includes specific transport systems in the ER, mitochondria, and plasma membrane. All these participating systems are also active at rest, therefore any changes in basal [Ca²⁺]_i levels indicate a modification of one or more of mentioned above transporting mechanisms. Slow buffering of Ca²⁺ is effectively examined by analysing the amplitude and time-course of the depolarisation-evoked calcium transients. To the first approximation, the rate constant of [Ca²⁺]_i recovery from the steady state ($=1/\tau$ where τ is the time constant) is a sum of rate constants of all participating systems (Mironov, 1995). The maximum amplitude (a new steady level attained during depolarisation) is determined by the product $J\tau$ where J is the Ca²⁺ influx into the cell.

For *in vivo* calcium measurements we used the neurons which demonstrated periodic activity in the form of rhythmic calcium transients accompanying the bursts of action potentials in spontaneously active cells in our preparation (for further details see Hartelt et al., 2008). In KO neurons the transients had bigger amplitudes than in WT neurons (0.16 ± 0.02 vs. 0.09 ± 0.02 μ M) and slower recovery time constants (5.1 ± 1.2 vs. 3.1 ± 0.8 s). The above numbers are the mean values for 24 neurons of each sort (n=24). Depolarisation with high-K⁺ evoked bigger transients with a slower decay (the mean amplitudes and recovery time constants in WT and KO neurons were 0.25 ± 0.3 vs. 0.39 ± 0.4 μ M and 6.1 ± 0.2 vs. 11.1 ± 0.2 s, respectively, n = 24). Such difference in time constants for spontaneous and evoked calcium transients can be explained by shorter duration of spontaneous bursts, after which the recovery of [Ca²⁺]_i is faster. In this case initial rates of Ca²⁺ do not attain homogeneous distribution in the cytoplasm and Ca²⁺ is additionally redistributed through diffusion after the Ca²⁺ influx ceases. Differences in kinetics for spontaneous and evoked calcium transients depend not only on faster recovery of [Ca²⁺]_i after spontaneous bursts, but also on each cell's size and geometry and give variable contributions to the time constants. In order to exclude these effects, we analysed the kinetics of calcium recovery after 5 s-long depolarisations. Such depolarisations resulted in uniform steady [Ca²⁺]_i levels in the cytoplasm that are indicated by distinct plateaus in Fig. 16A and subsequent Figures.

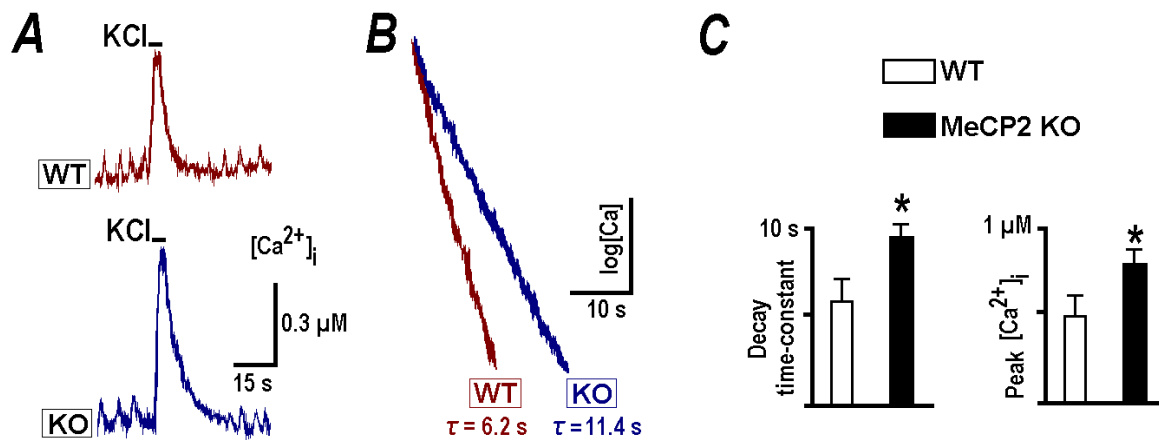


Figure 16. Calcium transients in WT and MeCP2 deficient mice (Mironov et al., 2009a).

(A) Typical depolarisation-induced calcium transients in spontaneously active preBötC neurons evoked by application of 50 mM K⁺ for 5 s. (B) The same transients are presented as semi-log plots to show the extended time-course of decay in KO mice. (C) Mean decay time-constants and peak increases during depolarisation, obtained in 6 to 8 different preparations at P21.

Fluorescence signals recorded in both KO and WT preparations had similar amplitudes and identical minimum and maximum values during calibration of with ionomycin (see Fig. 6). Thus one can conclude that the changes in calcium levels and time constants of recovery between WT and KO neurons were not due to differential expression of D3cpv sensor or changes in its properties.

Mitochondria and ER are the main systems of slow calcium buffering. We analysed their role by applying protonophore carbonyl cyanide m-chlorophenylhydrazone (CCCP), a respiratory chain uncoupler, and thapsigargin (Tg), a sarcoplasmic reticulum Ca^{2+} -ATPase (SERCA) inhibitor. These agents released Ca^{2+} from the corresponding internal store and significantly increased both the peak amplitude and time constant of recovery after depolarisation (Fig. 17A-D). Notably, in the KO neurons that were maintained in culture in presence of BDNF (10 ng/ml), the depolarisations-evoked calcium transients acquired the time-courses and amplitudes identical to their WT counterparts. At P28 the respective mean values ($n = 12$) were 6.4 ± 0.5 s vs. 7.1 ± 0.6 s and 0.26 ± 0.06 μM vs. 0.29 ± 0.07 μM in WT and KO. The same results were obtained at P14 and P2. On the other hand, pretreatment of WT slices with TrkB blocker K252a produced opposite effects, and calcium transients acquired the form typical for KO neurons (Fig 17G, H). The specificity of TrkB blockade was confirmed by applying the inactive analogue K-252b, which showed no effects ($n = 4$).

Application of BDNF alone always induced an immediate transient increase and subsequent slow $[\text{Ca}^{2+}]_i$ decrease (see Fig. 18). Both effects were related to Ca^{2+} handling by ER. They did not depend on extracellular Ca^{2+} because they were abolished after application of thapsigargin and they were not affected by CCCP. The fast transient to BDNF represents a Ca^{2+} release (Bramham and Messaoudi, 2005; Lang et al., 2007), because this effect was not observed after activation of metabotropic receptors with ATP, t-ACPD, substance P nor in the presence of thapsagargin, each of which depletes ER Ca^{2+} . Depolarisation-induced calcium transients recorded during the secondary long-lasting decrease had smaller amplitudes and rates of decay (Fig. 18B) and resembled the responses of WT neurons. The data obtained indicate that BDNF stimulates SERCA that in turn improves calcium removal from the cytoplasm. Application of TrkB blocker K252a (100 nM, 20 min) abolished all effects of BDNF on $[\text{Ca}^{2+}]_i$ (Fig. 18B).

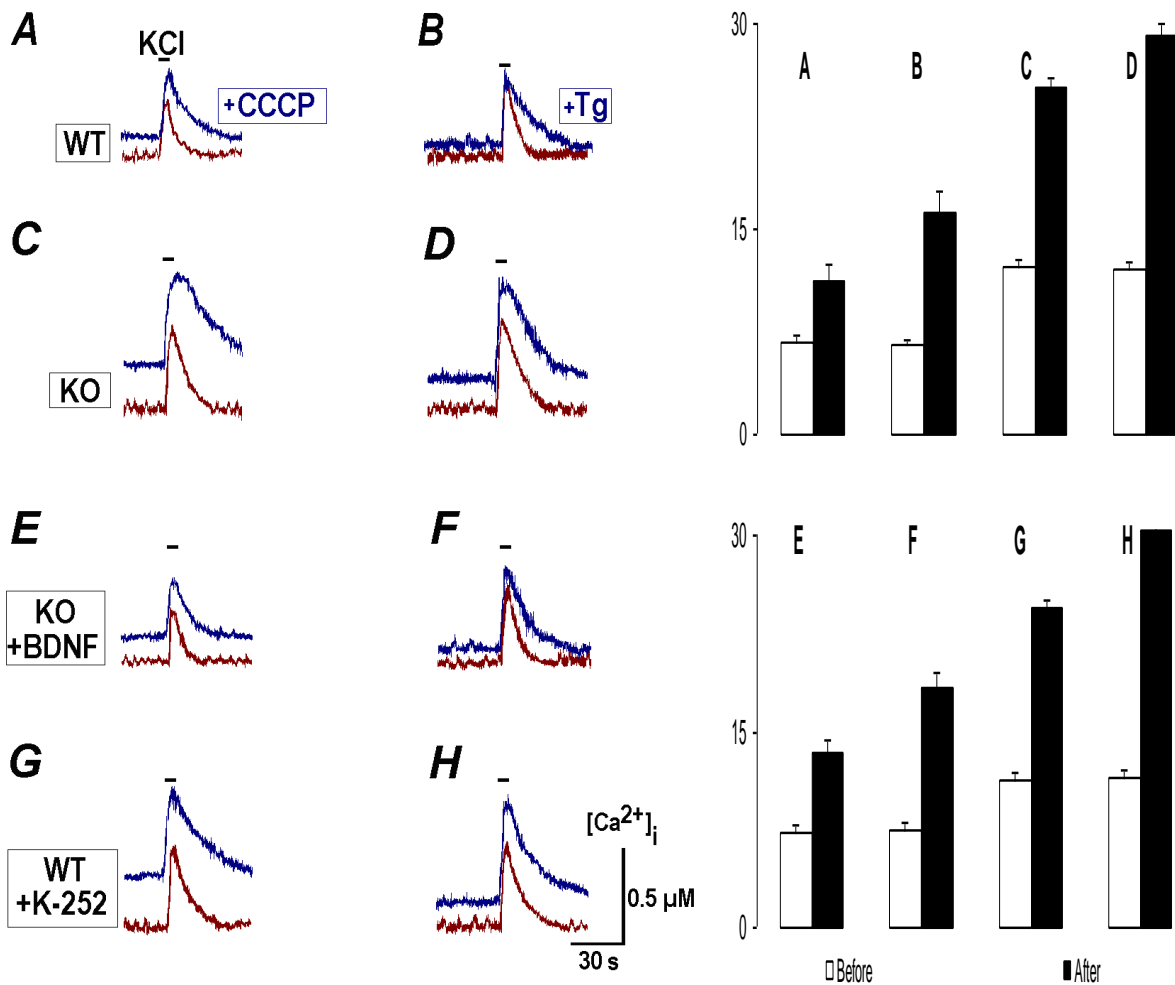


Figure 17. Contributions of mitochondria and ER to the slow calcium buffering in preBötC neurons (Mironov et al., 2009a).

Depolarisations with 50 mM K^+ were induced before and 2 min after applications of 1 μ M CCCP (**A**, **C**, **E**, **G**) and 1 μ M Tg (**B**, **D**, **F**, **H**). Uncoupling of mitochondria with CCCP and inhibition of SERCA with thapsigargin led to an increase in basal calcium levels and prolonged the decay of calcium transients after membrane depolarisation in both wild-type and KO neurons. After pretreatment with BDNF (20 ng/ml, 20 min), the time-courses of transients in KO neurons became closer to those measured in WT cells (**E**, **F**). After pretreatment with TrkB blocker 100 nM K252a for 20 min, the transients in WT neurons acquired the amplitudes and decay times typical for KO neurons (**G**, **H**). Time constants of $[Ca^{2+}]_i$ recovery obtained in 15 to 25 neurons presented in the histograms on the right panel. Experimental data and corresponding histograms are marked with same letters.

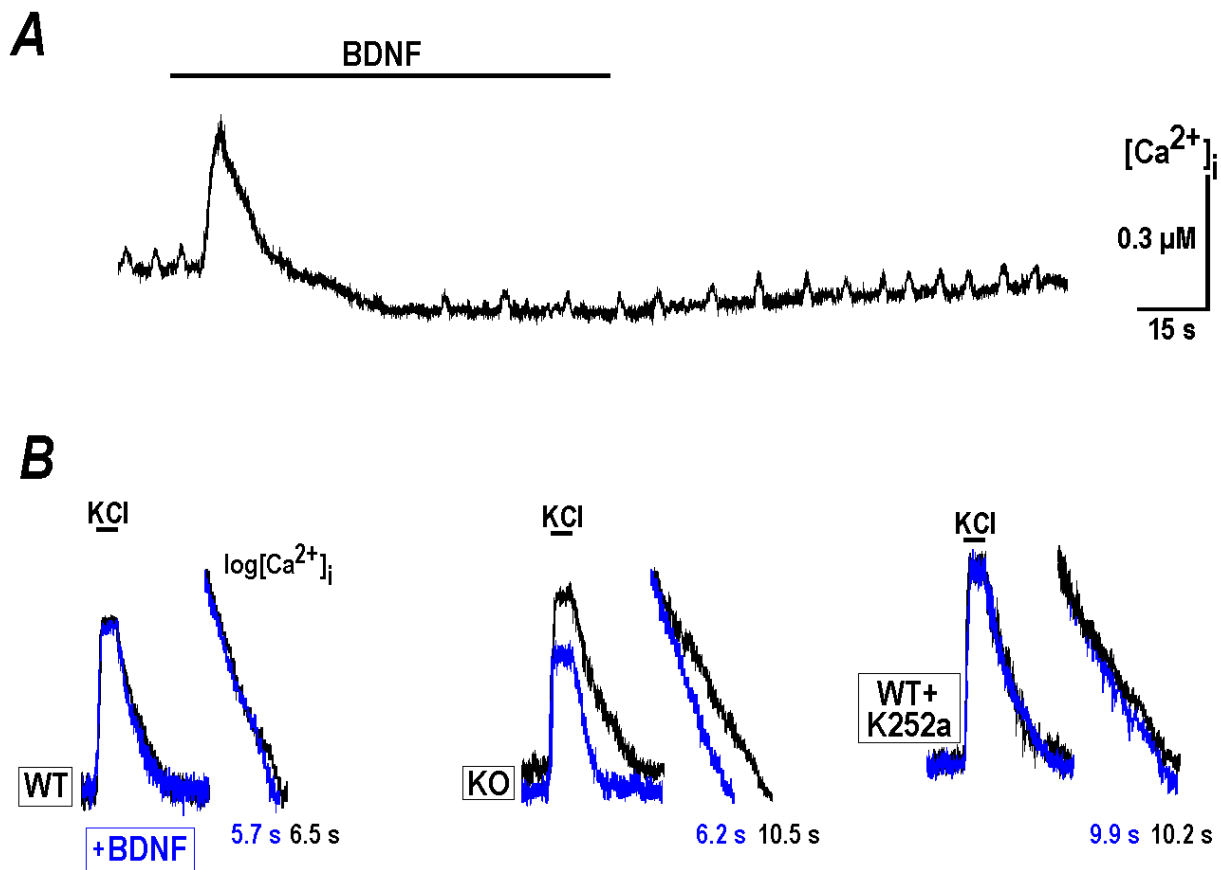


Figure 18. BDNF and calcium homeostasis (Mironov et al., 2009a).

(A) Initial transient increase and long-lasting $[Ca^{2+}]_i$ decrease during BDNF application. (B) Representative calcium transients due to depolarisation recorded at P28 in wild-type and MeCP2 deficient slices and in WT slice treated with 100 nM K252a. Semi-log plots near original traces show the differences in $[Ca^{2+}]_i$ recovery times. The traces recorded in the presence of BDNF are grey-coded (online, blue).

5.9 Hypoxia and retraction of neurites

Respiratory network function in RS mouse models shows disturbances consisting of alternating periods of high respiratory frequency and apneas that can produce brief periods of hypoxia (Viemari et al., 2005; Stettner et al., 2007). We examined the effects of hypoxia by applying 200 μ M KCN. The effects of KCN on respiratory neurons *in vivo* are identical to oxygen depletion (Brockhaus et al., 1993). As in the data observed in the functionally intact preparation (Mironov and Langohr, 2005), the neurons in organotypic slices responded with an initial augmentation of activity, followed by a simultaneously developing depression with a calcium increase (Fig. 20).

After hypoxia $[Ca^{2+}]_i$ levels slowly returned to control values, taking much more time for KO than WT neurons. The decay of depolarisation-induced transients after hypoxia was also much slower for KO neurons. Notably, after a pretreatment of slices with BDNF (lowermost trace in Fig. 19), the two hypoxia-related parameters of calcium homeostasis were practically identical to the WT responses. After a brief application of chemical hypoxia (KCN) we also observed the retraction of neuronal processes (Fig. 20A, row 1). The effects developed within 1 h and showed a clear correlation with $[Ca^{2+}]_i$ increase during hypoxia (Fig. 20B). The retractions in KO neurons were about twice as frequent as observed in the WT neurons. Pretreatment with BDNF produced much smaller effects during subsequent application of hypoxia that were in a range observed in WT neurons (Fig. 20A, row 2). The effects of CCCP and thapsigargin on the retraction of neurites were similar to those of hypoxia (rows 3 and 4 in Fig. 20A). From the viewpoint of calcium buffering this can be explained by an influence of the largest contributions to calcium increases by efflux of Ca^{2+} from ER and mitochondria which are known to be evoked during hypoxia (Mironov and Langohr, 2005).

Calcium-induced retraction of neurites was observed only for relatively long lasting (\approx 1 min) calcium elevations, while calcium transients elicited by brief depolarisations did not produce noticeable changes. Some neurites were retracted after longer lasting transients occurring in some neurons without any treatment, interrupting the intrinsic activity (Fig. 21A). However, such events were extremely seldom, e. g., in the field of view containing 8-10

neurons, only few of these events could be recorded within a 1 h observation time (Fig. 21B). These treatment-independent events were more frequently observed in KO neurons (Fig. 21B), where they had larger amplitudes ($0.64 \pm 0.12 \mu\text{M}$) and slower rates of decay ($21.2 \pm 1.2 \text{ s}$). After such specific transients the neurites were retracted – the relative decrease in twelve KO neurons was $16 \pm 5 \%$ and in six WT neurons was $6 \pm 3 \%$ (measured 1 h after the transient). The differences can be explained by larger amplitudes and durations of spontaneous transients in KO neurons (Fig. 21A).

After brief incubation of KO neurons with BDNF the values of basal calcium changed from 0.16 ± 0.02 to $0.08 \pm 0.02 \mu\text{M}$ (means for 6 to 10 single neurons measured in four different experiments) and became close to those measured in WT neurons. This can be explained using a model developed on the basis of examination of hippocampal and thalamic neurons (Mironov, 1994). There are several systems that participate in calcium removal, but normally SERCA gives the most significant contribution. $[\text{Ca}^{2+}]_i$ levels are determined by a balance between calcium influx and its removal from the cytoplasm. Therefore under assumption that the influx of Ca^{2+} is constant, the ratio of removal speed values measured in the two different conditions e. g. one calcium removal system is not active or weakly expressed, is given by the ratio of calcium levels. The decay times give another estimation of removal speed values. Both approaches give the apparent values of $[\text{Ca}^{2+}]_i$ removal speed in WT and KO neurons which differ by a factor of 2.

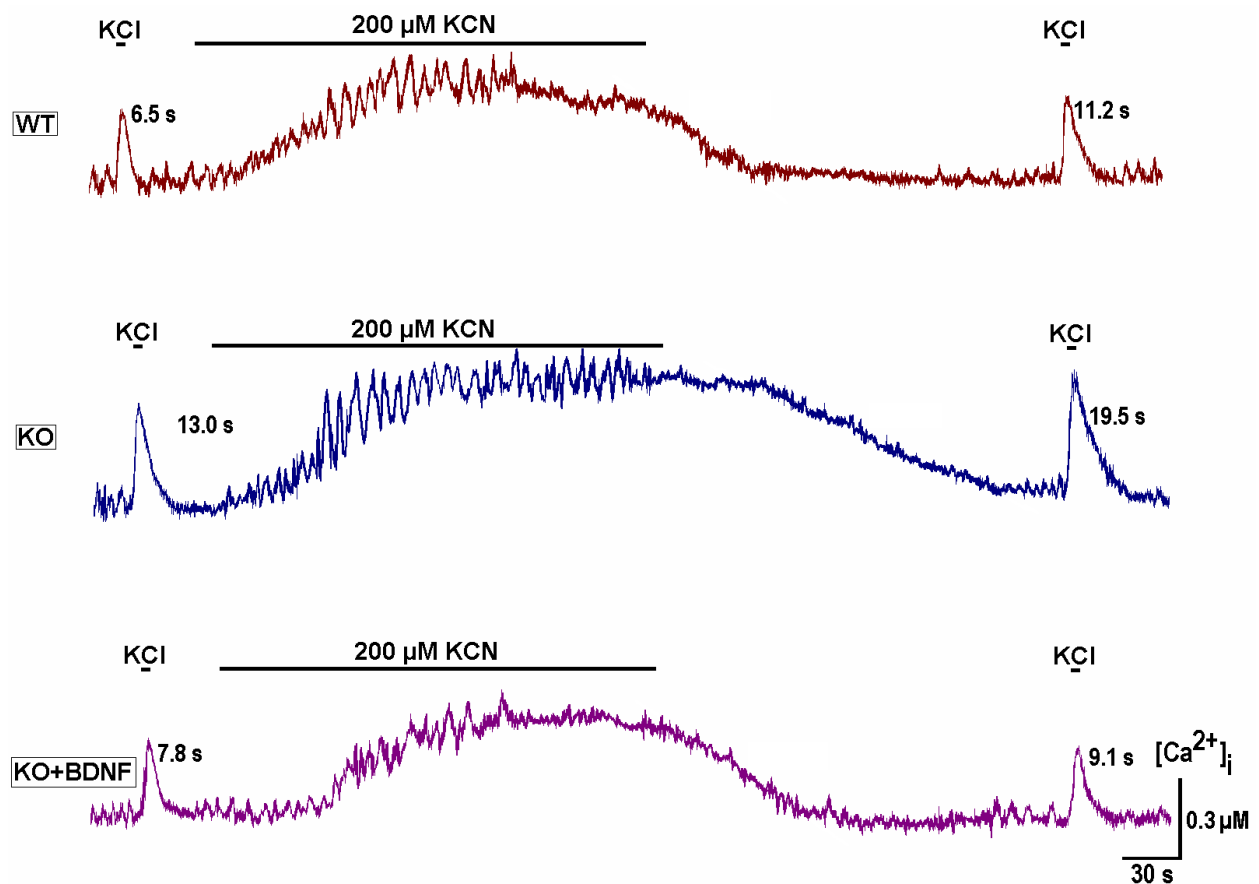


Figure 19. Calcium responses to hypoxia and their modification by BDNF (Mironov et al., 2009a).

Chemical hypoxia was induced by KCN (200 μM) and the slow calcium buffering was assessed by applying high- K^+ before and after this treatment. The time constants of $[\text{Ca}^{2+}]_i$ decay and the rates of $[\text{Ca}^{2+}]_i$ recovery after hypoxia are indicated near each trace. Note the prolonged recovery of calcium levels after hypoxia in neurons from *Mecp2* KO mice that was corrected to WT levels after applying BDNF (20 ng/ml for 20 min). The traces shown are representative of the experiments performed in four different preparations.

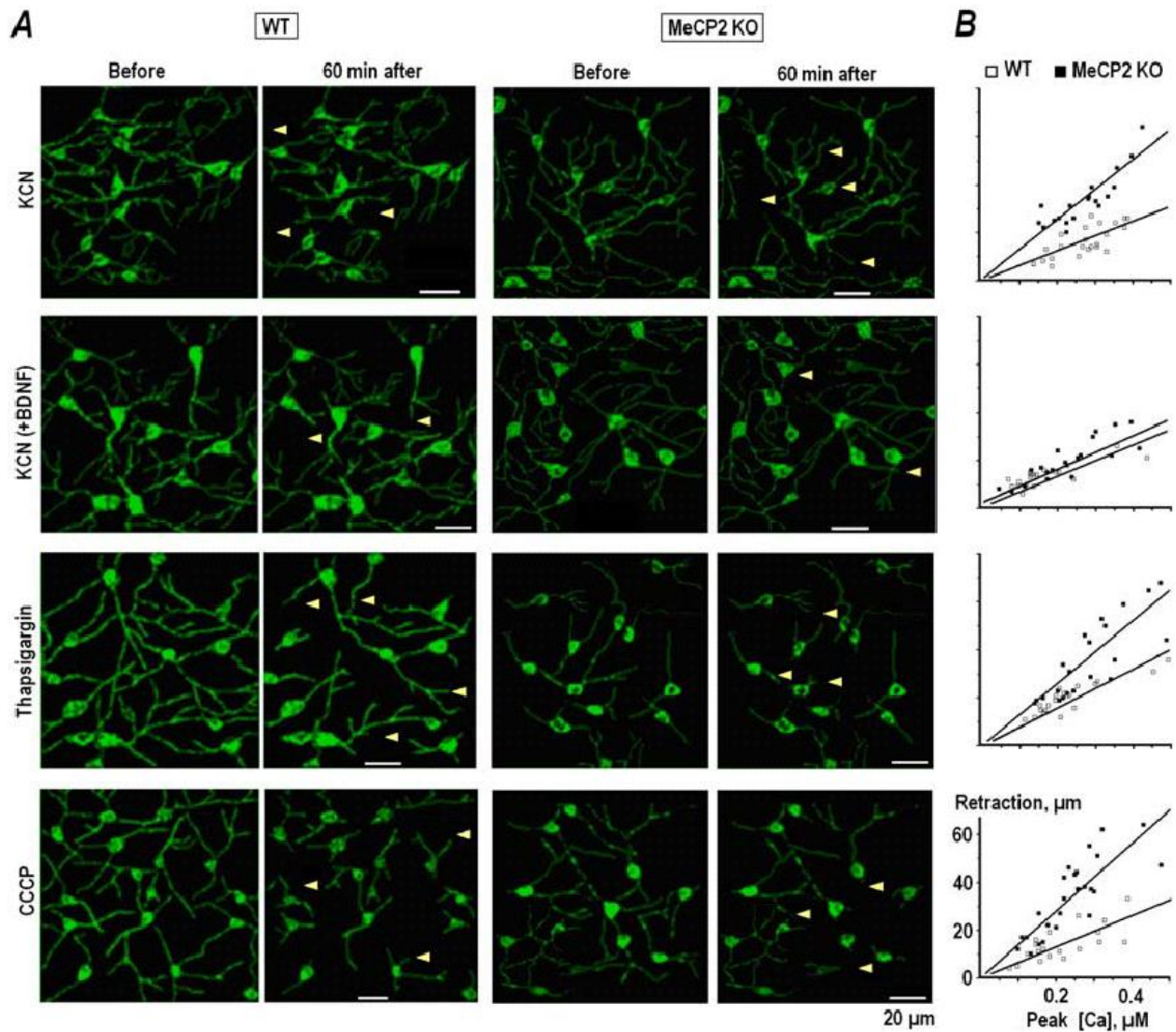


Figure 20. Retraction of neuronal processes after global calcium increases.

(A) Images of the respiratory network in wild-type and *Mecp2* KO mice at P28 obtained before and 60 min after application of the agents which produced long-lasting calcium increases – a chemical hypoxia (200 µM KCN) in control and after pretreatment with 20 ng/ml BDNF for 20 min, 1 µM thapsigargin and 1 µM CCCP. The positions of some retracted processes are indicated by arrowheads. (B) Correlations between relative shortening of the processes and measured peak $[Ca^{2+}]_i$. Straight lines show linear regression of the data (all correlation coefficients are >0.95). Cited from erratum to the article Mironov et al., 2009a, re-calculated by Dr. S.L. Mironov.

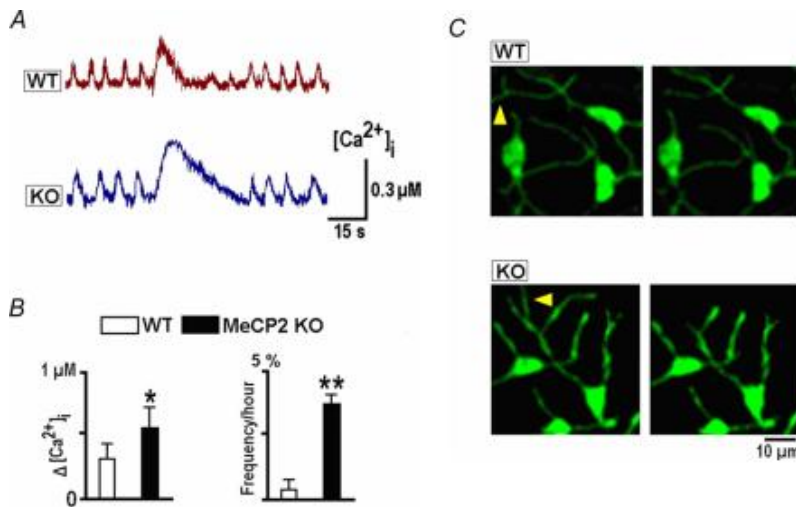


Figure 21. Spontaneous $[Ca^{2+}]_i$ increases and retraction of neuronal processes (Mironov et al., 2009a).

(A) Selected episodes of spontaneous rhythmic activity interrupted by long-lasting calcium transients. (B) Mean amplitudes and frequencies of observation of these transients. (C) The images taken before and 60 min after spontaneous transients show the retractions of neuronal processes as indicated by arrowheads.

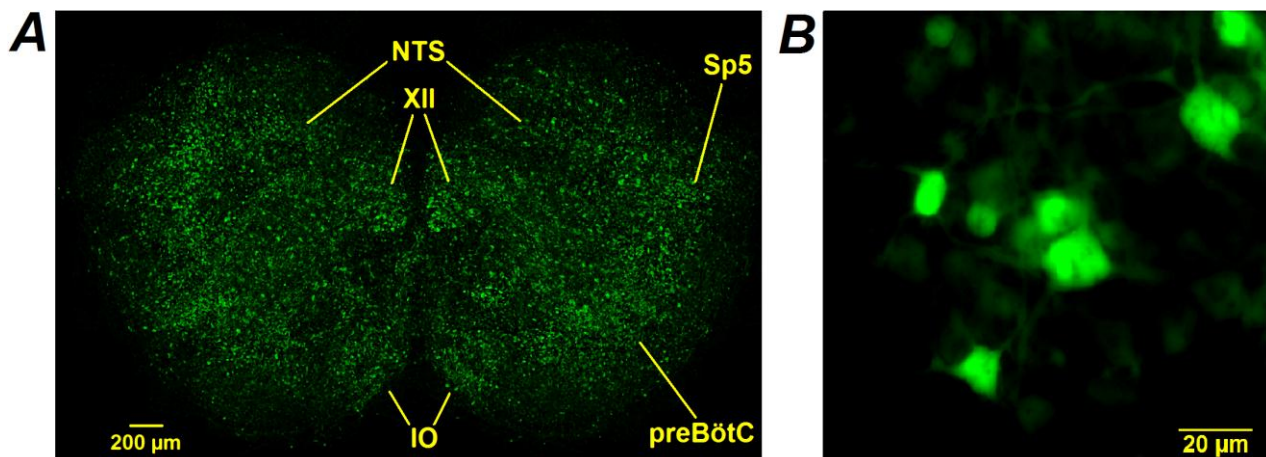


Figure 22. Expression of neuron-specific Epac1-camps (Mironov et al., 2009b).

(A) Representative original images of AAV-Epac1-camps-transduced organotypic slice which contained pre-Bötzinger complex (preBötC) and other characteristic nuclei (XII – *Nucleus hypoglossus*, NTS – *Nucleus tractus solitarii*, IO – *inferior olive*, Sp5 - *spinal nucleus*); (B) Neurons in preBötC. The images were acquired at x10 (A) and x40 (B) magnification. To obtain the panoramic view of the whole slice in (A), the images with overlapping parts were taken in the same horizontal plane and then combined.

5.10 Neuron-specific expression of cAMP and calcium dependent changes

Application of AAV-Epac1-camps vector produced sensor expression in many neurons in the organotypic brainstem slice (Fig. 22A). The neurons were combined into groups with organisation corresponding to the characteristic nuclei in this section of the brainstem (Ruangkittisakul et al., 2006). The sensitivity of Epac1-camps to register $[cAMP]_i$ changes was first examined in tests where the activities of AC and PDE were modulated. Applications of 1 μ M forskolin (a specific AC activator), 50 μ M isobutylmethylxanthine (IBMX, non-specific PDE inhibitor), 1 μ M rolipram (a specific inhibitor of PDE4 (de Boer et al., 1992), and 0.1 mM 2'5'-dideoxyadenosine (DDA, membrane-permeable AC inhibitor) induced changes in $[cAMP]_i$ which were in line with the presumed targets of the drugs (Fig. 23). Induced drug-based effects were reversible and the responses could be repeatedly elicited after washing them out for 15 min. Rolipram was the most effective among PDE inhibitors - the increases in $[cAMP]_i$ induced by PDE3 inhibitor milrinone (1 μ M) and PDE2 inhibitor EHNA (10 μ M) were 0.58 ± 0.05 and 0.21 ± 0.06 μ M, respectively. These effects were smaller than those induced by rolipram, which was in an agreement with their efficacy shown in cardiomyocytes (Nikolaev et al., 2006). Specific actions of rolipram in preBötC neurons are in line with its stimulating effect on the respiratory motor output (Ruangkittisakul et al., 2006). Activation of metabotropic receptors led to delayed $[cAMP]$ increases. The bottom two panels in Fig. 23 show the actions of 5-HT and mGluR1/5 agonist (S)-3,5-dihydroxyphenylglycine (DHPG) which are consistent with activation of G-protein-coupled receptors for serotonin and glutamate. The data describing the kinetics of changes in cAMP levels presented on Table 3. More detailed analysis was not performed because the time courses of changes in cAMP concentration can be determined by several factors that we here can not correctly estimate.

cAMP-signalling pathways are often activated by Ca^{2+} influx (Huang and Kandel, 1998; Alberts et al., 2002) via an increase in AC activity and modulation of cAMP-hydrolyzing phosphodiesterase (Antoni, 1997; Ang and Antoni, 2002; Cooper, 2003; Hurley, 2006). On the contrary cAMP and PKA modulations of Ca^{2+} channels and plasma membrane Ca^{2+} -ATPases

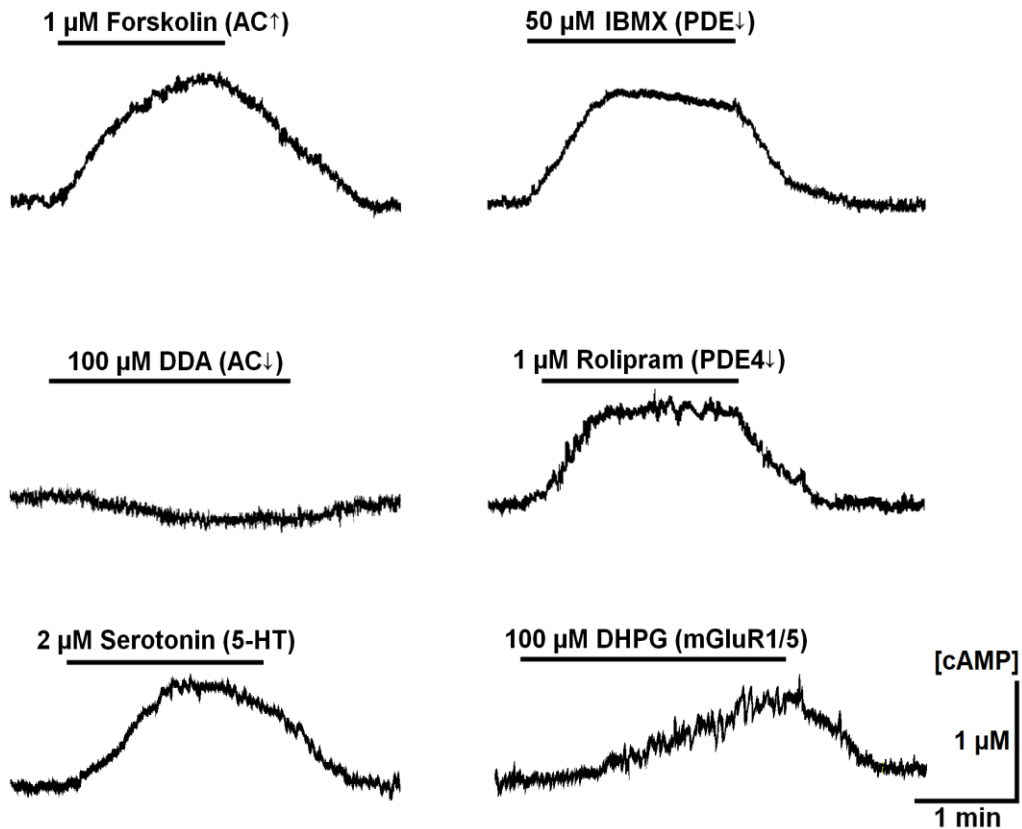


Figure 23. $[cAMP]_i$ changes in preBötC neurons after modulation of cAMP-signalling pathway (Mironov et al., 2009b).

Representative responses due to modulation of activity of AC, PDE and activation of metabotropic receptors are shown. AC was stimulated with forskolin and inhibited with 2'5'-dideoxyadenosine (DDA), PDE was antagonized with IBMX and rolipram, and Group I metabotropic glutamate receptors were activated with (S)-3,5-dihydroxyphenylglycine (DHPG). Fluorescence signals were averaged over the soma of neurons and transformed into cAMP concentrations as described in Methods.

Table 3. Mean $[cAMP]_i$ changes observed after modulation of cAMP signaling pathway and activation of G-protein coupled glutamate and serotonin receptors (Mironov et al., 2009b).

Forskolin 1 μ M	IBMX 50 μ M	DDA 100 μ M	Rolipram 1 μ M	DHPG 100 μ M	5-HT 2 μ M
1.62 \pm 0.12	1.45 \pm 0.07	-0.12 \pm 0.05	1.19 \pm 0.08	0.74 \pm 0.07	0.81 \pm 0.05

Mean data \pm S. E. M. were obtained in 4 to 8 neurons in four different preparations and are presented as changes from the resting cAMP level (mean = 0.09 \pm 0.03 μ M). Group I metabotropic glutamate receptors (mGluR1/5) were activated with (S)-3,5-dihydroxyphenylglycine (DHPG).

are known to influence Ca^{2+} signal transduction (Nakade et al., 1994; Dean et al., 1997; Bruce et al., 2003; Holz et al., 2006). In order to examine possible mechanisms of crosstalk between Ca^{2+} and cAMP, we loaded transduced neurons with fura-2 (Harbeck et al., 2006) and evoked $[Ca^{2+}]_i$ changes by applying brief membrane depolarisations with high- K^+ or inducing Ca^{2+} release from internal stores. The first pattern is similar to the tetanic stimulation which is often used in the analysis of neuronal plasticity (Huang and Kandel, 1998). At the peak of $[Ca^{2+}]_i$ transient $[cAMP]_i$ started to increase and reached its maximum during $[Ca^{2+}]_i$ recovery to the resting value (see Fig. 24A). Induction of calcium release from ER with 1 mM ATP (Mironov, 1994) also produced delayed $[cAMP]_i$ increases with amplitude and duration similar to those induced by membrane depolarisation.

Various isoforms of AC and PDE are known to be differentially activated by Ca^{2+} (Willoughby and Cooper, 2007). Ca^{2+} -dependent stimulation of PDE would decrease $[cAMP]_i$; however, our observations show the opposite indicating a dominating role of AC modulation in Ca^{2+} -dependent increases. After blockade of AC activity with DDA, the amplitude of $[Ca^{2+}]_i$ transients became smaller (Fig. 24B). Thus a decreased production of cAMP promotes dephosphorylation of Ca^{2+} channels and leads to decrease in their activity (Landa et al., 2005). Conversely, the $[Ca^{2+}]_i$ transients showed increased amplitude after blockade of PDE (Fig. 24C) that points at PKA stimulation and subsequent phosphorylation of the channels (Landa et al., 2005).

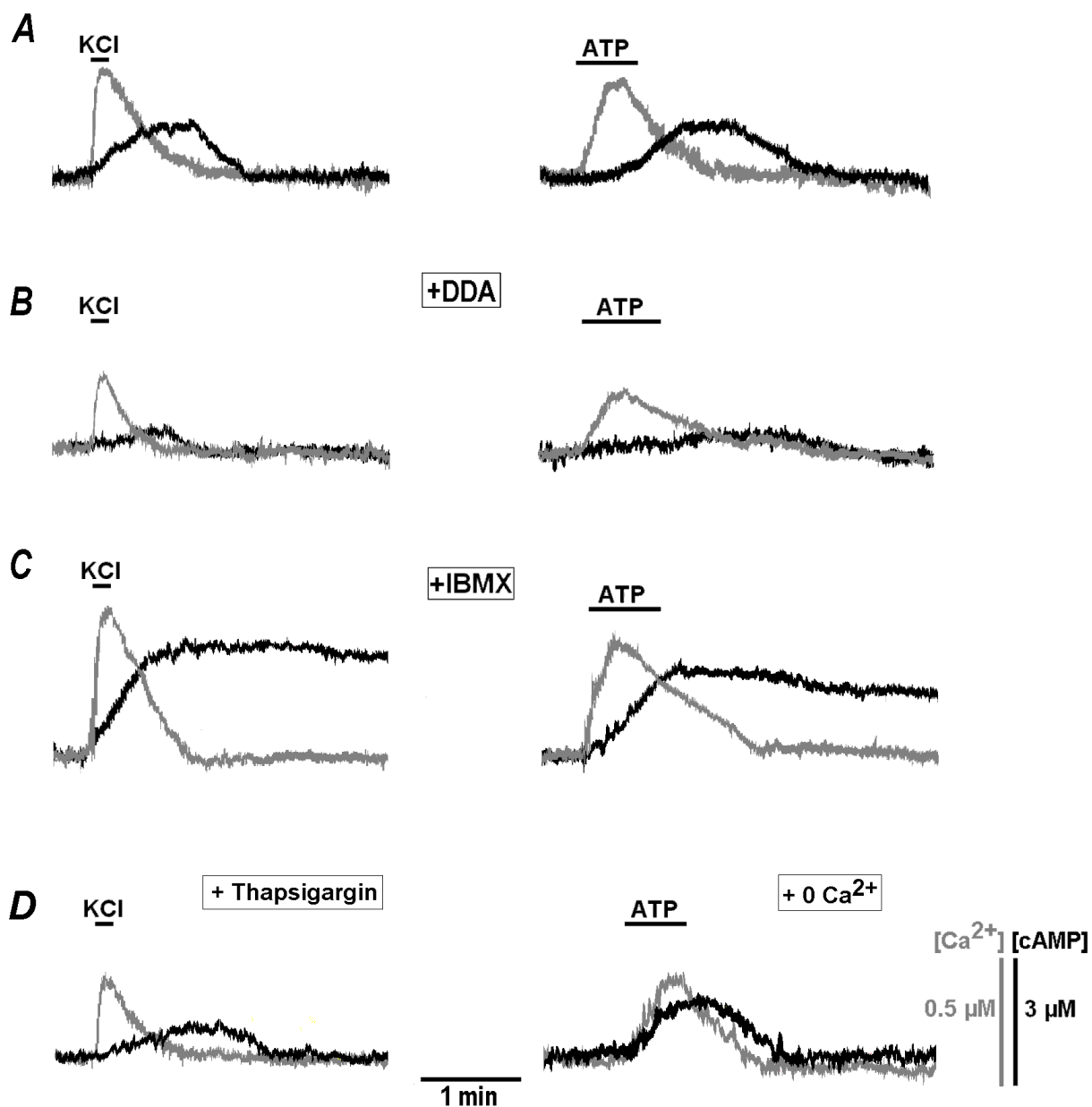


Figure 24. Interrelationships between calcium and cAMP transients measured with fura-2 and Epac-1-camps (Mironov et al., 2009b).

Cytoplasmic calcium and cAMP (grey and black traces, respectively) were recorded with fura-2 and Epac-1-camps during testing challenges to 50 mM K^+ and 1 mM ATP as indicated. The applications were made in control (**A**) and in the presence of 0.1 mM DDA (**B**) or 50 μ M IBMX (**C**) to inhibit the activity of AC and PDE, respectively. Note changes in the amplitude of both calcium and cAMP transients after the treatments. The two panels in (**D**) show $[Ca^{2+}]_i$ and $[cAMP]_i$ changes recorded after 10 min preincubation with 1 μ M thapsigargin to deplete calcium stores (*left*) and in Ca^{2+} -free solution (*right panel*). Values representing mean $[Ca^{2+}]_i$ and $[cAMP]_i$ increases and Ca^{2+} release in the presence of drugs modulating cAMP and Ca^{2+} homeostasis presented on Table 4 and Table 5, Fig. 25 and Fig. 26.

Table 4. Mean $[Ca^{2+}]_i$ and $[cAMP]_i$ increases due to membrane depolarisation and Ca^{2+} release in the presence of drugs modulating cAMP and Ca^{2+} homeostasis (Mironov et al., 2009b).

High- K^+ (50 mM)					
	Control	IBMX 50 μ M	DDA 100 μ M	Tg 2 μ M	0 Ca^{2+}
$[Ca^{2+}]_i$	0.44 ± 0.07	0.72 ± 0.08	0.24 ± 0.06	0.31 ± 0.05	0.01 ± 0.01
τ (s), Ca decay	14.2 ± 1.5	16.4 ± 1.8	14.1 ± 1.4	13.8 ± 1.6	n.s.
$[cAMP]_i$	1.52 ± 0.09	3.22 ± 0.17	0.25 ± 0.04	0.94 ± 0.08	0.04 ± 0.01
$t_{1/2}$ (s), cAMP rise	15.6 ± 2.5	19.5 ± 1.9	16.2 ± 2.3	24.2 ± 2.7	1,2 – n. s., 2,4 – $p < 0.1$
$t_{1/2}$ (s), cAMP decay	12.2 ± 1.5	n. d.	10.2 ± 1.5	14.1 ± 1.5	n. s.

Mean data \pm S. E. M. were obtained in 4 to 8 neurons in four different preparations.

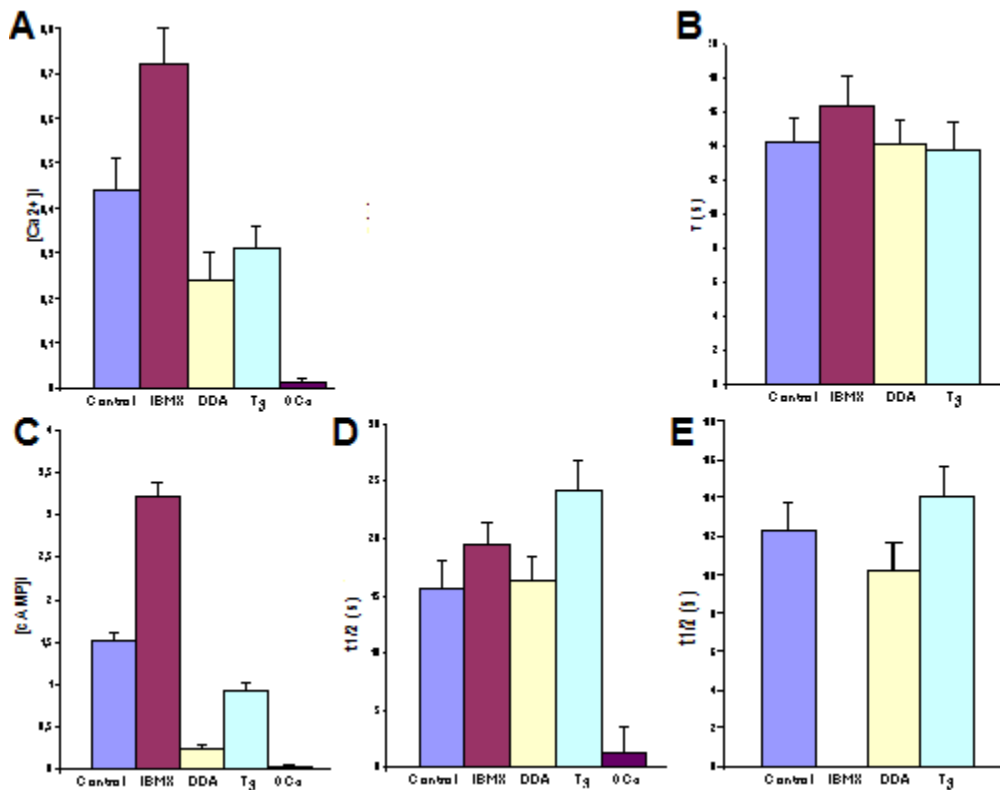


Figure 25. Kinetics of $[Ca^{2+}]_i$ and $[cAMP]_i$ increases due to membrane depolarisation and Ca^{2+} release in the presence of of drugs modulating cAMP and Ca^{2+} homeostasis (after Mironov et al., 2009b).

Mean $[Ca^{2+}]_i$ increase (A) and mean Ca decay time (B) due to membrane depolarisation induced by high K^+ (50 mM)- Columns represent cells in control, in presence of IBMX, DDA, and thapsigargin respectively. Violet bar, when present, indicates absence of Ca^{2+} . Second row represents mean $[cAMP]_i$ increase (C), mean rise (D) and decay (E) time in presence of IBMX (blue bars), DDA (purple bars), thapsigargin (cyan bars), or in the absence of Ca^{2+} (violet bars).

Table 5. Mean $[Ca^{2+}]_i$ and $[cAMP]_i$ increases due to membrane depolarisation and Ca^{2+} release in the presence of drugs modulating cAMP and Ca^{2+} homeostasis (Mironov et al., 2009b).

ATP (1 mM)					
	Control	IBMX 50 μ M	DDA 100 μ M	Tg 2 μ M	0 Ca^{2+}
$[Ca^{2+}]_i$	0.39 ± 0.07	0.52 ± 0.08	0.22 ± 0.05	0.02 ± 0.01	0.31 ± 0.05
$t_{1/2}$ (s), Ca rise	9.2 ± 1.2	8.5 ± 1.0	9.1 ± 1.1	n. d.	14.1 ± 1.5 , $p < 0.1$
τ (s), Ca decay	22.2 ± 3.1	24.2 ± 2.7	24.4 ± 2.5	n. d.	21.4 ± 1.7
$[cAMP]_i$	1.44 ± 0.08	2.24 ± 0.07	0.36 ± 0.03	0.04 ± 0.01	1.42 ± 0.08
$t_{1/2}$ (s), cAMP rise	42.4 ± 4.5	32.2 ± 3.4	54.2 ± 5.5	1,3 – n. s. 2,5 – $p < 0.1$	18.6 ± 2.5
$t_{1/2}$ (s), cAMP decay	24.2 ± 2.5	n. d.	27.4 ± 3.2	26.4 ± 3.1	15.4 ± 2.5

Here n.s. refers to non-significant differences, n.d. – to non determined. Mean data \pm S. E. M. were obtained in 4 to 8 neurons in four different preparations.

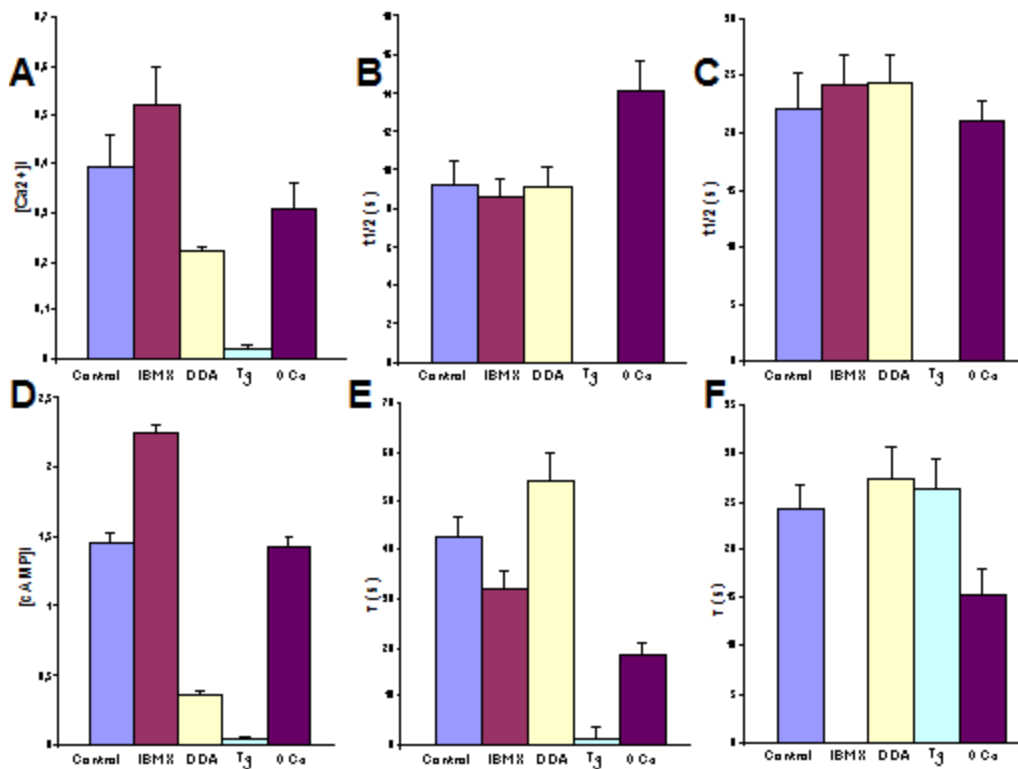


Figure 26. Kinetics of $[Ca^{2+}]_i$ and $[cAMP]_i$ increases due to membrane depolarisation and Ca^{2+} release in the presence of of drugs modulating cAMP and Ca^{2+} homeostasis (after Mironov et al., 2009b).

Mean $[Ca^{2+}]_i$ increase (A) and mean Ca rise (B) and decay time (C) due to membrane depolarisation induced by 1 mM ATP. Columns represent cellis in control, in presense of IBMX, DDA, and thapsigargin respectively. Violet bar, when present, indicates absence of Ca^{2+} . Second row represents mean $[cAMP]_i$ increase (D), mean rise (E) and decay (F) time in presense of IBMX (blue bars), DDA (purple bars), thapsigargin (cyan bars), or in the absence of Ca^{2+} (violet bars).

Removal of extracellular Ca^{2+} or introduction of 0.1 mM Cd^{2+} , which blocks all pathways of Ca^{2+} entry into the cell, abolished the changes in $[\text{cAMP}]_i$ induced by depolarisation. In Ca^{2+} -free solution the effects of ATP were still present (the right panel in Fig. 24D) that excludes the role of Ca^{2+} influx after activation of ionotropic P2X receptors. After depletion of ER with Tg the effects caused by membrane depolarisations were reduced (the left panel in Fig. 24D). Together, these results show that Ca^{2+} -induced Ca^{2+} release (CICR, Fabiato and Fabiato, 1979) from the ER via PLC-IP₃ signalling pathway amplifies in part cyclic nucleotide signalling induced by Ca^{2+} influx.

Ca^{2+} -related Epac1-camps responses can potentially report cGMP changes as it was recently found in presynaptic boutons of *Drosophila* neurons (Shakiryanova and Levitan, 2008), despite the sensor having lower affinity for cGMP ($K_d = 11 \mu\text{M}$) than that for cAMP (Nikolaev et al., 2004). One possible explanation is that in this case the presynaptic calcium transients had higher amplitude, inhibited [cAMP] production and made [cGMP] changes dominant. Since NO/cGMP signalling pathway plays an important role in preBötC neurons (Mironov and Langohr, 2007), we examined whether cGMP changes underlie, at least partially, the responses of Epac1-camps. When guanylyl cyclase inhibitor 1H-[1,2,4]-oxadiazolo-[4,3-a]-quinoxalin-1-one (ODQ, 100 μM), the NOS inhibitor N-monomethyl-L-arginine (L-NMMA), and the NO donor S-nitroso-N-acetylpenicillamine (SNAP, 300 μM) were applied, neither resting nor stimulus-induced Epac1-camps signals were changed ($n \geq 3$ for each treatment).

Ca^{2+} and cAMP changes showed a considerable crosstalk. When paired stimuli were applied, second $[\text{Ca}^{2+}]_i$ increases induced greater effects (Fig. 27A). The enhancement of responses can be mediated by Ca^{2+} -driven stimulation of PKA with subsequent increase in the activity of voltage-sensitive Ca^{2+} channels (Hoogland et al., 2004). In order to test this hypothesis, we applied PKA inhibitor H-89 (N-[2-(p-bromocinnamylamino)ethyl]-5-isoquinoline sulfonamide hydrochloride, 10 μM for 10 min). Potentiation of secondary $[\text{Ca}^{2+}]_i$ and $[\text{cAMP}]_i$ increases was abolished after pretreatment with H-89 (Fig. 27A). Ca^{2+} release from ER also led to enhanced $[\text{cAMP}]_i$ responses and the effects were inhibited by H-89 (Fig. 27B, C).

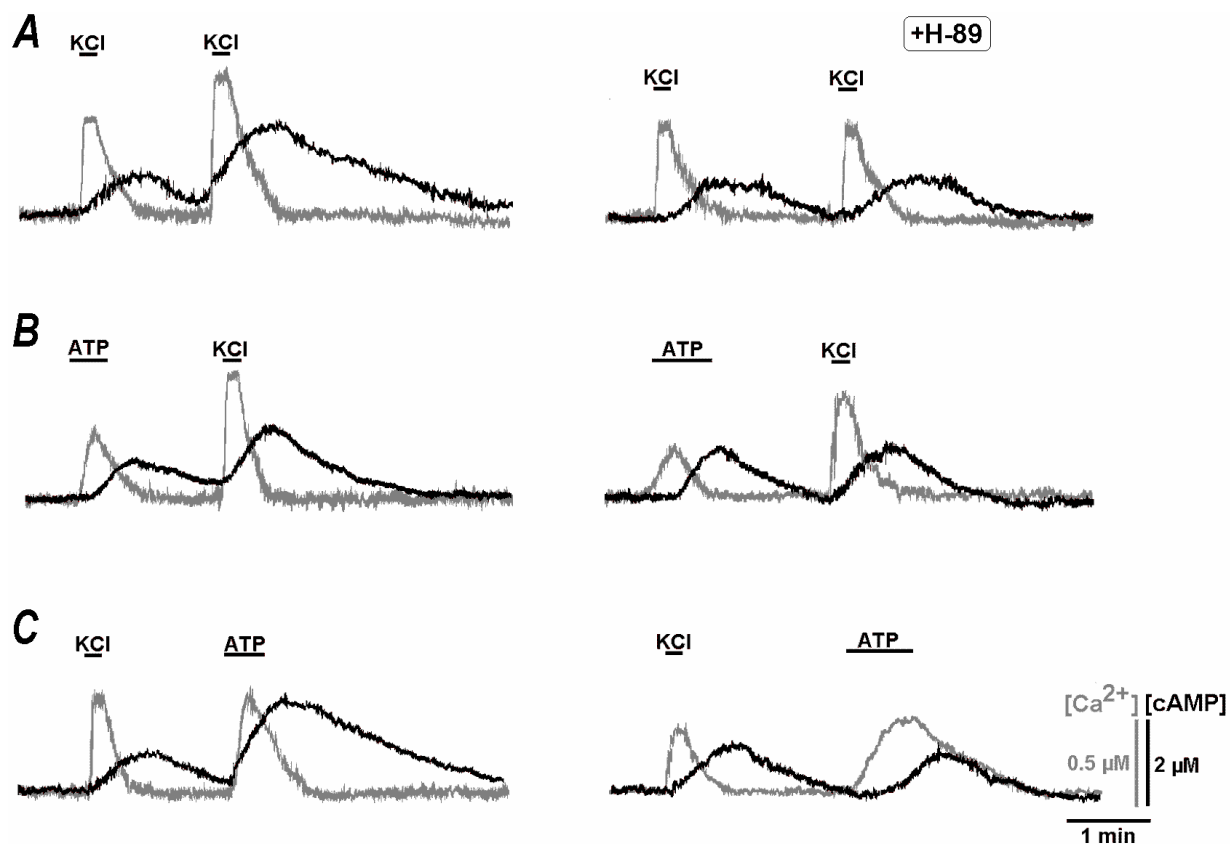


Figure 27. Non-linear interactions between Ca^{2+} influx and Ca^{2+} release in $[\text{cAMP}]$ increases (Mironov et al., 2009b).

Testing applications of 50 mM K^+ and 100 μM ATP were made as indicated by horizontal bars. Changes in $[\text{Ca}^{2+}]_i$ and $[\text{cAMP}]_i$ are shown by grey and black traces, respectively. The experiments were done in control (*left*) and repeated 20 min after pretreatment with PKA inhibitor H-89 (10 μM , *right*). (A) Two depolarisations with high K^+ . (B) A Ca^{2+} release from ER followed by a depolarisation. (C) Depolarisation and Ca^{2+} release. Note that potentiation of $[\text{cAMP}]$ increases during the second treatments was abolished by H-89.

5.11 Deregulated cAMP homeostasis in *Mecp2*^{-/-} neurons

Resting [cAMP]_i in living cells is normally slightly below 1 μM (Willoughby and Cooper, 2007) and determined by basal activities of adenylate cyclase and phosphodiesterase. As described previously (Mironov et al., 2009a), during calibrations we first set a ‘zero’ cAMP level by inhibiting AC with membrane-permeable inhibitor 2’5’-dideoxyadenosine (DDA, 0.1 mM) and then applied a specific Epac1-camps activator 8-Bromo-2’-O-methyl-cAMP (BrOMecAMP, Kang et al., 2003) in a step-like fashion. A greater decrease of signal by DDA in KO neurons is shown in Fig. 28A indicating a lower [cAMP]_i level. Subsequent addition of BrOMecAMP produced identical increases in WT and KO neurons (Fig. 28B) that excludes differences in the expression of the sensor or modification of its properties in the two types of cells.

The resting cAMP was 0.56 ± 0.06 μM in WT and 0.12 ± 0.02 μM in KO neurons; the differences were maintained up to postnatal day P35 (Fig. 28C). Brief membrane depolarisations imposed by applications of 45 mM KCl for 10 s induced Ca²⁺ influx that resulted in slow increase in cAMP levels (Fig. 24). Initially lower [cAMP]_i level in KO neurons, its smaller increase and faster decay is demonstrated in Fig. 28D. The time-constants of decay were 15.6 ± 2.1 and 9.0 ± 1.2 s in WT and KO neurons, respectively (n = 6 for both).

The responses in WT and KO neurons to activation of AC with forskolin and inhibition of PDE4 with rolipram (Yamashita et al., 1997) were distinctly different (Fig. 29). In order to interpret the data, we used a simple model of cAMP homeostasis described by the first order ordinary differential equation

$$dC/dt = \alpha - \beta C \tag{4}$$

where C is a mean [cAMP]_i concentration within the cell, and α and β are the rate constants for cAMP production by AC and its degradation by PDE, respectively.

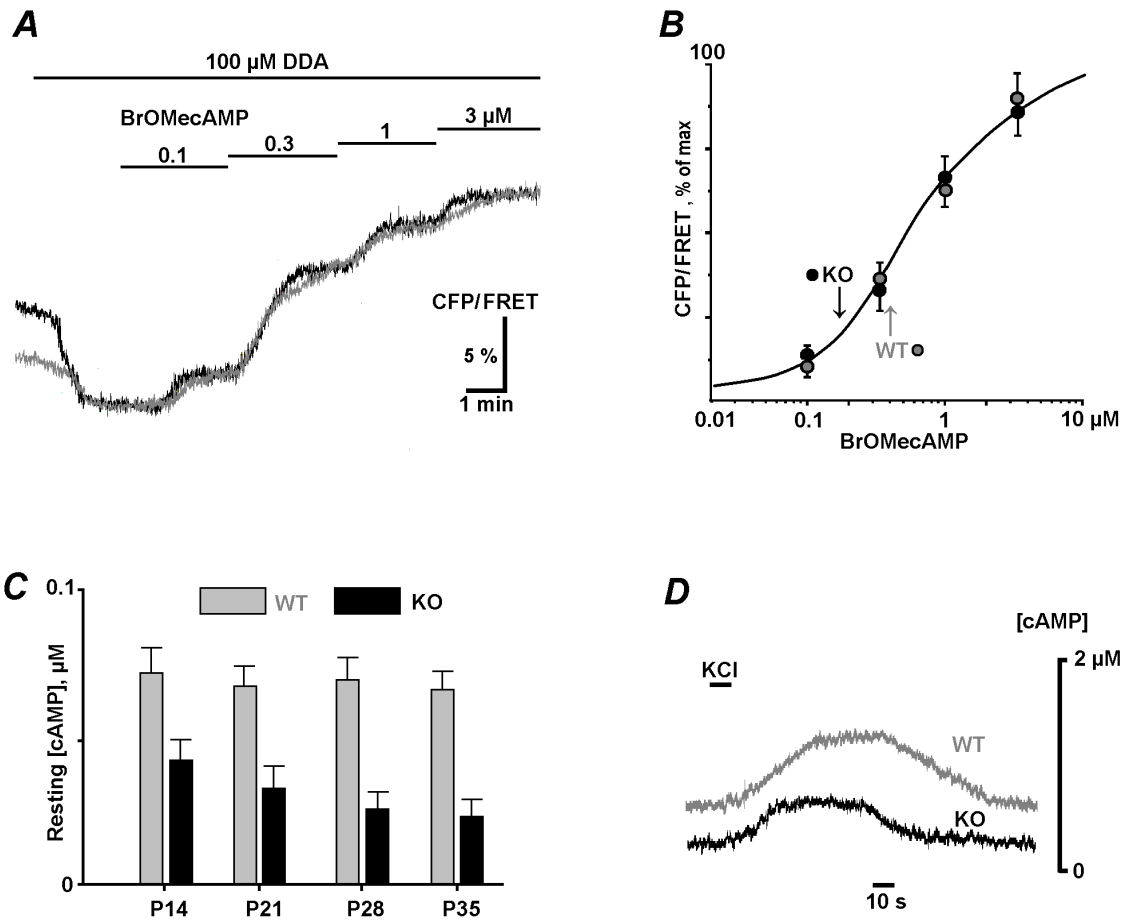


Fig. 28. Resting cAMP and its time-dependent changes in preBötC neurons.

(A) Decreases in 470/535 nm emission ratio (CFP/FRET) after addition of AC inhibitor (100 μ M DDA) and its increases after application of membrane-permeable Epac activator 8-Bromo-2'-OMe-cAMP. (B) Mean ratios \pm S. E. M. were obtained as steady state levels at different concentrations of the agonist and normalized to the maximal signal obtained at 30 μ M. The data in both animal types were approximated by a single Michaelis – Menten-like curve ($K_d = 1.5 \mu$ M) that coincides with EC_{50} describing the binding of cAMP to Epac1-camps (Mironov et al., 2009a). (C) Resting levels of [cAMP]_i in WT and KO neurons. Preparations were made at the P3, transduced at P5 and examined at days indicated. (D) Representative responses of WT and KO neurons at P14. Brief membrane depolarisation via elevation of cytoplasmic calcium (see Mironov et al., 2009a) produced a slow increase in [cAMP] (horizontal bar). Notice a lower initial [cAMP]_i level in KO neurons, its smaller increase and faster kinetics.

The solution of Eq. (1)

$$C = \alpha/\beta(1 - e^{-\beta t}) + C_0 e^{-\beta t} \quad (5)$$

predicts that a steady state of level $[cAMP]_i = \alpha/\beta$ is established exponentially according to the time constant $\tau = 1/\beta$. The values of β in WT and KO neurons were 0.063 s^{-1} vs. 0.11 s^{-1} , respectively, and the resting cAMP levels give $\alpha = 0.11$ vs. $0.10 \mu\text{M}^{-1}\text{s}^{-1}$. Thus, the rate of basal cAMP production is about the same in both cases, whereas cAMP degradation in WT is about twice as fast as in KO neurons. $[cAMP]_i$ increases induced by forskolin in KO neurons were 2.1 ± 0.2 -fold smaller compared to WT cells (Fig. 29A, $n = 6$) that can be explained by higher values of β in the mutant KO cells. In the presence of forskolin the time-constants of $[cAMP]_i$ decay were not modified ($16.4 \pm 2.6 \text{ s}$ in WT and $8.1 \pm 1.8 \text{ s}$ in KO cells). After inhibition of PDE4 with rolipram, the increases in cAMP were similar both in WT and KO neurons (Fig. 29B) and cAMP decay became slower (the time constants were $26.7 \pm 3.5 \text{ s}$, WT; and $25.1 \pm 3.8 \text{ s}$, KO). Obtained values correspond to $\beta \approx 0.04 \text{ s}^{-1}$ and represent the rate of $[cAMP]_i$ degradation by other phosphodiesterases. Subtracting this from the value measured before adding rolipram, we obtain for intrinsic activity of PDE4 $\beta' \approx 0.02 \text{ s}^{-1}$ in WT and $\beta' \approx 0.06 \text{ s}^{-1}$ in KO cells, i. e., PDE4 is about three times more active in the KO neurons. We also examined BDNF based effects on $[cAMP]_i$ homeostasis because previously observed positive influence of BDNF on responses in the mouse model of RS (Mironov et al., 2009) can be gated by both calcium- and cAMP-dependent processes. After pretreatment with BDNF (20 ng/ml, 30 min), the responses to forskolin, rolipram and membrane depolarisation in WT and KO neurons became identical (Fig. 29C, D). These effects of BDNF in KO neurons were not observed in the presence of 100 nM TrkB blocker K252a ($n = 6$). Electrical stimulation, a treatment that is often used to study neuronal plasticity (Byrne and Kandel, 1996), elicited $[cAMP]_i$ responses that were similar to those evoked by high- K^+ . The amplitude of the transients increased with the number of pulses in a sequence (Fig. 30). They had smaller amplitudes that can be explained by smaller calcium increases that caused weaker stimulation of AC. Both forskolin and rolipram increased the amplitude of transients, but only rolipram changed their time-

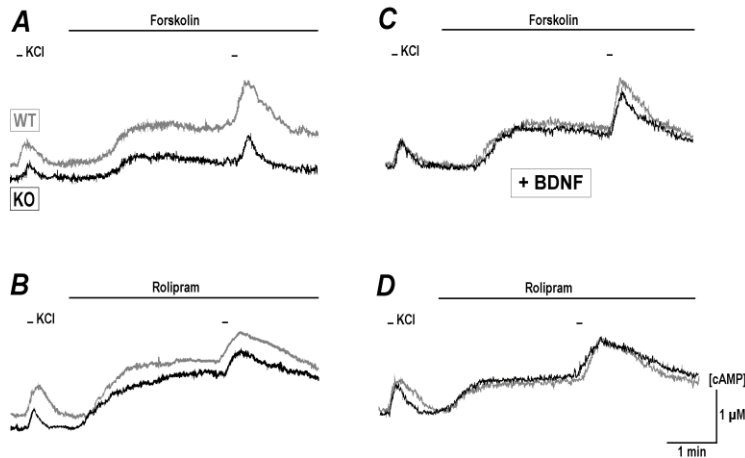


Figure 29. $[cAMP]_i$ changes induced by forskolin and rolipram and their modulation by BDNF.

High K^+ (45 mM) was applied before and after additions of 1 μ M forskolin and 1 μ M rolipram to activate AC and inhibit PDE4, respectively. The responses were measured in the wild-type and KO neurons in control (**A**, **B**) and after pretreatment of slices with 20 ng/ml BDNF for 30 min (**C**, **D**).

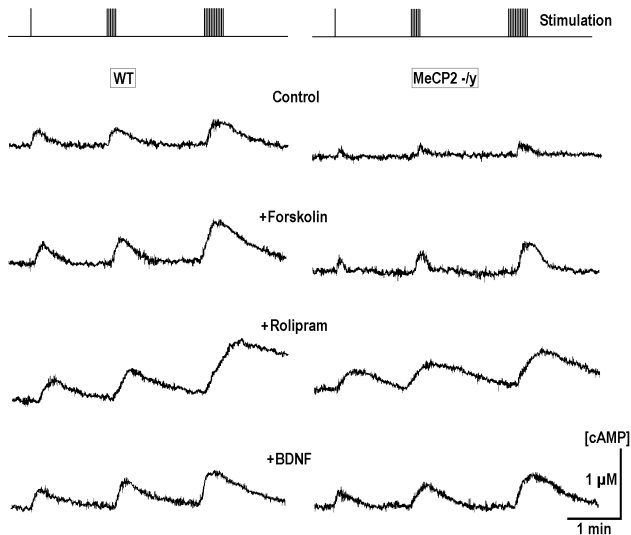


Figure 30. $[cAMP]_i$ changes evoked by electrical stimulation.

Electric pulses (10 ms, +15 V, interval 1 s) were applied to slices through bath electrodes as shown in the uppermost inset. Four rows of traces present the responses obtained in control and in the presence of 1 μ M forskolin, 1 μ M rolipram and 20 ng/ml BDNF. Note different amplitudes and time-courses of stimulus-evoked cAMP transients in WT and KO neurons and their similarity after pretreatment with BDNF.

course. WT and KO neurons showed similar differences in kinetics as described above and these differences were removed after pretreatment with BDNF (20 ng/ml for 30 min) as the two bottom traces in Fig. 30 show. This again indicates a positive role of BDNF on $[cAMP]_i$ homeostasis that can be attributed to the enhanced activity of PDE4 in KO neurons. The results of our studies point to a diminished activity of K-ATP channels in the KO neurons which play an important role in their reaction to hypoxia (Mironov et al., 1999a) and intrinsic activity (Mironov et al., 1999b) and demonstrate a crucial role of BDNF as an important factor in neurodevelopment.

6. Discussion.

This work is devoted to the investigation of morphological and physiological changes during maturation of the inspiratory neurons in the preBötC complex and their functional difference with *Mecp2* null cells used as a model of Rett Syndrome (RS). Recent findings reveal multiple physiological properties of RS, which include 1) modification of synapses during the first two weeks of development (Nelson et al., 2006; Chao et al., 2007), 2) impaired hippocampal plasticity (Asaka et al., 2006), 3) long-term potentiation (Asaka et al., 2006; Moretti et al., 2006), 4) breathing irregularities (Viemari et al., 2005; Stettner et al., 2007), 5) increased neuronal vulnerability during excitotoxicity in the cerebellum (Russell et al., 2007), and 6) enhanced susceptibility to hypoxia in the hippocampus (Fisher et al., 2008). Molecular mechanisms of RS development are still a matter of investigations (Chahrour et al., 2008; Hite et al., 2009; Gonzales and LaSalle, 2010), yet some manifestations of these genetic disturbances have already been studied with the newly-developed powerful physiology tools.

It is well known that Ca^{2+} participates in a wide range of physiological processes of signal transduction, neurotransmitter release, and is one of key players in the respiratory rhythm generation and neuronal plasticity. Here we investigated whether the origin, rates, and kinetic properties of Ca^{2+} release differ in wild-type (WT) and *Mecp2* knockout neurons (KO) under normal and hypoxic conditions. We hypothesised that disbalance in slow Ca^{2+} buffering and cAMP homeostasis may induce certain differences in the morphological organisation and mechanism of rhythmogenesis in the preBötC complex. Experiments with the use of corresponding mice KO models have recently documented that changes in *Mecp2* expression levels modify organisation of synapses, neuronal plasticity, and vulnerability, and play essential role in the development of breathing disorders in early postnatal life (Chen et al., 2001; Roloff 2005). Since deficit in *Mecp2* expression corresponds to many if not all of the clinical signs of RS (Roloff 2005; Ogier and Katz, 2008) we used KO mice as a model for RS.

6.1 Electrophysiology

The breathing activity and rhythmogenesis is a complex process that correlates with the periodic changes in oxygen consumption (Brockhaus et al., 1993), intracellular calcium (Baker et al., 1995; Koshiya and Smith, 1999; Thoby-Brisson et al., 2003; Mironov and Langohr,

2005; Potts and Paton, 2006; Ruangkittisakul et al., 2006), mitochondrial properties (Mironov et al., 2005a,b), and activity of K-ATP-sensitive channels (Haller et al., 2001). One of the most important elements of this system of respiration control and supervision is represented by the preBötC (Smith et al., 1991). Although the brainstem contains at least one more oscillator - the parafacial respiratory group (pFRG) - it is still under discussion whether the preBötC is the primary site of rhythmogenesis at all stages of development or it is overridden with the pFRG at birth (Forster, 2006; Onimaru et al., 2006). Nevertheless in normal adult animals the process of generating of breathing “rhythm” is normally dominated by preBötC while pFRG is mostly involved in providing “drive” (Janczewski et al., 2002; Borday et al., 2004; Janczewski and Feldman, 2006).

A lot of important information on the respiratory rhythmogenesis was delivered from electrophysiological studies of single respiratory neurons and from the slices showing rhythmic respiration-related activity (Matheison and Maler, 1988; Burnard et al., 1990; Nolan and Waldrop, 1993; da Costa and Behbehani, 1995; Martin-Caraballo and Greer, 1999). Our patch-clamp recordings performed in brainstem slices showed that modulation of K-ATP channel and neuronal activities by ATP and BDNF in cerebellum granule and preBötC cells are qualitatively similar. Both ATP and BDNF elicited the effects which were similar to those observed in the primary culture of preBotC neurons. This substantiates the results of detailed investigations of K-ATP channels in culture suggesting common operating mechanisms. The only difference between the effects in slices and in culture is the time-course of the responses that can be attributed to a slower delivery of the drugs to the bulk of the slice.

In the patch-clamp studies of *Mecp2* null mice the initial activity of K-ATP channels was much reduced as manifested by distinctly smaller probability of opening. Activation of these channels produces membrane hyperpolarization and enhances stability of the resting state (“a decreased vulnerability”, Yamada et al., 2001; Allen and Brown, 2004). Thus *Mecp2* $-/y$ neurons with their lower levels of channel activity should possess an enhanced excitability as compared to the wild-type. Weaker activity of ‘protective’ K-ATP channels (Ballanyi, 2004) may produce the intrinsic disturbances in calcium and cAMP homeostasis having such consequences as improper development of the synapses in *Mecp2* $-/y$ neurons as discussed below. Notably, after pretreatment with exogenous BDNF the K-ATP channels activity in the *Mecp2* $-/y$ neurons resembled that observed in the wild-type. Such positive effects of BDNF in

both cerebellum and brain stem indicate that disturbances in K-ATP channel activity in *Mecp2* null cells are probably caused by low BDNF levels and this can be compensated at least in vitro. This is in line with the recent observations demonstrating that at least some types of *Mecp2* null and BDNF lacking neurons are more vulnerable than WT cells (Fisher et al., 2008; Russell et al., 2007). Moreover, the recent findings reveal physiological properties of MeCP2 deficient cells, such as modification of synapses during the first two weeks of development (Nelson et al., 2006; Chao et al., 2007), impaired hippocampal plasticity (Asaka et al., 2006), long-term potentiation (Asaka et al., 2006; Moretti et al., 2006), and breathing irregularities (Stettner et al., 2007; Viemari et al., 2005).

It is worth noting that the results of electrophysiological studies must be treated with caution because in some cases KO genotype produces relatively small obvious phenotype compared to the one expected from the pharmacological blockade of the channels. Moreover, KO cells may compensate through reconfiguration and appropriate tuning of neuronal conductance's (Marder and Goaillard, 2006). Electrophysiological studies can provide information about electrical properties of a single cell, but to understand interaction between neurons one should examine at least a representative part of the whole network. This challenging task requires changing from electrophysiology to optical imaging.

6.2 Disturbances in network topology and neurite retraction in *Mecp2* KO mice

Calcium transients correlate with rhythmogenesis in respiratory neurons (Baker et al., 1995, Koshiya and Smith 1999, Onimaru et al 2006). At low resolution functionally intact slices demonstrate calcium transients in phase with inspiratory bursts (Mironov, 2009). Respiratory motor output is generated within the preBötC in the dispersed structures that can be associated with the unit predicted by 'group pacemaker' hypothesis (Mironov, 2009). Single-channel recordings show that inspiratory bursts appear after activation of mGluR1/5 (Mironov, 2009). Activation of this receptor in turn produces calcium waves that reach soma and activate calcium-activated nonselective cation TRPM4 channels (Mironov, 2008). These two types of channels are thought to be functionally coupled through dendritic calcium waves generated by mGluR at least in cortex (Larkium et al., 2003; Hangenston et al., 2008) and in preBötC (Mironov, 2008). Fine structure of networks can be revealed in immunofluorescence studies on

fixed cells. In the respiratory kernel, this technique was used to visualize the neurons which express NK-1, HT-5, and μ -opioid receptors, proposed to form a population of inspiratory neurons (Gray et al., 1999; Guyenet and Wang, 2001; Alheid et al., 2002; Manzke et al., 2003). Such high-resolution methods provide important data about the wiring within the networks, but say little about the function and do not allow any estimation of physiological condition of the cell.

This problem can be solved by *in vivo* imaging. However, commercial calcium indicators such as fura-2 or fluo-3 stain neurons as well as glia, producing blurred images. We used adeno associated virus leading to expression of EGFP under the neuron-specific promoter *synapsin1* to transduce neurons in the respiratory network, to map them, and to reveal their connections. AAV-mediated transduction made the neurons in slice clearly visible and, at the same time, the cells transduced with AAV retained rhythmic activity, remained electrically excitable and reacted on depolarisation. The images obtained from AAV transduction sharply contrast with the blurred pictures of neuronal somata obtained by non-selective staining with out-of-focus fluorescence from the glial cells around. These improvements in the imaging of neuronal processes allowed us to reveal the details of the fine structure of neuronal organisation of preBötC under physiological conditions and gave new unexpected results on the organization of the respiratory network. The information obtained from exclusive neuronal staining was used to analyse interactions between the neurons that formed small clusters, to reveal their structure and connections, and to obtain the wiring diagrams within the network (Mironov, 2009).

There is no clear evidence that brains of RS patients and *Mecp2* null mice exhibit morphological abnormalities (Ogier and Katz, 2008 vs. Kitt and Wilcox, 1995). The neurological dysfunction is rather profound during RS and reduction in brain size is postulated to be the only morphological change. These changes in morphology can be explained by a decrease in neuronal size rather than in the number of cells: for cortex, thalamus, basal ganglia, and hippocampus this decrease was shown by Kitt and Wilcox (1995), for dysmorphic olfactory neurons by Ronnett et al., 2003. Kitt and Wilcox also reported a decrease in the number of neurons in *substantia nigra pars compacta* (SNpc) as evidence for cell death in RS. Our data for the preBötC neurons support this finding rather than a 'no detectable cell loss' presented by Ogier and Katz in their recent review (Ogier and Katz, 2008). In our investigation,

Mecp2 null neurons of preBötC were of smaller size and had fewer connections. These data were in accordance with Larimore and Wenk, who pointed to this effect as a hallmark for RS (Larimore et al., 2008, Wenk, 1997).

The entire respiratory network in neonatal mice was estimated to consist of about 600 neurons (Feldman and Del Negro, 2006). The morphology of neurons in WT slices as well as their organisation did not change significantly within the first two postnatal months, while the morphology of neurons and network organisation in KO mice was apparently reorganized (Mironov et al., 2009). As we showed, the number of neurons, their processes and connections were decreasing in KO slices during this time, while developing in WT. In the case of strictly limited number of cells, even a small reduction in connectivity can produce irregularities in rhythm generation similar to irregularities generally observed in rhythmogenesis of RS network (for more details see Mironov, 2009). Brief hypoxia produced global calcium increase and subsequent retraction of some neuronal processes, and could decrease neuronal connectivity in the KO slices. If the network functioning becomes unstable, interruptions in breathing produce new hypoxic episodes leading to further decreases in neuronal connectivity until no rhythmic pattern is generated. Among other symptoms, the RS mouse model B6.129P2(C)-*Mecp2*^{tm1-1Bird} is characterised by spontaneous interruptions of breathing activity (Viemari et al., 2005; Stettner et al., 2007) that increase in severity and frequency. We conclude that the above time-dependent retraction results in an instability related to the appearance and progression of breathing disorders in RS.

Relevant compensatory mechanisms must be active to counteract these deleterious effects during normal development. These mechanisms should include at least one factor ubiquitously present in the brain and involved in the development of neuronal network (e.g., participating in regulation of survival and growth of neurons during development, or the establishment and maintenance of synaptic plasticity). One of the promising candidates is IGF-1 factor that participates in changes in brain structure development in *Mecp2* mutant mice. IGF1 is directly involved in development of brain size (Beck et al., 1995) and endogenous brain *Igf1* expression peaks during postnatal development (Werner et al., 1989; Daftary and Gore, 2003). IGF-1 is barely detected in the normal adult murine brain (Andersson et al., 1988; Rotwein et al., 1988; Bondy, 1991), and treatment with exogenous IGF-1 significantly improves brain reduction in mutant mice (Tropea et al., 2009). Another possible candidate is

BDNF: this highly conserved growth factor with widespread functions is ubiquitously present in soma as well as in processes of the neurons in the developing brain. BDNF is involved in survival, growth of neurons during development, and the establishment and maintenance of synaptic plasticity (Bekinschtein et al., 2008). On the other hand, BDNF transcription depends on CREB-CREST complexes and thereby involves intracellular Ca^{2+} stores and voltage-sensitive calcium channels (VSCC) into processes of regulation and formation of dendritic tree (Wong and Ghosh, 2002). We showed that cultivation of KO-neurons in presence of BDNF resulted in a normal development of neuronal network and morphology within a slice: the neurons were excitable and demonstrated a rhythmic bursting activity. Thus the process of brain degradation is at least partially reversed by a treatment with IGF-1 (Beck et al, 1995) and BDNF (Mironov et al., 2009) that both participate in early postnatal development of the brain. Worth noting that calcium signalling that regulates neurite outgrowth may change during development from an IP(3)R-mediated pathway to a RyR-mediated pathway (Arie et al., 2009) and may be another starting point for further investigations of the changes in the development of *Mecp2* null neuronal network.

Reduction of the brain size is associated not only with the decreased number of cells but also with the abnormalities in neuronal branching and maturation. RS affected organisms show reduction in dendritic branching of the pyramidal neurons in the frontal, temporal, and motor cortices (Armstrong, 2005), shortening of dendritic spines (Belichenko et al., 1994), reduced cortical dendritic arborisation (Kishi and Macklis, 2004), delayed neuronal maturation and synaptogenesis in the cerebral cortex (Fukuda et al., 2005), and reductions in synapse number in the hippocampus (Chao et al., 2007; Ogier and Katz, 2008). In view of our results we propose that spontaneous retraction of neuronal processes caused by higher levels of the resting calcium can be responsible for the diminished wiring which we observed in maturing preBötC of *Mecp2* null mice.

Dynamic process of the dendritic tree formation is characterized by extension and retraction of branches, followed by stabilization and growth (Konur and Ghosh, 2005). The early development of dendrites is regulated by either molecular signals that control various aspects of dendritic development, growth and branching or specific cell-intrinsic programs (reviewed in McAllister, 2000, Scott and Luo, 2001, Cline, 2001, Miller and Kaplan, 2003, and Jan and Jan, 2003). Semaphorin 3A, which regulates apical dendrite orientation (Polleux et al.,

2000), neurotrophins, which regulate layer-specific dendritic growth and branching (McAllister et al., 1996 and McAllister et al., 1997), Notch1, which restricts dendritic growth (Sestan et al., 1999; Redmond et al., 2000; Redmond and Ghosh, 2001), Slit-1, which acts as a dendritic branching factor (Whitford et al., 2002b), and classical cadherins and their signalling partners β -catenins, which play a role in the stabilization of dendrites and spines (Togashi et al., 2002; Yu and Malenka, 2003; Abe et al., 2004). Recent observations suggest that most of these effects are mediated by calcium signalling (Spitzer et al., 2002; Wong and Ghosh, 2002; Henley and Poo, 2004; Hua et al., 2005; McAllister, 2007).

Transient elevations of intracellular calcium are known to trigger either elongation or retraction of neuronal processes *in vivo* and *in vitro*. Many regions of the brain, including the retina, the hippocampus, and the cortex, show spontaneous calcium transients before the onset of sensory experience (Yuste et al., 1995; Feller et al., 1996; Ben-Ari et al., 1997; Garaschuk et al., 2000). This period of spontaneous network activity corresponds to a period of rapid dendritic growth, and emerging evidence suggests that dendritic growth and branching during this period are dependent on calcium signalling. The amplitude, duration, and spatial spread of calcium increases determine the resulting effect on the cell: local fast transients facilitate the attraction of neuronal processes, whereas the global long-lasting calcium increases promote their repulsion (Wong and Ghosh, 2002; Ciccolini et al., 2003; Henley and Poo, 2004; McAllister, 2007). For example, dendrites in retina are retracted after thapsigargin-induced calcium release from ER (Lohmann et al., 2002). Similar effects were observed in the preBötC neurons in response to global calcium increases induced by brief hypoxia and Ca^{2+} efflux from ER and mitochondria. The amount of retraction of neurites evoked by chemical hypoxia, CCCP, and thapsigargin in organotypic slices correlated with the amplitude of the calcium transients.

While much of the study of mechanisms of activity-dependent dendritic development has focused on intracellular mechanisms, several observations suggest that neuronal activity might also regulate dendritic patterning by regulating the production and release of factors that in turn affect dendritic growth. One such mediator is BDNF: its expression is regulated by calcium signalling in cortical neurons, and BDNF exerts a major influence on cortical dendrite development (Shieh et al., 1998; Tao et al., 1998; Gorski et al., 2003). The effects of BDNF on dendritic growth are mediated by MAP kinase and PI3-kinase signalling (Dijkhuizen and

Ghosh, 2005).

Local calcium signalling events have been shown to affect multiple aspects of dendrite elaboration including dendrite spine dynamics and formation, initiation of filopodia, and dendrite branch stability (Maletic-Savatic et al., 1999; Wu et al., 2001; Wong and Gosh, 2002). During development it may also mediate local translational events in response to activity as reported for cultured hippocampal neurons (Sutton et al., 2004). In addition to the fast local signalling effects of calcium on dendrite structure, neuronal activity initiates a delayed, prolonged response on dendrite development. In vitro studies have demonstrated that calcium influx can activate a program of signalling that propagates to the neuronal nucleus and regulates gene transcription. These nuclear events are crucial because their inhibition prevents calcium-induced dendrite growth (Redmond and Ghosh, 2005).

Calcium levels in neurons are regulated by influx through calcium channels as well as by release of calcium from the intracellular stores. Calcium influx is mediated mainly by voltage-sensitive calcium channels (VSCC) and NMDA receptors. Release from the stores principally involves calcium-induced calcium release (CICR) or activation by ligands that leads to the production of IP₃, which acts on internal stores.

Calcium increases converge onto activation of calcium/calmodulin dependent protein kinases (CaMK) and the mitogen activated protein kinase (Ras/MAPK) pathway. Two major signalling targets of calcium influx are calcium/calmodulin-dependent protein kinases (CaMKs) and mitogen-activated kinase (MAPK). Upon calcium entry via VSCC or NMDA receptors, calmodulin binds multiple calcium ions and can activate various intracellular effectors, including CaMKs (reviewed in Ghosh and Greenberg, 1995).

Regulation of the dendritic growth by calcium influx via VSCCs appears to involve calcium-dependent transcription (Redmond et al., 2002). Calcium-dependent transcription is regulated by the calcium-responsive transactivator (CREST), which contributes to the activity-induced expression of genes controlling dendrite morphology. These genes include the candidate plasticity gene-15 (cpg15), Arc, Homer, and Bdnf. Decoding the origin of calcium signalling events is coordinated by specification of the transcription of these genes; how the proteins encoded by these genes exert specific effects on dendrite morphology is yet to be revealed (Redmond and Ghosh, 2005).

6.3 Impaired calcium homeostasis in the mouse model of Rett syndrome

Besides regulating of transcription and participation in the dendritic tree formation, the intracellular calcium is a key regulator of up- and downstream processes in neuronal development (Mattson et al., 2000). We examined physiological principles underlying abnormal development of the respiratory network in RS with use of AAV-based probe with inserted coding sequence of the Ca^{2+} sensor protein D3cpv (Palmer et al., 2006). This probe provided us *in vivo* images with fine details of neuronal processes in neurons of *Mecp2* null mouse strain B6.129P2(C)-*Mecp2*^{tm1-1Bird} under physiological conditions. We have found specific alterations in calcium homeostasis in preBötC neurons of the *Mecp2* null mice. KO neurons had higher resting $[\text{Ca}^{2+}]_i$ levels and showed relatively large amplitudes of depolarisation-induced calcium transients (Mironov et al., 2009). Decay times in KO neurons were also prolonged compared to those of WT neurons thus supporting the hypothesis of improper regulation of calcium levels in the KO neurons. Higher levels of resting calcium in KO cells could cause a previously observed compromised wiring due to a decrease in the number of connections and neurons (Hartelt et al., 2008; Mironov et al., 2009). An imbalance in the intracellular calcium regulation in KO neurons might also underlie long-lasting calcium transients with large-amplitude after which neuronal processes are retracted.

Calcium resting values were set up to that typical in WT by the pretreatment of KO neurons with BDNF. Experiments with thapsigargin and CCCP point to the fact that the intracellular ER store was involved in developing both immediate transient increase with Ca^{2+} release and subsequent Ca decrease (Mironov et al., 2009). Kinetic properties of long-lasting BDNF-dependent Ca^{2+} release and experiments with thapsigargin and BDNF suggest that BDNF most probably stimulates endogenous endoplasmic reticulum Ca ATPase SERCA thus decreasing resting Ca^{2+} level. These data are also supported by the results obtained from the cerebellar granule cells pretreated with 10 ng/ml BDNF (Mhyre et al., 2000).

6.4 Interplay between calcium and cAMP

Many vitally important processes in neurons are controlled by both cAMP and Ca^{2+} (Alberts et al., 2002). Fluctuations of $[\text{Ca}^{2+}]_i$ and $[\text{cAMP}]_i$ in non-excitabile cells are often interrelated (Borodinsky and Spitzer, 2006) and linked via an increase in an AC activity or

through modulation of phosphodiesterases (Antoni, 1997; Hurley, 2006; Cooper, 2003; Willoughby and Cooper, 2007). cAMP and PKA - dependent modulations of channels and plasma membranes are known in turn to influence Ca^{2+} signal transduction. (Nakade et al., 1994; Dean et al., 1997; Holz et al., 1999 ; Bruce et al., 2003). Different isoforms of AC can be either stimulated or inhibited by Ca^{2+} (Willoughby and Cooper, 2007).

Interplay between Ca^{2+} and cAMP involves intermediate mediators and few branching steps (Alberts et al., 2002). cAMP activates cAMP-dependent protein kinase PKA, which can directly modulate effector proteins by phosphorylation at PKA-specific serine or threonine residues or can alter the levels of the effector proteins themselves by modulating gene expression. Promoters containing cAMP/ Ca^{2+} -response elements (CREs) are regulated by the transcription factor, CRE-binding protein (CREB) (Mayr and Montminy, 2001; Impey et al., 2004), which can be activated by extracellular signals that increase the intracellular levels of cAMP or Ca^{2+} (Lonze and Ginty, 2002; West et al., 2002; Conkright et al., 2003). cAMP-dependent regulation of transcription via CREB has been implicated in neurogenesis, cell survival, synaptic transmission, and cognitive function in the normal nervous system and may be defective in developmental, psychiatric and neurodegenerative disorders (Barco et al., 2002; Lonze and Ginty, 2002; Nguyen and Woo, 2003; Carlezon et al., 2005).

The changes in the $[\text{cAMP}]_i$ levels in response to the $[\text{Ca}^{2+}]_i$ transients may themselves be differentially changed by various downstream targets, e. g., PKA, CREB and Rap to initiate events such as gene expression and cell differentiation. PKA-mediated phosphorylation of channels is important for normal functioning of the channels and for maintainance of their activity mediating Ca^{2+} entry into the cytoplasm and its release from internal stores. Such phosphorylation/dephosphorylation reactions thus close the loop of regulatory feedback between Ca^{2+} and cAMP. Recently cAMP has been shown to activate not only PKA but also the guanine exchange factor Epac (de Rooij et al., 1998; Kawasaki et al., 1998). Epac in turn activates phospholipase C (PLC) (Schmidt et al., 2001), and could therefore activate PKC (Parekh et al., 2000)

Unfortunately, changes in the intracellular cAMP levels are less described than the ones of Ca^{2+} , especially those occurring in response to changes in neuronal activity. New observations involve applications of cAMP sensors which have been developed in the last decade to different neuronal preparations (Adams et al., 1991; Zaccolo et al., 2000; DiPilato et al., 2004; Nikolaev

et al., 2004; Ponsioen et al., 2004). Until now such studies have been made only in some cell lines (Terrin et al., 2006) and isolated neurons in primary culture (Dunn and Feller, 2008). Nevertheless, they reveal the complexity of cAMP dynamics in the cytoplasm. Interactions with the neighbouring neurons and the surrounding glial cells and intrinsic electrical activity of the neurons both have an important impact on $[cAMP]_i$ patterns on different time scales. Ca^{2+} fluxes of different amplitude and time-courses and spontaneous Ca^{2+} release from the internal stores can substantially modulate spatial $[cAMP]_i$. Such changes can underlie different vital cellular functions such as neuronal plasticity, differentiation, and development (Kononenko and Mironov, 1980; Huang and Kandel, 1998; Ooashi et al., 2000; West et al., 2001; Alberts et al., 2002; Liu et al., 2003; Hoogland and Saggau, 2004). Although studies of the cAMP dynamics are very promising, these investigations were restricted due to the absence of adequate tools for *in vivo* studies. Currently used cAMP sensors are bulky proteins, and the first obstacle in cAMP imaging is the delivery of the probe into the cytoplasm. There are several ways to solve this problem, each with its own advantages and difficulties. A straightforward way is a single cell injection (Adams et al., 1991) though with relatively low output and mechanical stress included. Transgenic animals would be an ideal solution and this approach has been successfully used to study cAMP signalling in the heart (Nikolaev et al., 2006), pancreatic islets (Kim et al., 2008), and the neurons of fruit-flies (Lissandron et al., 2007). Alternative possibility presents a non-cytotoxic viral gene transfer which application is not limited to a particular animal and tissue (Kügler et al., 2003; Teschemacher et al., 2005). We used a strictly neuron-specific promoter (Syn1) (Kügler et al., 2003) to deliver cAMP sensor Epac1-camps (Nikolaev et al., 2004) into the neurons in organotypic slices. As a proof of this concept, we demonstrated that Epac1-camps sensor is expressed in many neurons and reports changes in $[cAMP]_i$ levels in μM range after various physiological stimuli. We estimated resting cAMP concentrations in WT and KO cells and observed that membrane depolarisation and calcium release from the internal stores produced $[cAMP]_i$ increases that led to a further enhancement of calcium entry or calcium release through PKA-dependent phosphorylation. We have also examined some effects of cAMP homeostasis in *Mecp2* null mice and proved that positive effects of incubation with BDNF can be gated by cAMP-dependent processes as well as by Ca^{2+} . After pretreatment with BDNF, KO neurons became identical to the WT in their reaction to forskolin, rolipram and membrane depolarization while in the absence of BDNF the responses in WT and KO neurons to activation

(forskolin) and inhibition (PDE4) of AC were rather different. The WT and KO neurons possessed similar rates of the basal cAMP production whereas cAMP degradation in the KO was nearly twice as fast as in the WT cells.

It is a challenging task for future studies to determine how the effects of these two second messengers are orchestrated, and how they influence the neuronal activity. We believe that the neuronal specificity, optical stability, and sensitivity of Epac1-camp based sensor provide a solid platform for further examinations of Ca^{2+} and cAMP interaction within the respiratory neurons.

7. References

1. Abbracchio M.P., Burnstock G., Verkhratsky A., Zimmermann H. Purinergic signaling in the nervous system: an overview. *Trends Neurosci.*, 2009, 32(1), pp. 19-29.
2. Abe R., Shimizu T., Yamagishi Sh., Shibaki A., Amano Sh., Inagaki Y., Watanabe H., Sugawara H., Nakamura H., Takeuchi M., Imaizumi T., and Shimizu H. Overexpression of Pigment Epithelium-Derived Factor Decreases Angiogenesis and Inhibits the Growth of Human Malignant Melanoma Cells in Vivo. *Am. J. Pathol.*, 2004, 164, pp. 1225-1232.
3. Adams S.R., Harootunian A.T., Buechler Y.J., Taylor S.S., Tsien R.Y. Fluorescence ratio imaging of cyclicAMP in single cells. *Nature*, 1991, 349, pp. 694-697.
4. Akbarian S. Clinical experts on Rett disorder. *Developmental Neurorehabilitation*, 2002, 5, pp. 117-118.
5. Alberts B., Johnson A., Walter P., Lewis J., Raff M., Roberts K. *Molecular Biology of the Cell*. 4th edition. London, Taylor and Francis Group; 2002.
6. Alheid G.F., Gray P.A., Jiang M.C., Feldman J.L., McCrimmon D.R. Parvalbumin in respiratory neurons of the ventrolateral medulla of the adult rat. *J. Neurocytol.*, 2002, 31, pp. 693–717.
7. Allen T.G., Brown D.A. Modulation of the excitability of cholinergic basal forebrain neurones by KATP channels. *J. Physiol.*, 2004, 554(2), pp. 353-370.
8. Altar C.A., Laeng P., Jurata L.W., Brockman J.A., Lemire A., Bullard J., Bukhman Y.V., Young T.A., Charles V., Palfreyman M.G. Electroconvulsive seizures regulate gene expression of distinct neurotrophic signaling pathways. *J. Neurosci.*, 2004, 24(11), pp. 2667-2677.
9. Amir R.E., Van den Veyver I.B., Wan M., Tran C.Q., Francke U., Zoghbi H.Y. Rett syndrome is caused by mutations in X-linked *MECP2*, encoding methyl-CpG-binding

- protein 2. *Nat. Genet.*, 1999, 23(2), pp. 185-188.
10. Andersson I.K., Edwall D., Norstedt G., Rozell B., Skottner A., Hansson H.A. Differing expression of insulin-like growth factor I in the developing and in the adult rat cerebellum. *Acta Physiol. Scand.*, 1988, 132(2), pp. 167-173.
 11. Ang K.L., Antoni F.A. Reciprocal regulation of calcium dependent and calcium independent cyclic AMP hydrolysis by protein phosphorylation. *J. Neurochem.*, 2002, 81(3), pp. 422-433.
 12. Antoni F.A. Calcium regulation of adenylyl cyclase relevance for endocrine control. *Trends Endocrinol. Metab.*, 1997, 8(1), pp. 7-14.
 13. Arie Y., Iketani M., Takamatsu K., Mikoshiba K., Goshima Y., Takei K. Developmental changes in the regulation of calcium-dependent neurite outgrowth. *Biochem. Biophys. Res. Commun.*, 2009, 379(1), pp. 11-15.
 14. Armstrong D.D. Can we relate MeCP2 deficiency to the structural and chemical abnormalities in the Rett brain? *Brain Dev.*, 2005, S72-S76.
 15. Armstrong D.D. Neuropathology of Rett syndrome. *J. Child Neurol.*, 2005, 20(9), pp. 747-753.
 16. Armstrong D.D. Neuropathology of Rett syndrome. *Ment. Retard. Dev. Disabil. Res. Rev.*, 2002, 8, 72-76.
 17. Asaka Y., Jugloff D.G., Zhang L., Eubanks J.H., Fitzsimonds R.M. Hippocampal synaptic plasticity is impaired in the *Mecp2*-null mouse model of Rett syndrome. *Neurobiol. Dis.*, 2006, 21(1), pp. 217-227.
 18. Augustine G.J., Santamaria F., Tanaka K. Local calcium signaling in neurons. *Neuron*, 2003, 40, pp. 331-346.
 19. Badie-Mahdavi H., Worsley M.A., Ackley M.A., Asghar A.U., Slack J.R., King A.E. A role for protein kinase intracellular messengers in substance P- and nociceptor afferent-

- mediated excitation and expression of the transcription factor Fos in rat dorsal horn neurons in vitro. *Eur. J. Neurosci.*, 2001, 14(3), pp. 426-434.
20. Bading H., Ginty D.D., Greenberg M.E. Regulation of gene expression in hippocampal neurons by distinct calcium signaling pathways. *Science*, 1993, 260(5105), pp. 181-186.
 21. Baker R.E., Ballantyne D., Bingmann D., Jones D., Widman G. Rhythm generation in organotypic medullary cultures of newborn rats. *Int. J. Dev. Neurosci.*, 1995, 13(8), pp. 799-809.
 22. Baker-Herman T.L., Fuller D.D., Bavis R.W., Zabka A.G., Golder F.J., Doperalski N.J., Johnson R.A., Watters J.J., Mitchell G.S. BDNF is necessary and sufficient for spinal respiratory plasticity following intermittent hypoxia. *Nat. Neurosci.*, 2004, 7(1), pp. 48-55.
 23. Balkowiec A., Katz D.M. Brain-derived neurotrophic factor is required for normal development of the central respiratory rhythm in mice. *J. Physiol.*, 1998, 510 (Pt 2), pp. 527-533.
 24. Balkowiec A., Kunze D.L., Katz D.M. Brain-derived neurotrophic factor acutely inhibits AMPA-mediated currents in developing sensory relay neurons. *J. Neurosci.*, 2000, 20(5), pp. 1904-1911.
 25. Ballanyi K., Protective role of neuronal KATP channels in brain hypoxia. *J. Exp. Biol.*, 2004, 207(18), pp. 3201-3212.
 26. Ballas N., Lioy D.T., Grunseich C., Mandel G. Non-cell autonomous influence of MeCP2-deficient glia on neuronal dendritic morphology. *Nat. Neurosci.*, 2009, 12(3), pp. 311-317.
 27. Banke T.G., Bowie D., Lee H., Huganir R.L., Schousboe A., Traynelis S.F. Control of GluR1 AMPA receptor function by cAMP-dependent protein kinase. *J. Neurosci.*, 2000, 20(1), pp. 89-102.
 28. Barco A., Alarcon J.M., Kandel E.R. Expression of constitutively active CREB protein

- facilitates the late phase of long-term potentiation by enhancing synaptic capture. *Cell*, 2002, 108(5), pp. 689-703.
29. Barnes B.J., Tuong C.M., Mellen N.M. Functional imaging reveals respiratory network activity during hypoxic and opioid challenge in the neonate rat tilted sagittal slab preparation. *J. Neurophysiol.*, 2007, 97, pp.2283–2292.
 30. Beck K.D., Powell-Braxton L., Widmer H.R., Valverde J., Hefti F. Igf1 gene disruption results in reduced brain size, CNS hypomyelination, and loss of hippocampal granule and striatal parvalbumin-containing neurons. *Neuron*, 1995, 14(4), pp. 717-730.
 31. Bekinschtein P., Cammarota M., Izquierdo I., Medina J.H. BDNF and memory formation and storage. *Neuroscientist*, 2008, 14(2), pp. 147-156.
 32. Bekinschtein P., Cammarota M., Kathe C., Slipczuk L., Rossato J.I., Goldin A., Izquierdo I., Medina J.H. BDNF is essential to promote persistence of long-term memory storage. *Proc. Natl. Acad. Sci. USA*, 2008, 105(7), pp. 2711-2716.
 33. Belichenko P.V., Oldfors A., Hagberg B., Dahlström A. Rett syndrome: 3-D confocal microscopy of cortical pyramidal dendrites and afferents. *Neuroreport.*, 1994, 5(12), pp. 1509-1513.
 34. Ben-Ari Y., Khazipov R., Leinekugel X., Caillard O., Gaiarsa J.L. GABAA, NMDA and AMPA receptors: a developmentally regulated 'ménage à trois'. *Trends Neurosci.*, 1997, 20(11), pp. 523-529.
 35. Berg J.M., Tymoczko J.L., Stryer L. *Biochemistry*. 5th ed. W. H. Freeman and Company, 2002.
 36. Berridge M.J. Neuronal calcium signaling. *Neuron*, 1998, 21(1), pp. 13-26.
 37. Beyer K.S., Blasi F., Bacchelli E., Klauck S.M., Maestrini E., Poustka A. Mutation analysis of the coding sequence of the MECP2 gene in infantile autism. *Hum Genet.* 2002;111:305–309.

38. Bianchi A., Denavit-Saubie M., Champagnat J. Central control of breathing in mammals: neuronal circuitry, membrane properties and neurotransmitters. *Physiol. Rev.*, 1995, 75, p. 1-45.
39. Bissonnette J.M., Knopp S.J. Effect of inspired oxygen on periodic breathing in methyl-CpG-binding protein 2 (*Mecp2*) deficient mice. *J. Appl. Physiol.*, 2008, 104(1), pp. 198-204.
40. Bissonnette J.M., Knopp S.J. Separate respiratory phenotypes in methyl-CpG-binding protein 2 (*Mecp2*) deficient mice. *Pediatr. Res.*, 2006, 59(4), pp. 513-518.
41. Bissonnette J.M., Knopp S.J., Maylie J., Thong T. Autonomic cardiovascular control in methyl-CpG-binding protein 2 (*Mecp2*) deficient mice. *Auton. Neurosci.*, 2007, 136(1-2), pp. 82-89.
42. Blackstone C., Murphy T.H., Moss S.J., Baraban J.M., Huganir R.L. Cyclic AMP and synaptic activity-dependent phosphorylation of AMPA-preferring glutamate receptors. *J. Neurosci.*, 1994, 14(12), pp. 7585-7593.
43. Blum R.K., Kafitz W., Konnerth A. Neurotrophin-evoked depolarization requires the sodium channel Na(V)1.9. *Nature*, 2002, 419, pp. 687-693.
44. Bondy C.A. Transient IGF-I gene expression during the maturation of functionally related central projection neurons. *J. Neurosci.*, 1991, 11(11), pp. 3442-3455.
45. Bonham A.C. Neurotransmitters in the CNS control of breathing. *Respir. Physiol.*, 1995, 101(3), pp. 219-330.
46. Borday C., Wrobel L., Fortin G., Champagnat J., Thaëron-Antônio C., Thoby-Brisson M. Developmental gene control of brainstem function: views from the embryo. *Prog. Biophys. Mol. Biol.*, 2004, 84(2-3), pp. 89-106.
47. Borodinsky L.N., Spitzer N.C. Second messenger pas de deux: the coordinated dance between calcium and cAMP. *Sci. STKE*, 2006, 336, pp. 22.

48. Bouvier J., Autran S., Dehorter N., Katz D.M., Champagnat J., Fortin G., Thoby-Brisson M. Brain-derived neurotrophic factor enhances fetal respiratory rhythm frequency in the mouse preBötzing complex in vitro. *Eur. J. Neurosci.*, 2008, 28(3), pp. 510-520.
49. Bouvier J., Autran S., Fortin G., Champagnat J., Thoby-Brisson M. Acute role of the brain-derived neurotrophic factor (BDNF) on the respiratory neural network activity in mice in vitro. *J. Physiol. Paris.*, 2006, 100(5-6), pp. 290-296.
50. Bramham C.R., Messaoudi E. BDNF function in adult synaptic plasticity: the synaptic consolidation hypothesis. *Prog. Neurobiol.*, 2005, 76(2), pp. 99-125.
51. Brockhaus J., Ballanyi K., Smith J.C., Richter D.W. Microenvironment of respiratory neurons in the in vitro brainstem-spinal cord of neonatal rats. *J. Physiol.*, 1993, 462, pp.421-445.
52. Browning K.N., Travagli R.A. The peptide TRH uncovers the presence of presynaptic 5-HT1A receptors via activation of a second messenger pathway in the rat dorsal vagal complex. *J. Physiol.*, 2001, 531(2), pp. 425-435.
53. Bruce J.I., Yule D.I., Shuttleworth T.J. Ca^{2+} -dependent protein kinase--a modulation of the plasma membrane Ca^{2+} -ATPase in parotid acinar cells. *J. Biol. Chem.*, 2002, 277(50), pp. 48172-48181.
54. Budden S., Meek M., Henighan C. Communication and oral-motor function in Rett syndrome. *Dev. Med. Child Neurol.*, 1990, 32(1), pp. 51-55.
55. Budden S.S., Dorsey H.C., Steiner R.D. Clinical profile of a male with Rett syndrome. *Brain Dev.*, 2005, 1, pp. 69-71.
56. Byrne J.H., Kandel E.R. Presynaptic facilitation revisited: state and time dependence. *J. Neurosci.*, 1996, 16(2), pp. 425-435.
57. Cai X., Gu Z., Zhong P., Ren Y., Yan Z. Serotonin 5-HT1A receptors regulate AMPA receptor channels through inhibiting Ca^{2+} /calmodulin-dependent kinase II in prefrontal

- cortical pyramidal neurons. *J. Biol. Chem.*, 2002, 277(39), pp. 36553-36562.
58. Cantallops I., Haas K., Cline H.T. Postsynaptic CPG15 promotes synaptic maturation and presynaptic axon arbor elaboration in vivo. *Nat. Neurosci.*, 2000, 3(10), pp. 1004-11.
59. Carlezon W.A. Jr, Duman R.S., Nestler E.J. The many faces of CREB. *Trends. Neurosci.*, 2005, 28(8), pp. 436-445.
60. Carney R.M., Wolpert C.M., Ravan S.A., Shahbazian M., Ashley-Koch A., Cuccaro M.L., Vance J.M., Pericak-Vance M.A. Identification of MeCP2 mutations in a series of females with autistic disorder. *Pediatr Neurol.* 2003;28:205–211.
61. Catterall W.A., Few A.P. Calcium channel regulation and presynaptic plasticity. *Neuron*, 2008, 59(6), pp. 882-901.
62. Chahrour M., Jung S.Y., Shaw C., Zhou X., Wong S.T., Qin J., Zoghbi H.Y. MeCP2, a key contributor to neurological disease, activates and represses transcription. *Science*, 2008, 320(5880), pp. 1224-1229.
63. Chahrour M., Zoghbi H.Y. The story of Rett syndrome: from clinic to neurobiology. *Neuron*, 2007, 56(3), pp. 422-437.
64. Champagnat J., Denavit-Saubié M., Henry J.L., Leviel V. Catecholaminergic depressant effects on bulbar respiratory mechanisms. *Brain Res.*, 1979, 160(1), pp. 57-68.
65. Chao H.T., Zoghbi H.Y., Rosenmund C. MeCP2 controls excitatory synaptic strength by regulating glutamatergic synapse number. *Neuron*, 2007, 56(1), pp. 58-65.
66. Chen R.Z., Akbarian S., Tudor M., Jaenisch R. Deficiency of methyl-CpG binding protein-2 in CNS neurons results in a Rett-like phenotype in mice. *Nat Genet.*, 2001, 27(3), pp. 327-331.
67. Chen W.G., Chang Q., Lin Y., Meissner A., West A.E., Griffith E.C., Jaenisch R.,

- Greenberg M.E. Derepression of BDNF transcription involves calcium-dependent phosphorylation of MeCP2. *Science*, 2003; 302(5646), pp. 885-889.
68. Chowdhury S., Shepherd J.D., Okuno H., Lyford G., Petralia R.S., Plath N., Kuhl D., Huganir R.L., Worley P.F. Arc/Arg3.1 interacts with the endocytic machinery to regulate AMPA receptor trafficking. *Neuron*, 2006, 52, pp. 445-459.
69. Ciccolini F., Collins T.J., Sudhoelter J., Lipp P., Berridge M.J., Bootman M.D. Local and global spontaneous calcium events regulate neurite outgrowth and onset of GABAergic phenotype during neural precursor differentiation. *J. Neurosci.*, 2003, 23(1), pp. 103-111.
70. Clayton-Smith J., Watson P., Ramsden S., Black G.C. Somatic mutation in MECP2 as a non-fatal neurodevelopmental disorder in males. *Lancet*, 2000, 356, pp. 830-832.
71. Cline H. Synaptogenesis: a balancing act between excitation and inhibition. *Curr. Biol.* 2005, 15(6), pp. 203-205.
72. Cline H.T. Dendritic arbor development and synaptogenesis. *Curr. Opin. Neurobiol.*, 2001, 11(1), pp. 118-126.
73. Collins A.L, Levenson J.M, Vilaythong A.P., Richman R., Armstrong D.L., Noebels J.L., David Sweatt J., Zoghbi H.Y. Mild overexpression of MeCP2 causes a progressive neurological disorder in mice. *Hum. Mol. Genet.*, 2004, 13(21), pp. 2679-2689.
74. Colwell C.S., Levine M.S. Excitatory synaptic transmission in neostriatal neurons: regulation by cyclic AMP-dependent mechanisms. *J. Neurosci.*, 1995, 15(3), pp. 1704-1713.
75. Conkright M.D., Guzmán E., Flechner L., Su A.I., Hogenesch J.B., Montminy M. Genome-wide analysis of CREB target genes reveals a core promoter requirement for cAMP responsiveness. *Mol. Cell.*, 2003, 11(4), pp. 1101-8. Erratum in: *Mol Cell.*, 2003, 11(5), p. 1417.
76. Cooper D.M. Regulation and organization of adenylyl cyclases and cAMP. *Biochem. J.*,

2003, 375(3), pp. 517-529.

77. Crowder E.A., Saha M.S., Pace R.W., Zhang H., Prestwich G.D., Del Negro C.A. Phosphatidylinositol 4,5-bisphosphate regulates inspiratory burst activity in the neonatal mouse preBötzinger complex. *J. Physiol.*, 2007, 582(3), pp. 1047-1058.
78. Daftary S.S., Gore A.C. Developmental changes in hypothalamic insulin-like growth factor-1: relationship to gonadotropin-releasing hormone neurons. *Endocrinology*, 2003, 144(5), pp. 2034-2045.
79. Dani V.S., Chang Q., Maffei A., Turrigiano G.G., Jaenisch R., Nelson S.B. Reduced cortical activity due to a shift in the balance between excitation and inhibition in a mouse model of Rett syndrome. *Proc. Natl. Acad. Sci. USA*, 2005, 102(35), pp. 12560-12565.
80. Davies A.M. The role of neurotrophins during successive stages of sensory neuron development. *Prog. Growth Factor Res.*, 1994, 5(3), pp. 263-289.
81. de Boer J., Philpott A.J., van Amsterdam R.G., Shahid M., Zaagsma J. Human bronchial cyclic nucleotide phosphodiesterase isoenzymes: biochemical and pharmacological analysis using selective inhibitors. *Br. J. Pharmacol.*, 1992, 106, pp. 1028-1034.
82. de Rooij J., Zwartkruis F.J., Verheijen M.H., Cool R.H., Nijman S.M., Wittinghofer A., Bos J.L. Epac is a Rap1 guanine-nucleotide-exchange factor directly activated by cyclic AMP. *Nature*, 1998, 396(6710), pp. 474-477.
83. Dean W.L., Chen D., Brandt P.C., Vanaman T.C. Regulation of platelet plasma membrane Ca²⁺-ATPase by cAMP-dependent and tyrosine phosphorylation. *J. Biol. Chem.*, 1997, 272(24), pp. 15113-15119.
84. Del Negro C.A., Koshiya N., Butera R.J. Jr, Smith J.C. Persistent sodium current, membrane properties and bursting behavior of pre-bötzinger complex inspiratory neurons in vitro. *J Neurophysiol.* 2002 Nov; 88(5), pp. 2242-2250.

85. Del Negro C.A., Morgado-Valle C., Hayes J.A., Mackay D.D., Pace R.W., Crowder E.A., Feldman J.L. Sodium and calcium current-mediated pacemaker neurons and respiratory rhythm generation. *J. Neurosci.*, 2005, 25(2), pp. 446-453.
86. Deng V, Matagne V, Banine F, Frerking M, Ohliger P, Budden S, Pevsner J, Dissen GA, Sherman LS, Ojeda SR. FXYD1 is an MeCP2 target gene overexpressed in the brains of Rett syndrome patients and *Mecp2*-null mice. *Hum Mol Genet.* 2007 Mar 15; 16(6), pp. 640-650.
87. Desai N.S., Rutherford L.C., Turrigiano G.G. BDNF regulates the intrinsic excitability of cortical neurons. *Learn Mem.* 1999 May-Jun; 6(3), pp. 284-291.
88. D'Esposito M., Quaderi N.A., Ciccodicola A., Bruni P., Esposito T., D'Urso M., Brown SD. Isolation, physical mapping, and northern analysis of the X-linked human gene encoding methyl CpG-binding protein, MECP2. *Mamm Genome* 1996; 7:533-535.
89. Di Fiore B., Palena A., Felsani A., Palitti F., Caruso M., Lavia P. Cytosine methylation transforms an E2F site in the retinoblastoma gene promoter into a binding site for the general repressor methylcytosine-binding protein 2 (MeCP2). *Nucleic Acids Res.* 1999 Jul 15; 27(14), pp. 2852-2859.
90. Dijkhuizen P.A., Ghosh A. BDNF regulates primary dendrite formation in cortical neurons via the PI3-kinase and MAP kinase signaling pathways. *J Neurobiol.* 2005 Feb 5; 62(2), pp. 278-288.
91. DiPilato L.M., Cheng X., Zhang J. Fluorescent indicators of cAMP and Epac activation reveal differential dynamics of cAMP signaling within discrete subcellular compartments. *Proc Natl Acad Sci USA* 2004, 101:16513-16518.
92. Dunn T.A., Feller M.B. Imaging second messenger dynamics in developing neural circuits. *Dev Neurobiol* 2008, 68:835-844.
93. Elsen F.P., Ramirez J.M. Calcium currents of rhythmic neurons recorded in the isolated respiratory network of neonatal mice. *J Neurosci.* 1998; 18:10652–10662.

94. Erickson J.T., Conover J.C., Borday V., Champagnat J., Barbacid M., Yancopoulos G., Katz D.M. Mice lacking brain-derived neurotrophic factor exhibit visceral sensory neuron losses distinct from mice lacking NT4 and display a severe developmental deficit in control of breathing. *J Neurosci.* 1996 Sep 1; 16(17), pp. 5361-5371.
95. Fabiato A., Fabiato F. Calcium and cardiac excitation-contraction coupling. *Annu Rev Physiol.* 1979; 41:473-484.
96. Fabiato A., Fabiato F. Use of chlorotetracycline fluorescence to demonstrate Ca^{2+} -induced release of Ca^{2+} from the sarcoplasmic reticulum of skinned cardiac cells. *Nature.* 1979 Sep 13; 281(5727), pp. 146-148.
97. Felder C.C. Muscarinic acetylcholine receptors: signal transduction through multiple effectors. *FASEB J.* 1995 May; 9(8), pp. 619-625.
98. Feldman J.L., Del Negro C.A. Looking for inspiration: new perspectives on respiratory rhythm. *Nat Rev Neurosci* 2006, 7:232-242.
99. Feldman J.L., Smith J.C. Cellular mechanisms underlying modulation of breathing pattern in mammals. *Ann N Y Acad Sci.* 1989; 563:114-130.
100. Feller M.B., Delaney K.R., Tank D.W. Presynaptic calcium dynamics at the frog retinotectal synapse. *J Neurophysiol.* 1996 Jul; 76(1), pp. 381-400.
101. Fields R.D., Burnstock G. Purinergic signalling in neuron-glia interactions. *Nat Rev Neurosci.* 2006 Jun; 7(6), pp. 423-436.
102. Fischer M., Reuter J., Gerich F.J., Hildebrandt B., Hägele S., Katschinski D., Müller M. Enhanced hypoxia susceptibility in hippocampal slices from a mouse model of rett syndrome. *J Neurophysiol.* 2009 Feb; 101(2), pp. 1016-1032.
103. Fong A., Krstew E., Barden J., and Lawrence A. (2002). Immunoreactive localisation of P2Y1 receptors within the rat and human nodose ganglia and rat brainstem: comparison with [α 33P]deoxyadenosine 5'-triphosphate autoradiography. *Neuroscience* 113, 809.

104. Forster H. V. The parafacial respiratory group (pFRG)/pre-Botzinger complex (preBotC) is the primary site of respiratory rhythm generation in the mammal. *J Appl Physiol* 100: 2103-2108, 2006.
105. Francke U. Mechanisms of disease: neurogenetics of MeCP2 deficiency. *Nat Clin Pract Neurol*. 2006 Apr; 2(4), pp. 212-221.
106. Frermann D., Keller B.U., Richter D.W. Calcium oscillations in rhythmically active respiratory neurones in the brainstem of the mouse. *J Physiol*. 1999 Feb 15; 515 (Pt 1), pp. 119-131.
107. Fukuda T., Itoh M., Ichikawa T., Washiyama K., Goto Y. Delayed maturation of neuronal architecture and synaptogenesis in cerebral cortex of *Mecp2*-deficient mice. *J Neuropathol Exp Neurol*. 2005 Jun; 64(6), pp. 537-544.
108. Funk G.D., Johnson S.M., Smith J.C., Dong X.W., Lai J., Feldman J.L. Functional respiratory rhythm generating networks in neonatal mice lacking NMDAR1 gene. *J Neurophysiol*. 1997; 78:1414–1420.
109. Funk G.D., Kanjhan R., Walsh C., Lipski J., Comer A.M., Parkis M.A., Housley G.D. P2 receptor excitation of rodent hypoglossal motoneuron activity in vitro and in vivo: a molecular physiological analysis. *J Neurosci*. 1997 Aug 15; 17(16), pp. 6325-6337.
110. Funke F., Dutschmann M., Muller M. Imaging of respiratory-related population activity with single-cell resolution. *Am J Physiol Cell Physiol*. 2007; 292, pp.508–516.
111. Garaschuk O., Linn J., Eilers J., Konnerth A. Large-scale oscillatory calcium waves in the immature cortex. *Nat Neurosci*. 2000 May; 3(5), pp. 452-459.
112. Gaultier C., Gallego J. Neural control of breathing: insights from genetic mouse models. *J Appl Physiol*. 2008 May; 104(5), pp. 1522-1530. Epub 2008 Jan 24. Review.
113. Ge Q., Feldman J.L. AMPA receptor activation and phosphatase inhibition affect neonatal rat respiratory rhythm generation. *J Physiol*. 1998 May 15; 509 (Pt 1), pp. 255-266.

114. Georgel P.T., Horowitz-Scherer R.A., Adkins N., Woodcock C.L., Wade P.A., Hansen J.C. Chromatin compaction by human MeCP2. Assembly of novel secondary chromatin structures in the absence of DNA methylation. *J Biol Chem.* 2003 Aug 22; 278(34), pp. 32181-32188.
115. Ghosh A., Carnahan J. and Greenberg M.E., Requirement for BDNF in activity-dependent survival of cortical neurons, *Science* 263 (1994), pp. 1618–1623.
116. Ghosh A., Greenberg M.E. Calcium signaling in neurons: molecular mechanisms and cellular consequences. *Science.* 1995 Apr 14; 268(5208), pp. 239-247. Review.
117. Gonzales M.L., LaSalle J.M. The role of MeCP2 in brain development and neurodevelopmental disorders. *Curr Psychiatry Rep.* 2010 Apr; 12(2), pp. 127-134.
118. Gonzalez M., Collins W.F. 3rd. Modulation of motoneuron excitability by brain-derived neurotrophic factor. *J Neurophysiol.* 1997 Jan; 77(1), pp. 502-506.
119. Gorski J.A., Zeiler S.R., Tamowski S., Jones K.R. Brain-derived neurotrophic factor is required for the maintenance of cortical dendrites. *J Neurosci.* 2003 Jul 30;23(17), pp. 6856-6865.
120. Gourine A.V., Atkinson L., Deuchars J., and Spyer K.M. (2003). Purinergic signaling in the medullary mechanisms of respiratory control in the rat: respiratory neurones express the P2X2 receptor subunit. *J Physiol* 552, 197–211.
121. Gourine A.V., Llaudet E., Dale N., and Spyer K.M (2005b). Release of ATP in the ventral medulla during hypoxia in rats: role in hypoxic ventilatory response. *J Neurosci* 25, 1211–1218.
122. Gourine A.V., Llaudet E., Dale N., and Spyer K.M. (2005a). ATP is a mediator of chemosensory transduction in the central nervous system. *Nature* 436, 108–111.
123. Gourine A.V., Wood J.D., Burnstock G. Purinergic signalling in autonomic control. *Trends Neurosci.* 2009 May; 32(5), pp. 241-248.

124. Gray P.A., Janczewski W.A., Mellen N., McCrimmon D.R., Feldman J.L. Normal breathing requires preBötzing complex neurokinin-1 receptor-expressing neurons. *Nat Neurosci.* 2001; 4:927–930.
125. Gray P.A., Rekling J.C., Bocchiario C.M., and Feldman J.L. Modulation of respiratory frequency by peptidergic input to rhythmogenic neurons in the preBotzinger complex. *Science*, 1999, 286, 1566–1568.
126. Greengard P, Jen J., Nairn A.C., Stevens C.F. Enhancement of the glutamate response by cAMP-dependent protein kinase in hippocampal neurons. *Science*. 1991 Sep 6; 253(5024), pp. 1135-8.
127. Greer P.L., Greenberg M.E. From synapse to nucleus: calcium-dependent gene transcription in the control of synapse development and function. *Neuron*. 2008 Sep 25; 59(6), pp. 846-860.
128. Grynkiewicz G., Poenie M., Tsien R.Y. A new generation of Ca^{2+} indicators with greatly improved fluorescence properties. *J Biol Chem*. 1985 Mar 25; 260(6), pp. 3440-3450.
129. Guy J., Gan J., Selfridge J., Cobb S., Bird A. Reversal of neurological defects in a mouse model of Rett syndrome. *Science*. 2007 Feb 23; 315(5815), pp. 1143-1147.
130. Guy J., Hendrich B., Holmes M., Martin J.E., Bird A. A mouse *Mecp2*-null mutation causes neurological symptoms that mimic Rett syndrome. *Nat Genet*. 2001 Mar; 27(3), pp. 322-326.
131. Guyenet P.G., Wang H. Pre-Bötzing neurons with preinspiratory discharges "in vivo" express NK1 receptors in the rat. *J Neurophysiol*. 2001 Jul; 86(1), pp. 438-446.
132. Hagberg B.; Aicardi J.; Dias K.; Ramos O. A progressive syndrome of autism, dementia, ataxia, and loss of purposeful hand use in girls: Rett's syndrome: report of 35 cases. *Ann Neurol* 1983 Oct; 14(4), pp. 471-479.
133. Hagenston A.M., Fitzpatrick J.S., Yeckel M.F. MGluR-mediated calcium waves that invade the soma regulate firing in layer V medial prefrontal cortical pyramidal neurons.

Cereb Cortex. 2008 Feb; 18(2), pp. 407-423.

134. Haji A., Ohi Y. Ryanodine receptor/ Ca^{2+} release mechanism in rhythmically active respiratory neurons of cats in vivo. *Neuroscience*. 2006; 140:343–354.

135. Haji A., Pierrefiche O., Lalley P.M., and Richter, D.W. Protein kinase C pathways modulate respiratory pattern generation in the cat. *J. Physiol*. 1996 494, pp. 297–306.

136. Haller M., Mironov S.L., Karschin A., Richter D.W. Dynamic activation of K-ATP channels in rhythmically active neurons. *J Physiol*. 2001 Nov 15; 537(Pt 1), pp. 69-81.

137. Hanoune J., Defer N. Regulation and role of adenylyl cyclase isoforms. *Annu Rev Pharmacol Toxicol*. 2001; 41:145-174.

138. Harbeck M.C., Chepurny O., Nikolaev V.O., Lohse M.J., Holz G.G. Simultaneous optical measurements of cytosolic Ca^{2+} and cAMP in single cells. *Sci STKE* 2006, (353), p. pl6.

139. Hartelt N., Skorova E., Suhr M., Manzke T., Mironova L., Kügler S., Mironov S.L. Imaging of respiratory network topology in living brain slices. *Mol Cell Neurosci* 2008, 37:425-431.

140. Henley J., Poo M.M. Guiding neuronal growth cones using Ca^{2+} signals. *Trends Cell Biol*. 2004 Jun; 14(6), pp. 320-330. Review.

141. Higley M.J. and Sabatini B.L. Calcium signaling in dendrites and spines: practical and functional considerations, *Neuron* 59, 2008, pp. 902–913.

142. Hite K.C., Adams V.H., Hansen J.C. Recent advances in MeCP2 structure and function. *Biochem Cell Biol*., 2009, 87(1), pp.:219-227.

143. Holz G.G., Leech C.A., Heller R.S., Castonguay M., Habener J.F. cAMP-dependent mobilization of intracellular Ca^{2+} stores by activation of ryanodine receptors in pancreatic beta-cells. A Ca^{2+} signaling system stimulated by the insulinotropic hormone glucagon-like peptide-1-(7-37). *J Biol Chem*., 1999, 274(20), pp.14147-14156.

144. Hong E.J., McCord A.E., Greenberg M.E. A biological function for the neuronal activity-dependent component of Bdnf transcription in the development of cortical inhibition. *Neuron*, 2008, 60(4), pp. 610-624.
145. Hong S.J., Li H., Becker K.G., Dawson V.L. and Dawson T.M., Identification and analysis of plasticity-induced late-response genes, *Proc. Natl. Acad. Sci. USA* 101, 2004, pp. 2145–2150.
146. Hoogland T.M., Saggau P. Facilitation of L-type Ca²⁺- channels in dendritic spines by activation of beta2 adrenergic receptors. *J Neurosci* 2004, 24:8416-8427.
147. Horike S., Cai S., Miyano M., Cheng J.F., Kohwi-Shigematsu T. Loss of silent-chromatin looping and impaired imprinting of DLX5 in Rett syndrome. *Nat Genet.*, 2005, 37(1), pp.31-40.
148. Hua J.Y., Smear M.C., Baier H., Smith S.J. Regulation of axon growth in vivo by activity-based competition. *Nature*, 2005, 434(7036), pp.1022-1026.
149. Huang Y.Y., Kandel E.R. Postsynaptic induction and PKA-dependent expression of LTP in the lateral amygdala. *Neuron*, 1998, 21, pp.169-178.
150. Hurley R.L., Barré L.K., Wood S.D., Anderson K.A., Kemp B.E., Means A.R., Witters L.A. Regulation of AMP-activated protein kinase by multisite phosphorylation in response to agents that elevate cellular cAMP. *J Biol Chem.*, 2006, 281(48), pp. 36662-36672.
151. Ide S., Itoh M., Goto Y. Defect in normal developmental increase of the brain biogenic amine concentrations in the *mecp2*-null mouse. *Neurosci Lett.*, 2005, 386(1), pp. 14-17.
152. Impey S., McCorkle S.R., Cha-Molstad H., Dwyer J.M., Yochum G.S., Boss J.M., McWeeney S., Dunn J.J., Mandel G., Goodman R.H. Defining the CREB regulon: a genome-wide analysis of transcription factor regulatory regions. *Cell*, 2004, 119(7), pp.1041-1054.
153. Isaacs A.M., Oliver P.L., Jones E.L., Jeans A., Potter A., Hovik B.H., Nolan P.M., Vizer L., Glenister P., Simon A.K., Gray I.C., Spurr N.K., Brown S.D., Hunter A.J., Davies K.E. A mutation in Af4 is predicted to cause cerebellar ataxia and cataracts in the robotic

mouse. *J Neurosci.*, 2003, 23(5), pp. 1631-1637.

154. Itoh M., Ide S., Takashima S., Kudo S., Nomura Y., Segawa M., Kubota T., Mori H., Tanaka S., Horie H., Tanabe Y., Goto Y. Methyl CpG-binding protein 2 (a mutation of which causes Rett syndrome) directly regulates insulin-like growth factor binding protein 3 in mouse and human brains. *J Neuropathol Exp Neurol.*, 2007, 6(2), pp.117-123.

155. Jan Y.N., Jan L.Y. The control of dendrite development. *Neuron*, 2003, 40(2), pp.229-242. Review.

156. Janczewski W.A., Feldman J.L. Novel data supporting the two respiratory rhythm oscillator hypothesis. Focus on "respiration-related rhythmic activity in the rostral medulla of newborn rats. *J Neurophysiol.*, 2006, 96(1), pp. 1-2.

157. Janczewski W.A., Onimaru H., Homma I., Feldman J.L. Opioid-resistant respiratory pathway from the preinspiratory neurones to abdominal muscles: in vivo and in vitro study in the newborn rat. *J Physiol.*, 2002, 545(3), pp.1017-1026.

158. Johnson S.M., Smith J.C., Feldman J.L. Modulation of respiratory rhythm in vitro: role of Gi/o protein-mediated mechanisms. *J Appl Physiol.*, 1996, 80(6), pp.2120-2133.

159. Jonas P. and Burnashev N. Molecular mechanisms controlling calcium entry through AMPA-type glutamate receptor channels. *Neuron*, 1995, 15, pp. 987–990.

160. Kamenetsky M., Middelhaufe S., Bank E.M., Levin L.R., Buck J., Steegborn C. Molecular details of cAMP generation in mammalian cells: a tale of two systems. *J Mol Biol.*, 2006, 362(4), pp. 623-639. Review.

161. Kameyama K., Lee H.K., Bear M.F., Huganir R.L. Involvement of a postsynaptic protein kinase A substrate in the expression of homosynaptic long-term depression. *Neuron*, 1998, 21(5), pp.1163-1175.

162. Kang G., Joseph J.W., Chepurny O.G., Monaco M., Wheeler M.B., Bos J.L., Schwede F., Genieser H.G., Holz G.G. Epac-selective cAMP analog 8-pCPT-2'-O-Me-cAMP as a stimulus for Ca²⁺-induced Ca²⁺ release and exocytosis in pancreatic beta-cells. *J. Biol.*

Chem., 2003, 278, pp. 8279-8285.

163. Kang H., Schuman E.M. Long-lasting neurotrophin-induced enhancement of synaptic transmission in the adult hippocampus, *Science*, 1995, 267, pp. 1658–1662.

164. Kanjhan R., Housley G.D., Burton L.D., Christie D.L., Kippenberger A., Thorne P.R., Luo L., Ryan A.F. Distribution of the P2X2 receptor subunit of the ATP-gated ion channels in the rat central nervous system. *J. Comp. Neurol.*, 1999, 407(1), pp. 11-32.

165. Kawasaki H., Springett G.M., Mochizuki N., Toki S., Nakaya M., Matsuda M., Housman D.E., Graybiel A.M. A family of cAMP-binding proteins that directly activate Rap1. *Science*, 1998, 282(5397), pp. 2275-2279.

166. Khawaja A.M. and Rogers D.F. Tachykinins: receptor to effector. *Int. J. Biochem. Cell Biol.*, 1996, 28(7), pp. 721-738.

167. Kim J.W., Roberts C.D., Berg S.A., Caicedo A., Roper SD. Imaging cyclic AMP changes in pancreatic islets of transgenic reporter mice. *PLoS ONE*, 2008, 3:e2127.

168. Kishi N., Macklis J.D. MECP2 is progressively expressed in post-migratory neurons and is involved in neuronal maturation rather than cell fate decisions. *Mol. Cell Neurosci.*, 2004, 27(3), pp. 306-321.

169. Kitt C.A., Wilcox B.J. Preliminary evidence for neurodegenerative changes in the substantia nigra of Rett syndrome. *Neuropediatrics*, 1995, 26(2), pp. 114-118.

170. Kononenko N.I., Mironov S.L. The effects of intracellular cAMP injection on the electric characteristics of snail neurons. *Neurophysiology*, 1980, 12, pp. 485-492.

171. Konur S., Ghosh A. Calcium signaling and the control of dendritic development. *Neuron*, 2005, 46(3), p. 401-405.

172. Korte M., Carroll P., Wolf E., Brem G., Thoenen H., Bonhoeffer T. Hippocampal long-term potentiation is impaired in mice lacking brain-derived neurotrophic factor. *Proc. Natl. Acad. Sci. USA*. 1995, 92(19), pp. 8856-8860.

173. Koshiya N., Smith J.C. Neuronal pacemaker for breathing visualized in vitro. *Nature*, 1999, 400, pp. 360–363.
174. Kovalchuk Y., Hanse E., Kafitz K.W., Konnerth A. Postsynaptic Induction of BDNF-Mediated Long-Term Potentiation. *Science*, 2002, 295(5560), pp. 1729-1734.
175. Kriaucionis S., Paterson A., Curtis J., Guy J., Macleod N., Bird A. Gene expression analysis exposes mitochondrial abnormalities in a mouse model of Rett syndrome. *Mol. Cell. Biol.*, 2006, 26(13), pp. 5033-5042.
176. Kron M., Mörschel M., Reuter J., Zhang W., Dutschmann M. Developmental changes in brain-derived neurotrophic factor-mediated modulations of synaptic activities in the pontine Kölliker-Fuse nucleus of the rat. *J. Physiol.*, 2007, 583(1), pp. 315-327.
177. Kron M., Zhang W., Dutschmann M. Developmental changes in the BDNF-induced modulation of inhibitory synaptic transmission in the Kölliker-Fuse nucleus of rat. *Eur. J. Neurosci.*, 2007, 26(12), pp. 3449-3457.
178. Kügler S., Hahnewald R., Garrido M., Reiss J. Long-term rescue of a lethal inherited disease by adeno-associated virus-mediated gene transfer in a mouse model of molybdenum-cofactor deficiency. *Am J Hum Genet.*, 2007, 80(2), pp. 291-297.
179. Kügler S., Kilic E., Bähr M. Human synapsin 1 gene promoter confers highly neuron-specific long-term transgene expression from an adenoviral vector in the adult rat brain depending on the transduced area. *Gene Ther.*, 2003, 10, pp. 337-247.
180. Kügler S., Meyn L., Holzmüller H., Gerhardt E., Isenmann S., Schulz J.B., Bähr M. Neuron-specific expression of therapeutic proteins: evaluation of different cellular promoters in recombinant adenoviral vectors. *Mol. Cell. Neurosci.*, 2001, 17(1), pp. 78-96.
181. Ladewig T., Keller B.U. Simultaneous patch-clamp recording and calcium imaging in a rhythmically active neuronal network in the brainstem slice preparation from mouse. *Pflugers Arch.*, 2000, 440, pp. 322–332.
182. Lalley P.M., Pierrefiche O., Bischoff A.M., Richter D.W. cAMP-dependent protein

kinase modulates expiratory neurons in vivo. *J. Neurophysiol.*, 1997, 77(3), pp. 1119-1131.

183. Landa L.R. Jr, Harbeck M., Kaihara K., Chepurny O., Kitiphongspattana K., Graf O., Nikolaev V.O., Lohse M.J., Holz G.G., Roe M.W. Interplay of Ca²⁺ and cAMP signaling in the insulin-secreting MIN6 beta-cell line. *J. Biol. Chem.*, 2005, 280, pp. 31294-31302.

184. Lang S.B., Stein V., Bonhoeffer T., Lohmann C. Endogenous brain-derived neurotrophic factor triggers fast calcium transients at synapses in developing dendrites. *J. Neurosci.*, 2007, 27(5), pp. 1097-105.

185. Larimore J.L., Chapleau C.A., Kudo S., Theibert A., Percy A.K., Pozzo-Miller L. Bdnf overexpression in hippocampal neurons prevents dendritic atrophy caused by Rett-associated MECP2 mutations. *Neurobiol. Dis.*, 2009, 34(2), pp. 199-211.

186. LaSalle J.M. The odyssey of MeCP2 and parental imprinting. *Epigenetics*, 2007, 2(1), pp. 5-10.

187. LaSalle J.M., Goldstine J., Balmer D., Greco C.M. Quantitative localization of heterogeneous methyl-CpG-binding protein 2 (MeCP2) expression phenotypes in normal and Rett syndrome brain by laser scanning cytometry. *Hum. Mol. Genet.*, 2001, 10, pp. 1729-1740.

188. Laurenza A., Sutkowski E.M., Seamon K.B. Forskolin: a specific stimulator of adenylyl cyclase or a diterpene with multiple sites of action? *Trends Pharmacol. Sci.*, 1989, 10(11), pp. 442-447.

189. Lee H.K., Barbarosie M., Kameyama K., Bear M.F., Huganir R.L. Regulation of distinct AMPA receptor phosphorylation sites during bidirectional synaptic plasticity. *Nature*, 2000, 405(6789), pp. 955-959.

190. Lesser S.S., Sherwood N.T., Lo D.C. Neurotrophins differentially regulate voltage-gated ion channels. *Mol. Cell. Neurosci.*, 1997, 10(3-4), pp. 173-183.

191. Levi-Montalcini R. The nerve growth factor: thirty-five years later. *Embo. J.*, 1987, 6(5), pp. 1145-1154. Review.

192. Lewin G.R., Barde Y.A. Physiology of the neurotrophins. *Annu. Rev. Neurosci.*, 1996, 19, p. 289-317.
193. Lewis J.D., Meehan R.R., Henzel W.J., Maurer-Fogy I., Jeppesen P., Klein F., Bird A. Purification, sequence, and cellular localization of a novel chromosomal protein that binds to methylated DNA. *Cell*, 1992, 69(6), pp. 905-914.
194. Li H., Gu X., Dawson V.L. and Dawson T.M., Identification of calcium- and nitric oxide-regulated genes by differential analysis of library expression (DAzLE), *Proc. Natl. Acad. Sci. USA*, 2004, 101, pp. 647–652.
195. Li Y., Irwin N., Yin Y., Lanser M., Benowitz L.I. Axon regeneration in goldfish and rat retinal ganglion cells: differential responsiveness to carbohydrates and cAMP. *J. Neurosci.*, 2003, 23(21), pp. 7830-7838.
196. Lin C.H., Juan S.H., Wang C.Y., Sun Y.Y., Chou C.M., Chang S.F., Hu S.Y., Lee W.S., Lee Y.H. Neuronal activity enhances aryl hydrocarbon receptor-mediated gene expression and dioxin neurotoxicity in cortical neurons. *J. Neurochem.*, 2008 104(5):1415-1429.
197. Liss B., Roeper J. ATP-sensitive potassium channels in dopaminergic neurons: transducers of mitochondrial dysfunction. *News Physiol. Sci.*, 2001, 16:214-217. Review.
198. Lissandron V., Rossetto M.G., Erbguth K., Fiala A., Daga A. Transgenic fruit-flies expressing a FRET-based sensor for in vivo imaging of cAMP dynamics. *Cell Signal*, 2007, 19, pp.2296-2303.
199. Liu Z., Geng L., Li R., He X., Zheng J.Q. Frequency modulation of synchronized Ca²⁺ spikes in cultured hippocampal networks through G-protein-coupled receptors. *J. Neurosci.*, 2003, 23, pp. 4156-4163.
200. Loewenstein Y., Sompolinsky H. Temporal integration by calcium dynamics in a model neuron. *Nat. Neurosci.*, 2003, 6(9), pp. 961-967.
201. Lohmann C., Myhr K.L., Wong R.O. Transmitter-evoked local calcium release

stabilizes developing dendrites. *Nature*, 2002, 418(6894), pp. 177-181.

202. Lonze B.E., Ginty D.D. Function and regulation of CREB family transcription factors in the nervous system. *Neuron*, 2002, 35(4), pp. 605-623. Review.

203. Lorier A.R., Huxtable A.G., Robinson D.M., Lipski J., Housley G.D. and Funk G.D. P2Y1 receptor modulation of the pre-Bötzinger complex inspiratory rhythm generating network in vitro. *J. Neurosci.*, 2007, 27, pp. 993–1005.

204. Lorier A.R., Lipski J., Housley G.D., Greer J.J., Funk G.D. ATP sensitivity of preBötzinger complex neurones in neonatal rat in vitro: mechanism underlying a P2 receptor-mediated increase in inspiratory frequency. *J. Physiol.*, 2008, 586(5), pp. 1429-1446.

205. Luikenhuis S., Giacometti E., Beard C.F., Jaenisch R. Expression of MeCP2 in postmitotic neurons rescues Rett syndrome in mice. *Proc. Natl. Acad. Sci. USA*, 2004, 101(16), pp. 6033-6038.

206. Lukyanetz E.A., Kostyuk P.G. Two distinct receptors operate the cAMP cascade to up-regulate L-type Ca channels. *Pflugers Arch.*, 1996, 432(2), pp. 174-181.

207. Maletic-Savatic M., Malinow R., Svoboda K. Rapid dendritic morphogenesis in CA1 hippocampal dendrites induced by synaptic activity. *Science*, 1999, 283: 1923-1927.

208. Manzke T., Guenther U., Ponimaskin E.G., Haller M., Dutschmann M., Schwarzacher S., Richter D.W. 5-HT₄(a) receptors avert opioid-induced breathing depression without loss of analgesia. *Science*. 2003 Jul 11; 301(5630):226-229.

209. Marder E., Goaillard J.M. Variability, compensation and homeostasis in neuron and network function. *Nat Rev Neurosci*. 2006 Jul; 7(7):563-574. Review.

210. Martinowich K., Hattori D., Wu H., Fouse S., He F., Hu Y., Fan G., Sun Y.E. DNA methylation-related chromatin remodeling in activity-dependent BDNF gene regulation. *Science*, 2003, 302, pp. 890-893.

211. Mattson M.P., LaFerla F.M., Chan S.L., Leissring M.A., Shepel P.N., Geiger J.D.

Calcium signaling in the ER: its role in neuronal plasticity and neurodegenerative disorders. *Trends Neurosci.*, 2000, 23 (5):222-229

212. Mayr B., Montminy M. Transcriptional regulation by the phosphorylation-dependent factor CREB. *Nat Rev Mol Cell Biol.* 2001 Aug; 2(8):599-609. Review.

213. McAllister A.K. Cellular and molecular mechanisms of dendrite growth. *Cereb Cortex.* 2000 Oct; 10(10):963-973. Review.

214. McAllister A.K. Dynamic aspects of CNS synapse formation. *Annu Rev Neurosci.*, 2007; 30:425-50.

215. McAllister A.K., Katz L.C. and Lo D.C., Opposing roles for endogenous BDNF and NT-3 in regulating cortical dendritic growth, *Neuron*, 1997, 18, pp. 767–778.

216. McAllister A.K., Katz L.C., Lo D.C. Neurotrophin regulation of cortical dendritic growth requires activity. *Neuron.* 1996 Dec; 17(6):1057-1064.

217. McAllister A.K., Lo D.C. and Katz L.C., Neurotrophins regulate dendritic growth in developing visual cortex, *Neuron*, 1995, 15, pp. 791–803.

218. McGill B.E., Bundle S.F., Yaylaoglu M.B., Carson J.P., Thaller C., Zoghbi H.Y. Enhanced anxiety and stress-induced corticosterone release are associated with increased Crh expression in a mouse model of Rett syndrome. *Proc Natl Acad Sci U S A.* 2006 Nov 28; 103(48):18267-18272.

219. McKay L.C., Janczewski W.A. and Feldman J.L. Sleep-disordered breathing after targeted ablation of preBotzinger complex neurons. *Nat. Neurosci.*, 2005, 8, pp. 1142–1144.

220. Medrihan L., Tantalaki E., Aramuni G., Sargsyan V., Dudanova I., Missler M., Zhang W. Early defects of GABAergic synapses in the brain stem of a MeCP2 mouse model of Rett syndrome. *J Neurophysiol.* 2008 Jan; 99(1):112-121.

221. Mhyre T.R., Maine D.N., Holliday J. Calcium-induced calcium release from intracellular stores is developmentally regulated in primary cultures of cerebellar granule

neurons. *J Neurobiol.* 2000 Jan; 42(1):134-147.

222. Miles G.B., Parkis M.A., Lipski J., Funk G.D. Modulation of phrenic motoneuron excitability by ATP: consequences for respiratory-related output in vitro. *J Appl Physiol.* 2002 May; 92(5):1899-1910.

223. Miller F.D., Kaplan D.R. Signaling mechanisms underlying dendrite formation. *Curr Opin Neurobiol.* 2003 Jun; 13(3):391-398. Review.

224. Mironov S.L, Langohr K., Richter D.W. A1 adenosine receptors modulate respiratory activity of the neonatal mouse via the cAMP-mediated signaling pathway. *J Neurophysiol.* 1999 Jan; 81(1):247-255.

225. Mironov S.L. Mechanisms of Ca^{2+} mobilization in chick sensory neurones. *Neuroreport.* 1994 Jan 12; 5(4):445-448.

226. Mironov S.L. Metabotropic ATP receptor in hippocampal and thalamic neurones: pharmacology and modulation of Ca^{2+} mobilizing mechanisms. *Neuropharmacology*, 1994, 33, p. 1-13.

227. Mironov S.L. Metabotropic glutamate receptors activate dendritic calcium waves and TRPM channels which drive rhythmic respiratory patterns in mice. *J. Physiol.*, 2008; 586, pp. 2277–2291.

228. Mironov S.L. Monovalent amidiniums block calcium channels in chick sensory neurons. *J Membr Biol.* 1994 Sep; 141(3):231-237.

229. Mironov S.L. Plasmalemmal and intracellular Ca^{2+} pumps as main determinants of slow Ca^{2+} buffering in rat hippocampal neurones. *Neuropharmacology.* 1995 Sep; 34(9):1123-1132.

230. Mironov S.L., Hartelt N., Ivannikov M.V. Mitochondrial K-ATP channels in respiratory neurons and their role in the hypoxic facilitation of rhythmic activity. *Brain Res.*, 2005, 1033(1), pp. 20-27.

231. Mironov S.L., Hermann A. Ethanol actions on the mechanisms of Ca^{2+} mobilization in rat hippocampal cells are mediated by protein kinase C. *Brain Res.* 1996, 714(1-2), pp. 27-37.
232. Mironov S.L., Ivannikov M.V., Johansson M. $[\text{Ca}^{2+}]_i$ signaling between mitochondria and endoplasmic reticulum in neurons is regulated by microtubules. From mitochondrial permeability transition pore to Ca^{2+} -induced Ca^{2+} release. *J Biol Chem.* 2005 Jan 7; 280(1):715-721.
233. Mironov S.L., Langohr K. Mechanisms of Na^+ and Ca^{2+} influx into respiratory neurons during hypoxia. *Neuropharmacology*, 2005, 48, pp. 1056-1065.
234. Mironov S.L., Langohr K. Modulation of synaptic and channel activities in the respiratory network of the mice by NO/cGMP signaling pathways. *Brain Res.*, 2007, 1130, pp. 73-82.
235. Mironov S.L., Langohr K., Haller M., Richter D.W. Hypoxia activates ATP-dependent potassium channels in inspiratory neurones of neonatal mice. *J. Physiol.*, 1998, 509 (3), pp. 755-766.
236. Mironov S.L., Langohr K., Richter D.W. A1 adenosine receptors modulate respiratory activity of the neonatal mouse via the cAMP-mediated signaling pathway. *J Neurophysiol.*, 1999, 81(1), pp. 247-255.
237. Mironov S.L., Langohr K., Richter D.W. Hyperpolarization-activated current, I_h , in inspiratory brainstem neurons and its inhibition by hypoxia. *Eur J Neurosci.* 2000 Feb; 12(2):520-526.
238. Mironov S.L., Richter D.W. Intracellular signaling pathways modulate K-ATP channels in inspiratory brainstem neurones and their hypoxic activation: involvement of metabotropic receptors, G-proteins and cytoskeleton. *Brain Res.* 2000 Jan 17;853(1), pp. 60-67
239. Mironov S.L., Richter D.W. L-type Ca^{2+} channels in inspiratory neurones of mice and their modulation by hypoxia. *J Physiol.* 1998 Oct 1; 512 (Pt 1):75-87.
240. Mironov S.L., Skorova E., Hartelt N., Mironova L.A., Hasan M.T., Kügler S.

Remodelling of the respiratory network in a mouse model of Rett syndrome depends on brain-derived neurotrophic factor regulated slow calcium buffering. *J Physiol.* 2009 Jun 1; 587(Pt 11):2473-2485.

241. Mironov S.L., Skorova E., Hartelt N., Mironova L.A., Hasan M.T., Kügler S. Erratum to “Remodelling of the respiratory network in a mouse model of Rett syndrome depends on brain-derived neurotrophic factor regulated slow calcium buffering”. *J Physiol.* 2011 Aug 1;589(Pt 15):3897.

242. Mironov S.L., Skorova E., Taschenberger G., Hartelt N., Nikolaev V.O., Lohse M.J., Kügler S. Imaging cytoplasmic cAMP in mouse brainstem neurons. *BMC Neurosci.*, 2009, 27, pp. 10-29.

243. Mironova L.A., Mironov S.L. Approximate analytical time-dependent solutions to describe large-amplitude local calcium transients in the presence of buffers. *Biophys. J.* 2008, 94, pp. 349-358.

244. Moretti P., Levenson J.M., Battaglia F., Atkinson R., Teague R., Antalffy B., Armstrong D., Arancio O., Sweatt J.D., Zoghbi H.Y. Learning and memory and synaptic plasticity are impaired in a mouse model of Rett syndrome. *J. Neurosci.*, 2006, 26, pp. 319–327.

245. Morgado-Valle C., Beltran-Parrazal L., DiFranco M., Vergara J.L., Feldman J.L. Somatic Ca²⁺ transients do not contribute to inspiratory drive in preBötzing Complex neurons. *J. Physiol.*, 2008, 586(18), pp. 4531-4540.

246. Morton R.E., Bonas R., Minford J., Kerr A., Ellis R.E. Feeding ability in Rett syndrome. *Dev. Med. Child Neurol.*, 1997, 39(5), pp. 331-335.

247. Morton R.E., Bonas R., Minford J., Tarrant S.C., Ellis R.E. Respiration patterns during feeding in Rett syndrome. *Dev. Med. Child Neurol.*, 1997, 39(9), pp. 607-613.

248. Murakami J.W., Courchesne E., Haas R.H., Press G.A., Yeung-Courchesne R. Cerebellar and cerebral abnormalities in Rett syndrome: a quantitative MR analysis. *AJR Am J Roentgenol.* 1992 Jul; 159(1):177-183.

249. Murakoshi T., Suzue T., Tamai S. A pharmacological study on respiratory rhythm in the isolated brainstem-spinal cord preparation of the newborn rat. *Br. J. Pharmacol.*, 1985, 86(1), pp. 95-104.
250. Nakade S., Rhee S.K., Hamanaka H., Mikoshiba K. Cyclic AMP-dependent phosphorylation of an immunoaffinity-purified homotetrameric inositol 1,4,5-trisphosphate receptor (type I) increases Ca^{2+} flux in reconstituted lipid vesicles. *J Biol Chem.* 1994 Mar 4; 269(9):6735-6742.
251. Nectoux J., Bahi-Buisson N., Guellec I., Coste J., De Roux N., Rosas H., Tardieu M., Chelly J., Bienvenu T. The p.Val66Met polymorphism in the BDNF gene protects against early seizures in Rett syndrome. *Neurology*, 2008, 70(22), pp. 2145-2151.
252. Nedivi E., Hevroni D., Naot D., Israeli D. and Citri Y. Numerous candidate plasticity-related genes revealed by differential cDNA cloning, *Nature*, 1993, 363, pp. 718–722.
253. Nedivi E., Wu G.Y., Cline H.T. Promotion of dendritic growth by CPG15, an activity-induced signaling molecule. *Science*. 1998 Sep 18; 281(5384):1863-1836.
254. Nelson E.D., Kavalali E.T., Monteggia L.M. MeCP2-dependent transcriptional repression regulates excitatory neurotransmission. *Curr. Biol.*, 2006, 16, 710–716.
255. Nestler E.J. Molecular mechanisms of opiate and cocaine addiction. *Curr Opin Neurobiol.* 1997 Oct; 7(5):713-9. Nguyen PV, Woo NH. Regulation of hippocampal synaptic plasticity by cyclic AMP-dependent protein kinases. *Prog Neurobiol.* 2003 Dec; 71(6):401-437.
256. Nikolaev V.O., Bünemann M., Hein L., Hannawacker A., Lohse M.J. Novel single chain cAMP sensors for receptor-induced signal propagation. *J. Biol. Chem.*, 2004, 279, p. 37215-37218.
257. Nikolaev V.O., Bünemann M., Schmitteckert E., Lohse M.J., Engelhardt S. Cyclic AMP imaging in adult cardiac myocytes reveals far-reaching beta1-adrenergic but locally confined beta2-adrenergic receptor-mediated signaling. *Circ. Res.*, 2006, 99, pp. 1084-1091.

258. North R.A., Uchimura N. 5-Hydroxytryptamine acts at 5-HT₂ receptors to decrease potassium conductance in rat nucleus accumbens neurones. *J Physiol.* 1989 Oct; 417:1-12.
259. Nuber U.A., Kriaucionis S., Roloff T.C., Guy J., Selfridge J., Steinhoff C., Schulz R., Lipkowitz B., Ropers H.H., Holmes M.C., Bird A. Up-regulation of glucocorticoid-regulated genes in a mouse model of Rett syndrome. *Hum Mol Genet.* 2005 Aug 1; 14(15):2247-2256.
260. Ogier M., Katz D.M. Breathing dysfunction in Rett syndrome: understanding epigenetic regulation of the respiratory network. *Respir. Physiol. Neurobiol.*, 2008, 164(1-2), pp. 55-63.
261. Ogier M., Wang H., Hong E., Wang Q., Greenberg M.E., Katz D.M. Brain-derived neurotrophic factor expression and respiratory function improve after ampakine treatment in a mouse model of Rett syndrome. *J. Neurosci.*, 2007, 27(40), pp. 10912-10917.
262. Oka M., Kimura Y., Itoh Y., Sasaki Y., Taniguchi N., Ukai Y., Yoshikuni Y., Kimura K. Brain pertussis toxin-sensitive G proteins are involved in the flavoxate hydrochloride-induced suppression of the micturition reflex in rats. *Brain Res.* 1996 Jul 15; 727(1-2):91-98.
263. Oldfors A., Sourander P., Armstrong D.L., Percy A.K., Witt-Engerström I., Hagberg B.A. Rett syndrome: cerebellar pathology. *Pediatr. Neurol.*, 1990, 6(5), pp. 310-314.
264. Onimaru H., Ballanyi K., Homma I. Contribution of Ca²⁺-dependent conductances to membrane potential fluctuations of medullary respiratory neurons of newborn rats in vitro. *J. Physiol.*, 2003, 552, pp. 727–741.
265. Onimaru H., Ballanyi K., Richter D.W. Calcium-dependent responses in neurons of the isolated respiratory network of newborn rats. *J. Physiol.*, 1996, 491, p. 677–695.
266. Onimaru H., Homma I., Feldman J.L. and Janczewski W.A. Point: Counterpoint: The parafacial respiratory group (pFRG)/ pre-Botzinger complex (preBötC) is the primary site of respiratory rhythm generation in the mammal. *J. Appl. Physiol.*, 2006, 100: 2094-2098.
267. Onimaru H., Kumagawa Y., Homma I. Respiration-related rhythmic activity in the rostral medulla of newborn rats. *J. Neurophysiol.*, 2006, 96(1), pp. 55-61.

268. Ooashi N., Futatsugi A., Yoshihara F., Mikoshiba K., Kamiguchi H. Cell adhesion molecules regulate Ca^{2+} -mediated steering of growth cones via cyclic AMP and ryanodine receptor type 3. *J. Cell. Biol.*, 2000, 170, pp. 1159-1167.
269. Opie L.H. *The heart: physiology from cell to circulation*. 2004, Philadelphia: Lippincott Williams and Wilkins.
270. Oyelese A.A., Rizzo M.A., Waxman S.G., Kocsis J.D. Differential effects of NGF and BDNF on axotomy-induced changes in GABA(A)-receptor-mediated conductance and sodium currents in cutaneous afferent neurons. *J Neurophysiol.* 1997 Jul; 78(1):31-42.
271. Pagliardini S., Adachi T., Ren J., Funk G.D. and Greer J.J. Fluorescent tagging of rhythmically active respiratory neurons within the pre-Botzinger complex of rat medullary slice preparations. *J. Neurosci.*, 2005, 25, p. 2591–2596.
272. Palmer A.E., Giacomello M., Kortemme T., Hires S.A., Lev-Ram V., Baker D., Tsien R.Y. Ca^{2+} indicators based on computationally redesigned calmodulin-peptide pairs. *Chem. Biol.*, 2006, 13(5), pp. 521-530.
273. Palmer A.E., Jin C., Reed J.C., Tsien R.Y. Bcl-2-mediated alterations in endoplasmic reticulum Ca^{2+} analyzed with an improved genetically encoded fluorescent sensor. *Proc. Natl. Acad. Sci. USA*, 2004, 101(50), pp. 17404-17409.
274. Palmer A.E., Tsien R.Y. Measuring calcium signaling using genetically targetable fluorescent indicators. *Nat. Protoc.*, 2006, 1(3), pp. 1057-1065.
275. Parekh D.B, Ziegler W., Parker P.J. Multiple pathways control protein kinase C phosphorylation. *EMBO J.* 2000 Feb 15; 19(4):496-503.
276. Park C.S., Gong R., Stuart J. and Tang S.J., Molecular network and chromosomal clustering of genes involved in synaptic plasticity in the hippocampus, *J. Biol. Chem.*, 2006, 281, pp. 30195–30211.
277. Patterson S.L., Abel T., Deuel T.A., Martin K.C., Rose J.C., Kandel E.R. Recombinant BDNF rescues deficits in basal synaptic transmission and hippocampal LTP in BDNF

knockout mice. *Neuron*. 1996 Jun; 16(6):1137-1145.

278. Peddada S., Yasui D.H., LaSalle J.M. Inhibitors of differentiation (ID1, ID2, ID3 and ID4) genes are neuronal targets of MeCP2 that are elevated in Rett syndrome. *Hum Mol Genet*. 2006 Jun 15; 15(12):2003-2014.

279. Pelka G.J., Watson C.M., Christodoulou J., Tam P.P. Distinct expression profiles of *Mecp2* transcripts with different lengths of 3'UTR in the brain and visceral organs during mouse development. *Genomics*, 2005; 85, pp. 441–452.

280. Pelka G.J., Watson C.M., Radziewicz T., Hayward M., Lahooti H., Christodoulou J., Tam PP. *Mecp2* deficiency is associated with learning and cognitive deficits and altered gene activity in the hippocampal region of mice. *Brain*. 2006 Apr; 129(Pt 4), pp. 887-898.

281. Pena F., Parkis M.A., Tryba A.K., Ramirez J.M. Differential contribution of pacemaker properties to the generation of respiratory rhythms during normoxia and hypoxia. *Neuron*, 2004, 43, pp. 105–117.

282. Pierrefiche O., Champagnat J., Richter D.W. Calcium-dependent conductances control neurones involved in termination of inspiration in cats. *Neurosci. Lett.*, 1995, 184, pp. 101–104.

283. Pierrefiche O., Foutz A.S., Denavit-Saubié M. Effects of GABAB receptor agonists and antagonists on the bulbar respiratory network in cat. *Brain Res*. 1993 Mar 5; 605(1):77-84.

284. Pierrefiche O., Foutz A.S., Denavit-Saubié M. Effects of GABAB receptor agonists and antagonists on the bulbar respiratory network in cat. *Brain Res.*, 1993, 605(1), pp. 77-84.

285. Pierrefiche O., Haji A., Bischoff A., Richter D.W. Calcium currents in respiratory neurons of the cat in vivo. *Pflugers Arch.*, 1999, 438, p. 817–826.

286. Polleux F., Morrow T., Ghosh A. Semaphorin 3A is a chemoattractant for cortical apical dendrites. *Nature*. 2000 Apr 6; 404(6778):567-573.

287. Ponsioen B., Zhao J., Riedl J., Zwartkruis F., Krogt G., Zacco M., Moolenaar W.H.,

- Bos J.L., Jalink K.. Detecting cAMP-induced Epac activation by fluorescence resonance energy transfer: Epac as a novel cAMP indicator. *EMBO Rep*, 2004, 5, pp. 1176-1180.
288. Potts J.T., Paton J.F. Optical imaging of medullary ventral respiratory network during eupnea and gasping in situ. *Eur J Neurosci*. 2006 Jun; 23(11):3025-33.
289. Ramírez M.B., Sánchez M.B., Fernández M.C., Lipp O.V., and Vila J. Differentiation between protective reflexes: Cardiac defense and startle, *Psychophysiology*, 2005, 42, pp. 732–739.
290. Ramirez J.M., Telgkamp P., Elsen F.P., Quellmalz U.J., Richter D.W. Respiratory rhythm generation in mammals: synaptic and membrane properties. *Respir. Physiol.*, 1997 110(2-3), pp. 71-85.
291. Redmond L., Ghosh A. Regulation of dendritic development by calcium signaling. *Cell Calcium*. 2005 May; 37(5):411-416.
292. Redmond L., Ghosh A. The role of Notch and Rho GTPase signaling in the control of dendritic development. *Curr Opin Neurobiol*. 2001 Feb; 11(1):111-117. Review.
293. Redmond L., Kashani A.H., Ghosh A. Calcium regulation of dendritic growth via CaM kinase IV and CREB-mediated transcription. *Neuron*. 2002 Jun 13; 34(6):999-1010.
294. Redmond L., Oh S.R., Hicks C, Weinmaster G, Ghosh A. Nuclear Notch1 signaling and the regulation of dendritic development. *Nat Neurosci*. 2000 Jan; 3(1):30-40.
295. Rekling J.C., Champagnat J., Denavit-Saubié M. Electroresponsive properties and membrane potential trajectories of three types of inspiratory neurons in the newborn mouse brain stem in vitro. *J. Neurophysiol.*, 1996, 75(2), pp. 795-810.
296. Rekling J.C., Feldman J.L. PreBötzinger complex and pacemaker neurons: hypothesized site and kernel for respiratory rhythm generation. *Annu. Rev. Physiol.*, 1998, 60, pp. 385-405.
297. Renieri A., Meloni I., Longo I., Ariani F., Mari F., Pescucci C., Cambi F. Rett

syndrome: the complex nature of a monogenic disease. *J. Mol. Med.*, 2003, 81(6), pp. 346-354.

298. Rett A. Uber ein cerebral-atrophisches Syndrom bei Hyperammonamie. *Wien Med Wochenschr.*, 1966, 116(37), pp. 723-726.

299. Rial Verde E.M, Lee-Osbourne J., Worley P.F., Malinow R., Cline H.T. Increased expression of the immediate-early gene *arc/arg3.1* reduces AMPA receptor-mediated synaptic transmission. *Neuron*, 2006, 52(3), pp. 461-474.

300. Richter D.W., Champagnat J., Jacquin T., Benacka R. Calcium currents and calcium-dependent potassium currents in mammalian medullary respiratory neurones. *J. Physiol.*, 1993, 470, pp. 23-33.

301. Richter D.W., Lalley P.M., Pierrefiche O., Haji A., Bischoff A.M., Wilken B., Hanefeld F. Intracellular signal pathways controlling respiratory neurons. *Respir. Physiol.*, 1997, 110(2-3), pp. 113-123.

302. Richter D.W., Mironov S.L., Büsselberg D., Bischof A.M., Lalley P.M. Respiratory rhythm generation: Plasticity of a neuronal network. *Neuroscientist*, 2000, 6, pp. 188-205.

303. Richter D.W., Pierrefiche O., Lalley P.M., Polder H.R. Voltage-clamp analysis of neurons within deep layers of the brain. *J. Neurosci. Methods*, 1996, 67(2), pp. 121-123.

304. Richter DW, Spyer KM. Studying rhythmogenesis of breathing: comparison of in vivo and in vitro models. *Trends Neurosci.* 2001 Aug; 24(8):464-472.

305. Roche K.W., O'Brien R.J., Mammen A.L., Bernhardt J., Huganir R.L. Characterization of multiple phosphorylation sites on the AMPA receptor GluR1 subunit. *Neuron*, 1996, 16(6), pp. 1179-1188.

306. Roloff T.-C., Identification of *Mecp2* target genes and of proteins related to *Mecp2*. Ph.D. Thesis. Free University of Berlin, Germany. 2005

307. Roloff T.C., Nuber U.A. Chromatin, epigenetics and stem cells. *Eur J Cell Biol.* 2005

Mar; 84(2-3):123-135.

308. Roloff T.C., Ropers H.H., Nuber U.A. Comparative study of methyl-CpG-binding domain proteins. *BMC Genomics*. 2003 Jan 16; 4(1):1.

309. Rong W., Gourine A.V., Cockayne D.A., Xiang Z., Ford A.P., Spyer K.M., Burnstock G. Pivotal role of nucleotide P2X2 receptor subunit of the ATP-gated ion channel mediating ventilatory responses to hypoxia. *J. Neurosci.*, 2003, 23(36), pp. 11315-11321.

310. Ronnett G.V., Leopold D., Cai X., Hoffbuhr K.C., Moses L., Hoffman E.P., Naidu S. Olfactory biopsies demonstrate a defect in neuronal development in Rett's syndrome. *Ann Neurol*. 2003 Aug; 54(2):206-218.

311. Rotwein P., Burgess S.K., Milbrandt J.D., Krause J.E. Differential expression of insulin-like growth factor genes in rat central nervous system. *Proc Natl Acad Sci U S A*. 1988 Jan; 85(1):265-269.

312. Roux J.C., Dura E., Moncla A., Mancini J., Villard L. Treatment with desipramine improves breathing and survival in a mouse model for Rett syndrome. *Eur. J. Neurosci.*, 2007, 25(7), pp. 1915-1922.

313. Ruangkittisakul A., Schwarzacher S.W., Secchia L., Poon B.Y., Ma Y., Funk G.D., Ballanyi K. High sensitivity to neuromodulator-activated signaling pathways at physiological $[K^+]$ of confocally imaged respiratory center neurons in on-line-calibrated newborn rat brainstem slices. *J. Neurosci.*, 2006, 26, p. 11870–11880.

314. Russell J.C., Blue M.E., Johnston M.V., Naidu S., Hossain M.A. Enhanced cell death in *MeCP2* null cerebellar granule neurons exposed to excitotoxicity and hypoxia. *Neuroscience*, 2007, 150(3), pp. 563-574.

315. Sala C., Futai K., Yamamoto K., Worley P.F., Hayashi Y., Sheng M. Inhibition of dendritic spine morphogenesis and synaptic transmission by activity-inducible protein Homer1a. *J. Neurosci.*, 2003, 23(15), pp. 6327-6337.

316. Samaco R.C., Fryer J.D., Ren J., Fyffe S., Chao H.T., Sun Y., Greer J.J., Zoghbi H.Y.,

Neul J.L. A partial loss of function allele of methyl-CpG-binding protein 2 predicts a human neurodevelopmental syndrome. *Hum. Mol. Genet.*, 2008, 17(12), pp. 1718-1727.

317. Schanen N.C., Kurczynski T.W., Brunelle D., Woodcock M.M., Dure L.S. 4th, Percy A.K. Neonatal encephalopathy in two boys in families with recurrent Rett syndrome. *J. Child. Neurol.*, 1998, 13(5), pp. 229-231.

318. Schinder A.F., Poo M. The neurotrophin hypothesis for synaptic plasticity. *Trends Neurosci.* 2000 Dec; 23(12):639-645.

319. Schmidt M., Evellin S., Weernink P.A., von Dorp F., Rehmann H., Lomasney J.W., Jakobs K.H. A new phospholipase-C-calcium signalling pathway mediated by cyclic AMP and a Rap GTPase. *Nat Cell Biol.* 2001 Nov; 3(11):1020-1024.

320. Schwartz R.D., Heuschneider G., Edgar P.P., Cohn J.A. cAMP analogs inhibit gamma-aminobutyric acid-gated chloride flux and activate protein kinase A in brain synaptoneuroosomes. *Mol Pharmacol.* 1991 Mar; 39(3):370-375.

321. Schwartzman J.S., De Souza A.M., Faiwichow G., Hercowitz L.H. Rett phenotype in patient with XXY karyotype: case report. *Arq. Neuropsiquiatr.*, 1998, 56(4), pp. 824-828.

322. Schwarzacher S.W., Smith J.C., Richter D.W. Pre-Bötzinger complex in the cat. *J Neurophysiol.* 1995 Apr; 73(4):1452-1461.

323. Scott E.K., Luo L. How do dendrites take their shape? *Nat Neurosci.* 2001 Apr; 4(4):359-365.

324. Sestan N., Artavanis-Tsakonas S., Rakic P. Contact-dependent inhibition of cortical neurite growth mediated by notch signaling. *Science.* 1999 Oct 22; 286(5440):741-746.

325. Shahbazian M., Young J., Yuva-Paylor L., Spencer C., Antalffy B., Noebels J., Armstrong D., Paylor R., Zoghbi H. Mice with truncated MeCP2 recapitulate many Rett syndrome features and display hyperacetylation of histone H3. *Neuron*, 2002, 35(2), pp. 243-254.

326. Shakiryanova D., Levitan E.S. Prolonged presynaptic posttetanic cyclic GMP signaling in *Drosophila* motoneurons. *Proc. Natl. Acad. Sci. USA*, 2008, 105, pp. 13610-13613.
327. Shao X.M., Feldman J.L. Acetylcholine modulates respiratory pattern: effects mediated by M3-like receptors in preBötzinger complex inspiratory neurons. *J. Neurophysiol.*, 2000, 83(3), pp. 1243-52.
328. Shao X.M., Ge Q., Feldman J.L. Modulation of AMPA receptors by cAMP-dependent protein kinase in preBötzinger complex inspiratory neurons regulates respiratory rhythm in the rat. *J. Physiol.*, 2003, 547(2), pp. 543-553.
329. Sherwood N.T., Lesser S.S., Lo D.C. Neurotrophin regulation of ionic currents and cell size depends on cell context. *Proc Natl Acad Sci U S A*. 1997 May 27; 94(11):5917-5922.
330. Shevtsova Z., Malik J.M., Michel U., Bahr M. and Kugler S. 2005, Promoters and serotypes: targeting of adeno-associated virus vectors for gene transfer in the rat central nervous system in vitro and in vivo, *Exp. Physiol.*, 2005, 90, pp. 53–59.
331. Shibayama A., Cook E.H., Jr, Feng J., Glanzmann C., Yan J., Craddock N., Jones I.R., Goldman D., Heston L.L., Sommer S.S. MECP2 structural and 3'-UTR variants in schizophrenia, autism and other psychiatric diseases: a possible association with autism. *Am J Med Genet*. 2004;128B:50–53.
332. Shieh P.B., Hu S.C., Bobb K., Timmusk T., Ghosh A. Identification of a signaling pathway involved in calcium regulation of BDNF expression. *Neuron*. 1998 Apr; 20(4):727-740.
333. Smith J.C., Ellenberger H.H., Ballanyi K., Richter D.W., Feldman J.L. Pre-Bötzinger complex: a brainstem region that may generate respiratory rhythm in mammals. *Science*, 1991, 254, pp. 726–729.
334. Soderling T.R., Derkach V.A. Postsynaptic protein phosphorylation and LTP. *Trends. Neurosci.*, 2000, 23(2), pp. 75-80.
335. Song H.J., Poo M.M. Signal transduction underlying growth cone guidance by

diffusible factors. *Curr Opin Neurobiol.* 1999 Jun; 9(3):355-363.

336. Soundarapandian M.M., Zhong X., Peng L., Wu D., Lu Y. Role of K(ATP) channels in protection against neuronal excitatory insults. *J Neurochem.* 2007 Dec; 103(5):1721-1729.

337. Spitzer N.C., Kingston P.A., Manning T.J., Conklin M.W. Outside and in: development of neuronal excitability. *Curr. Opin. Neurobiol.*, 2002, 12(3), pp. 315-23.

338. Spyer K.M., Thomas T. Sensing arterial CO₂ levels: a role for medullary P2X receptors. *J. Auton. Nerv. Syst.*, 2000, 81, pp. 228–235

339. Stancheva I., Collins A.L., Van den Veyver I.B., Zoghbi H., Meehan R.R. A mutant form of MeCP2 protein associated with human Rett syndrome cannot be displaced from methylated DNA by notch in *Xenopus* embryos. *Mol Cell.* 2003 Aug; 12(2):425-435.

340. Stettner G.M., Huppke P., Brendel C., Richter D.W, Gärtner J., Dutschmann M. Breathing dysfunctions associated with impaired control of postinspiratory activity in *Mecp2*-*y* knockout mice. *J. Physiol.*, 2007, 579(3), pp. 863-876.

341. Stettner G.M., Huppke P., Gärtner J., Richter D.W, Dutschmann M. Disturbances of breathing in Rett syndrome: results from patients and animal models. *Adv. Exp. Med. Biol.*, 2008, 605, pp. 503-507.

342. Stettner G.M., Zanella S., Hilaire G., Dutschmann M. 8-OH-DPAT suppresses spontaneous central apneas in the C57BL/6J mouse strain. *Respir. Physiol. Neurobiol.*, 2008, 161(1), pp. 10-15.

343. Stettner G.M., Zanella S., Huppke P., Gärtner J., Hilaire G., Dutschmann M. Spontaneous central apneas occur in the C57BL/6J mouse strain. *Respir. Physiol. Neurobiol.*, 2008, 160(1), pp. 21-27.

344. Stornetta R.L., Rosin D.L., Wang H., Sevigny C.P., Weston M.C. and Guyenet P.G. A group of glutamatergic interneurons expressing high levels of both neurokinin-1 receptors and somatostatin identifies the region of the pre-Botzinger complex. *J. Comp. Neurol.*, 2003, 455, pp. 499–512.

345. Sun Y.E., Wu H. The ups and downs of BDNF in Rett syndrome. *Neuron*, 2006, 49(3), pp. 321-323.
346. Sutton M.A., Wall N.R., Aakalu G.N., Schuman E.M. Regulation of dendritic protein synthesis by miniature synaptic events. *Science*. 2004 Jun 25; 304(5679):1979-1983.
347. Swope S.L., Moss S.J., Blackstone C.D., Huganir R.L. Phosphorylation of ligand-gated ion channels: a possible mode of synaptic plasticity. *FASEB J.*, 1992, 6(8), pp. 2514-2523.
348. Tao X., Finkbeiner S., Arnold D.B., Shaywitz A.J., Greenberg M.E. Ca^{2+} influx regulates BDNF transcription by a CREB family transcription factor-dependent mechanism. *Neuron*. 1998 Apr; 20(4):709-726.
349. Terrin A., Di Benedetto G., Pertegato V., Cheung Y.F., Baillie G., Lynch M.J., Elvassore N., Prinz A., Herberg F.W., Houslay M.D., Zaccolo M: PGE(1) stimulation of HEK293 cells generates multiple contiguous domains with different [cAMP]: role of compartmentalized phosphodiesterases. *J. Cell. Biol.*, 2006, 175, pp. 441-451.
350. Teschemacher A.G., Paton J.F., Kasparov S. Imaging living central neurones using viral gene transfer. *Adv. Drug. Deliv. Rev.*, 2005, 57, pp. 79-93.
351. Thoby-Brisson M., Cauli B., Champagnat J., Fortin G., Katz D.M. Expression of functional tyrosine kinase B receptors by rhythmically active respiratory neurons in the pre-Bötzing complex of neonatal mice. *J. Neurosci.*, 2003, 23(20), pp. 7685-7689.
352. Thoby-Brisson M., Greer J.J. Anatomical and functional development of the pre-Bötzing complex in prenatal rodents. *J. Appl. Physiol.*, 2008, 104(4), pp. 1213-1219.
353. Thoby-Brisson M., Telgkamp P., Ramirez J.M. The role of the hyperpolarization-activated current in modulating rhythmic activity in the isolated respiratory network of mice. *J. Neurosci.*, 2000, 20(8), pp. 2994-3005.
354. Thoby-Brisson M., Trinh J.B., Champagnat J., Fortin G. Emergence of the pre-Bötzing respiratory rhythm generator in the mouse embryo. *J. Neurosci.*, 2005, 25(17), pp. 4307-4318.

355. Thomas T., Ralevic V., Bardini M., Burnstock G. and Spyer K.M. Evidence for the involvement of purinergic signaling in the control of respiration. *Neuroscience*, 2001, 107, pp. 481–490.
356. Thomas T., Ralevic V., Gadd C.A. and Spyer K.M. Central CO₂ chemoreception: a mechanism involving P₂ purinoceptors localized in the ventrolateral medulla of the anaesthetized rat. *J. Physiol.*, 1999, 517, pp. 899–905.
357. Thomas T., Spyer K.M. ATP as a mediator of mammalian central CO₂ chemoreception. *J. Physiol.*, 2000, 523, pp. 441–447.
358. Togashi H., Abe K., Mizoguchi A., Takaoka K., Chisaka O., Takeichi M. Cadherin regulates dendritic spine morphogenesis. *Neuron*. 2002 Jul 3; 35(1):77-89.
359. Traynelis S.F., Wahl P. Control of rat GluR6 glutamate receptor open probability by protein kinase A and calcineurin. *J Physiol*. 1997 Sep 15; 503 (Pt 3), pp. 513-531.
360. Tropea D., Giacometti E., Wilson N.R., Beard C., McCurry C., Fu D.D., Flannery R., Jaenisch R., Sur M. Partial reversal of Rett Syndrome-like symptoms in MeCP2 mutant mice. *Proc Natl Acad Sci U S A*. 2009 Feb 10; 106(6):2029-2034.
361. Turrigiano G. Homeostatic signaling: the positive side of negative feedback. *Curr. Opin. Neurobiol.*, 2007, 17(3), pp. 318-324.
362. Ulrey C.L., Liu L., Andrews L.G., Tollefsbol T.O. The impact of metabolism on DNA methylation. *Hum. Mol. Genet.*, 2005, 1, pp. 139-147.
363. Van Esch H., Bauters M., Ignatius J., Jansen M., Raynaud M., Hollanders K., Lugtenberg D., Bienvenu T., Jensen L.R., Gecz J., Moraine C., Fryns J.P., Froyen G. Duplication of the MECP2 region is a frequent cause of severe mental retardation and progressive neurological symptoms in males. *Am J Hum Genet*. 2005;77:442–453
364. Vasilakos K., Wilson R.J., Kimura N., and Remmers J.E. Ancient gill and lung oscillators may generate the respiratory rhythm of frogs and rats. *J. Neurobiol.*, 2005, 62, pp. 369–385.

365. Viemari J.C., Maussion G., Bévengut M., Burnet H., Pequignot J.M., Népote V., Pachnis V., Simonneau M., Hilaire G. Ret deficiency in mice impairs the development of A5 and A6 neurons and the functional maturation of the respiratory rhythm. *Eur. J. Neurosci.*, 2005, 22(10), pp. 2403-2412.
366. Viemari J.C., Roux J.C., Tryba A.K., Saywell V., Burnet H., Peña F., Zanella S., Bévengut M., Barthelemy-Requin M., Herzing L.B., Moncla A., Mancini J., Ramirez J.M., Villard L., Hilaire G. *Mecp2* deficiency disrupts norepinephrine and respiratory systems in mice. *J. Neurosci.*, 2005, 25(50), pp. 11521-11530.
367. Wallace D.J., Meyer zum Alten Borgloh S., Astori S., Yang Y., Bausen M., Kügler S., Palmer A.E., Tsien R.Y., Sprengel R., Kerr J.N., Denk W., Hasan M.T. Single-spike detection in vitro and in vivo with a genetic Ca^{2+} sensor. *Nat. Methods*, 2008, 5(9), pp. 797-804.
- 368.** Wan M., Lee S., Zhang X., Houwink-Manville I., Song H.-R., Amir R.E., Budden S., Naidu S., Pereira J.L.P., Lo I.F.M., Zoghbi H.Y., Schanen N. C., Francke U. Rett syndrome and beyond: recurrent spontaneous and familial *MECP2* mutations at CpG hotspots. *Am J Hum Genet* 1999; 65: 1520–1529.
369. Wang H., Cao R., Xia L., Erdjument-Bromage H., Borchers C., Tempst P., Zhang Y. Purification and functional characterization of a histone H3-lysine 4-specific methyltransferase. *Mol. Cell.*, 2001, 8, pp. 1207-1217.
370. Wang H., Chan S.A., Ogier M., Hellard D., Wang Q., Smith C., Katz D.M. Dysregulation of brain-derived neurotrophic factor expression and neurosecretory function in *Mecp2* null mice. *J Neurosci.* 2006 Oct 18; 26(42):10911-10915.
371. Wang L.Y., Salter M.W., MacDonald J.F. Regulation of kainate receptors by cAMP-dependent protein kinase and phosphatases. *Science.* 1991 Sep 6; 253(5024):1132-1135.
372. Wang L.Y., Taverna F.A., Huang X.P., MacDonald J.F., Hampson D.R. Phosphorylation and modulation of a kainate receptor (GluR6) by cAMP-dependent protein kinase. *Science.* 1993 Feb 19; 259(5098):1173-1175.

373. Wayman G.A., Davare M., Ando H., Fortin D., Varlamova O., Cheng H.Y., Marks D., Obrietan K., Soderling T.R., Goodman R.H., Impey S. An activity-regulated microRNA controls dendritic plasticity by down-regulating p250GAP. *Proc. Natl. Acad. Sci. USA*, 2008, 105(26), pp. 9093-9098.
374. Weese-Mayer D.E., Lieske S.P., Boothby C.M., Kenny A.S., Bennett H.L., Silvestri J.M., Ramirez J.M. Autonomic nervous system dysregulation: breathing and heart rate perturbation during wakefulness in young girls with Rett syndrome. *Pediatr. Res.*, 2006, 60(4), pp. 443-449.
375. Wenk G.L. Rett syndrome: neurobiological changes underlying specific symptoms. *Prog. Neurobiol.*, 1997, 51(4), pp. 383-391.
376. Werner H., Woloschak M., Adamo M., Shen-Orr Z., Roberts C.T. Jr, LeRoith D. Developmental regulation of the rat insulin-like growth factor I receptor gene. *Proc Natl Acad Sci U S A*. 1989 Oct; 86(19):7451-7455.
377. West A.E., Chen W.G., Dalva M.B., Dolmetsch R.E., Kornhauser J.M., Shaywitz A.J., Takasu M.A., Tao X., Greenberg M.E. Calcium regulation of neuronal gene expression. *Proc. Natl. Acad. Sci. USA*, 2001, 98, pp. 11024-11031.
378. West A.E., Griffith E.C., Greenberg M.E. Regulation of transcription factors by neuronal activity. *Nat Rev Neurosci*. 2002 Dec; 3(12):921-931.
379. Westenbroek R.E., Hell J.W., Warner C., Dubel S.J., Snutch T.P., Catterall W.A. Biochemical properties and subcellular distribution of an N-type calcium channel alpha 1 subunit. *Neuron*, 1992, 9(6), pp. 1099-1115.
380. Whitford K.L., Dijkhuizen P., Polleux F., Ghosh A. Molecular control of cortical dendrite development. *Annu Rev Neurosci*. 2002; 25:127-149.
381. Whitford K.L., Marillat V., Stein E., Goodman C.S., Tessier-Lavigne M., Chédotal A., Ghosh A. Regulation of cortical dendrite development by Slit-Robo interactions. *Neuron*. 2002 Jan 3; 33(1):47-61.

382. Willoughby D., Cooper D.M. Organization and Ca^{2+} regulation of adenylyl cyclases in cAMP microdomains. *Physiol. Rev.*, 2007, 87, p. 965-1010.
383. Wilson R.J., Vasilakos K., Harris M.B., Straus C., and Remmers J.E. Evidence that ventilatory rhythmogenesis in the frog involves two distinct neuronal oscillators. *J. Physiol.*, 2002, 540, pp. 557–570.
384. Wojcik W.J., Neff N.H. Gamma-aminobutyric acid B receptors are negatively coupled to adenylate cyclase in brain, and in the cerebellum these receptors may be associated with granule cells. *Mol. Pharmacol.*, 1984, 25(1), pp. 24-28.
385. Wong R.O., Ghosh A. Activity-dependent regulation of dendritic growth and patterning. *Nat. Rev. Neurosci.*, 2002, 3(10), pp. 803-812.
386. Wu G.Y., Deisseroth K., Tsien R.W. Spaced stimuli stabilize MAPK pathway activation and its effects on dendritic morphology. *Nat Neurosci.* 2001 Feb; 4(2):151-8.
387. Yamada K. and Inagaki N. ATP-Sensitive K^+ Channels in the Brain: Sensors of Hypoxic Conditions. *News in Physiological Sciences*, Vol. 17, No. 3, 127-130, June 2002.
388. Yamada K., Ji J.J., Yuan H., Miki T., Sato S., Horimoto N., Shimizu T., Seino S., Inagaki N. Protective role of ATP-sensitive potassium channels in hypoxia-induced generalized seizure. *Science*. 2001 May 25; 292(5521):1543-1546.
389. Yamashita N., Hayashi A., Baba J., Sawa A. Rolipram, a phosphodiesterase-4-selective inhibitor, promotes the survival of cultured rat dopaminergic neurons. *Jpn. J. Pharmacol.*, 1997, 75(2), pp. 155-159.
390. Yamashita N., Miyashiro M., Baba J., Sawa A. Rolipram, a selective inhibitor of phosphodiesterase type 4, pronouncedly enhanced the forskolin-induced promotion of dopamine biosynthesis in primary cultured rat mesencephalic neurons. *Jpn. J. Pharmacol.*, 1997, 75(1), pp. 91-95.
391. Yao S.T., Barden J.A., Finkelstein D.I., Bennett M.R. and Lawrence A.J. Comparative study on the distribution patterns of P2X_1 - P2X_6 receptor immunoreactivity in the brainstem

of the rat and the common marmoset (*Callithrix jacchus*): Association with catecholamine cell groups. *J. Comp. Neurol.*, 2000, 427, 485–507.

392. Yu F., Thiesen J., Strätling W.H. Histone deacetylase-independent transcriptional repression by methyl-CpG-binding protein 2. *Nucleic. Acids. Res.*, 2000, 28(10), pp. 2201-2206.

393. Yu X., Malenka R.C. Beta-catenin is critical for dendritic morphogenesis. *Nat Neurosci.* 2003 Nov; 6(11):1169-1177.

394. Yuste R., Nelson D.A., Rubin W.W., Katz L.C. Neuronal domains in developing neocortex: mechanisms of coactivation. *Neuron.* 1995 Jan; 14(1):7-17.

395. Zaccolo M., De Giorgi F., Cho C.Y., Feng L., Knapp T., Negulescu P.A., Taylor S.S., Tsien R.Y., Pozzan T. A genetically encoded, fluorescent indicator for cyclic AMP in living cells. *Nat. Cell. Biol.*, 2000, 2, pp. 25-29.

396. Zanella S., Mebarek S., Lajard A.M., Picard N., Dutschmann M., Hilaire G. Oral treatment with desipramine improves breathing and life span in Rett syndrome mouse model. *Respir. Physiol. Neurobiol.*, 2008, 160(1), pp. 116-121.

397. Zhao M.G., Hulsmann S., Winter S.M., Dutschmann M., Richter D.W. Calcium-regulated potassium currents secure respiratory rhythm generation after loss of glycinergic inhibition. *Eur. J. Neurosci.*, 2006, 24, p. 145–154.

398. Zhou Z., Hong E.J., Cohen S., Zhao W.N., Ho H.Y., Schmidt L., Chen W.G., Lin Y., Savner E., Griffith E.C., Hu L., Steen J.A., Weitz C.J., Greenberg M.E. Brain-specific phosphorylation of MeCP2 regulates activity-dependent *Bdnf* transcription, dendritic growth, and spine maturation. *Neuron*, 2006, 52(2), pp. 255-269.

399. Zieg J., Greer P.L., Greenberg M.E. SnapShot. Ca^{2+} -dependent transcription in neurons. *Cell*, 2008, 134(6), pp. 1080-1080.

400. Zoghbi H.Y. Postnatal neurodevelopmental disorders: meeting at the synapse? *Science.* 2003, 302(5646), pp. 826-830.

8. Curriculum vitae

Name	Ekaterina Skorova
E-mail	eskorova@gmail.com
Telephone	+17670193107
Address	Gosslerstr 33b, 56, 37073 Göttingen, Germany
Citizenship	Russian Federation

Education

1987-1999 Moscow State School

1997-2000 Evening biological school patronized by the Moscow State University

1999-2004 Department of Cell Biology and Histology Lomonosov Moscow State University, Moscow, Russia

2004 Master of Science in Physiology, Department of Cell Biology and Histology, Moscow State University, Moscow, Russia. Graduated with Honour

Research Experience

2002- 2003 Undergraduate research, Department of Cell Biology and Histology, Moscow State University (Supervisor: Dr. E. A. Smirnova)
Research topic: "Synchronization of the root meristem cells *Allium cepa* L. during the late S-phase"

2003-2004 Master research work, Department of Cell Biology and Histology, Moscow State University (Supervisors: Dr. E. A. Smirnova and Dr. N. A. Shanina)
Master thesis: "Identification and characterization of dynein - like protein in higher plant cells: *Allium cepa* L., *Triticum aestivum* L. and *Haemanthus katherinae* Baker."

2005-2010 Research assistant, Center of Molecular Physiology of the Brain (CMPB) , Georg-August University, Dept. Neuro- und Sensory Physiology, Göttingen, Germany, BAT IIa/2

2010-2011 Laboratory of cardiovascular experimental electrophysiology and imaging,
Heart centre, Georg-August University, Göttingen, Germany, HV

Research Courses

- 2001 Summer practical course on modern biology methods at S.N.Skadovsky
Biological station (ZBS MSU)
- 2002 Summer practical course on biophysical and biochemical methods at the
Pushchino Scientific Centre of Russian Academy of Sciences (PSC/RAS)
- 2012 10th Summer Course on Computational Neuroscience, Bernstein Center for
Computational Neuroscience (BCCN) Göttingen

Research Techniques

Cell culture, Slice preparation, Patch-clamp, Electrophoresis in PAA gel, Western blotting,
Immunocytochemistry, Optical imaging, Quantum Dots, Biological Data Processing.

Conferences Presentations

Skorova E., Shanina N., Chentsov Y., Smirnova E. “High molecular weight polypeptide
immunologically related to dynein heavy chain of Dictyostelium is found in higher plant cells”
American Society for Cell Biology, 44th Annual Meeting, 2004. (poster presentation)

Skorova E. “Calcium and cAMP homeostasis determine network organisation of respiratory
preBoetzing neurons in Mecp-2 null mice in vitro” V international young scientists’
conference “Biology: from a molecule up to the biosphere”, 2010. (Best Oral Presentation
Reward)

Prises and Awards

Best Oral Presentation Reward on V international young scientists’ conference “Biology: from

a molecule up to the biosphere”, 2010.

Journal Publications

1. Hartelt N., Skorova E., Manzke T., Suhr M., Mironova L., Kügler S., Mironov S.L. Imaging of respiratory network topology in living brainstem slices. *Mol. Cell Neurosci.* 2008 Mar; 37(3):425-31. Epub 2007 Oct 30.
2. Shanina N.A., Lazareva E.M., Skorova E.Y., Chentsov Y.S., Smirnova E.A. A high molecular weight polypeptide cross-reacting with the antibodies to the dynein heavy chain localizes to the subset of Golgi complex in higher plant cells. *Cell Biol. Int.* 2009 Mar; 33(3):290-300. Epub 2008 Dec 24.
3. Mironov S.L., Skorova E., Hartelt N., Mironova L.A., Hasan M.T., and Kügler S. Remodelling of the respiratory network in a mouse model of Rett syndrome depends on brain-derived neurotrophic factor regulated slow calcium buffering. *J. Physiol.* 2009 June 1; 587(Pt 11): 2473–2485. Epub 2009 April 9.
4. Mironov S.L., Skorova E., Taschenberger G., Hartelt N., Nikolaev V.O., Lohse M.J., and Kügler S. Imaging cytoplasmic cAMP in mouse brainstem neurons. *BMC Neurosci.* 2009; 10: 29. Published online 2009 March 27.
5. Mironov S.L., Skorova E.Yu. Stimulation of bursting in pre-Bötzinger neurons by Epac through calcium release and modulation of TRPM4 and K-ATP channels. *J. Neurochem.* 2011 Apr;117(2):295-308. Epub 2011 Feb 24.
6. Mironov S.L., Skorova E.Yu., Kügler S. Epac-mediated cAMP-signalling in the mouse model of Rett Syndrome. *Neuropharmacology.* 2011 May; 60(6):869-77. Epub 2011 Jan 11.